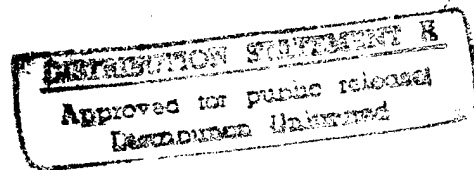


VOLUME III
SYSTEMS PHASE

CHAPTER 10
AEROELASTICITY/
AIRCRAFT STRUCTURES



19970117 013

USAF TEST PILOT SCHOOL
EDWARDS AFB, CA

Nov. 90

DTIC QUALITY INSPECTED 1

12.1 INTRODUCTION

Aeroelasticity is the science which deals with the mutual interaction of aerodynamic, elastic, and inertial forces and the aircraft's structural responses to these forces. If aircraft could be designed as perfectly rigid structures, then the interaction of these forces would not be important. The weight penalties and the resultant loss of aircraft performance make this design option impractical. This chapter is intended to introduce the flight test crew to the subject of aeroelastic phenomena in aircraft. Paragraph 12.3 deals with material used in aircraft structures, including structural design considerations and use of composite materials in aircraft structures. Paragraph 12.4 introduces aircraft structural response to loads and Paragraph 12.5 presents static and dynamic aeroelastic phenomena due to the interaction of the forces mentioned above.

This subject area has taken on increased importance to the flight test crew in recent years. New high strength-to-weight and high stiffness-to-weight materials are being used in aircraft. New aircraft design and fabrication techniques allow the structural weight to be minimized, thus increasing the flexibility of today's aircraft. Active feedback control surface actuation to alleviate dynamic loads and flutter on aircraft is being used to further decrease aircraft structural weight and thus gain increased performance. New composite aircraft structures require the test crew to better understand materials and structural response to loads. This chapter is intended to introduce the test team to this important subject area.

12.2 ABBREVIATIONS AND SYMBOLS

A, a	amplitude or area
ac	aerodynamic center
b	semi-chord or torsional damping
c	wing chord or distance from neutral axis to outermost fiber
cg	center of gravity
$C_{L_{\max}}$	variation of lift coefficient with angle of attack
$C_{L_{\alpha}}$	variation of the lift coefficient with angle of attack
$C_{L_{\delta_a}}$	variation of the lift coefficient with aileron deflection
d	linear damping or diameter
E	modulus of elasticity (Young's Modulus)
e	strain or the distance between the aerodynamic center and the elastic axis
EA	elastic axis
F, f	force or frequency
f_b	bending stress
f_c	compressive stress
f_n	normal stress or natural frequency
f_p	proportional limit stress
f_s	shear stress
f_t	tensile stress
G	Modules of Rigidity
g	gravity or flutter damping
h	vertical displacement
I	moment of inertia
J	polar moment of inertia

K	spring stiffness
K_{α}	torsional stiffness
K_x	bending stiffness
L	lift or length
L_{δ_a}	lift due to aileron deflection
$L_{\Delta\theta}$	variation in lift due to wing twist
ΔL_{δ_a}	variation in lift due to aileron deflection
M	Mach or moment
m	mass
M_{aero}	aerodynamic moment
M_{ac}	moment about the aerodynamic center
$M_{\text{ac}\delta_a}$	moment about the aerodynamic center due to aileron deflection
P	load
q	dynamic pressure
q_D	dynamic pressure at divergence speed
q_R	dynamic pressure at aileron reversal speed
r	radius
S	wing area or shear force
T	axial force
t	material thickness or time
U_D	divergence speed
U_F	flutter speed
U_R	aileron reversal speed
α	angle of attack or coefficient of thermal expansion
ω	frequency

ω_d	damping frequency
ω_F	flutter frequency
ω_n	undamped natural frequency
ω_α	undamped natural torsional frequency
σ	stress
σ_{ENG}	engineering stress
σ_{TR}	true stress
σ_u	ultimate stress
σ_y	yield stress
ϵ	strain
ϵ_{ENG}	engineering strain
ϵ_{TR}	true strain
γ	shear strain
μ	Poisson's ratio
δ	change in length
a	aileron deflection
ζ	damping ratio
ϕ	phase angle

12.3 AIRCRAFT STRUCTURAL MATERIALS

12.3.1 Introduction to Design

The primary responsibility of the engineer is the design, construction, and maintenance of structures and machinery, etc. In his function as a designer, he makes use of the principles of thermodynamics, electricity, and the statics and dynamics of solids and fluids, but he is ultimately limited by the materials at his disposal. In the past, design of a mechanism or system

has often been a function separate from the consideration of the material of which the mechanism was to be constructed. This process was adequate when there were a very limited number of materials available. Now, it is estimated that a designer must choose from as many as 75,000 alternative materials. In addition, the capability of designing specific materials for an application exists. This has a far reaching effect on the process of design; now the designer must consider from the outset the materials and fabrication techniques to be used.

Perhaps even more significant is the growing tendency toward development and use of metamorphic materials: those that change properties as the service environment changes. Some examples are metals that form metal oxide coatings in a corrosive environment and inhibit further corrosion, steels that are "self-healing" in order to prevent crack propagation, and polymers that are formed into final shape "in place." These materials demand a unified design approach that considers the material as a dynamic part of the system rather than passive and static.

Because of the intimate interaction between the part and the material, it is necessary that designers understand basic material properties and materials engineers understand the design process. At least, they must be able to communicate in a mutually comprehensible manner since they must work together throughout the design process. The purpose of this section is to briefly introduce the design process and some material properties of concern to the "designer." The design process is discussed first, then material properties, fabrication, and finally an example of their interaction.

12.3.2 The Design Process

The formulation of aircraft performance, size, and carriage requirements by using commands starts the design process. These requirements are carried through the acquisition process, modified through cost and current (and projected) state-of-the-art and off-the-shelf technology compromises. The end product of the acquisition cycle is the contractual specification that defines as specifically as possible the performance requirements the system must meet. It is this specification that dictates the design and the design process.

For a new development of an aircraft or weapon system, the definition of its mission dictates the design. While the iterations of the design cycle may

be similar among cargo, fighter, and heavy bomber aircraft, the tolerances, structural requirements, and size limitations differ widely. The typical flight profiles dictate the loads and mission load cycles to be considered by the structural designers. Wing and control surface sizes and locations are, in part, determined by the performance requirements, and these in turn influence the structural load paths to ensure proper margins of safety. Static and dynamic loads are analyzed according to the required flight characteristics and internal and external carriage requirements. Sizing, structural design, material selection, propulsion interface and support, avionics locations and functions, control system development, aerodynamic considerations, radar and IR signatures, and human factors engineering are analyzed, developed, coordinated, compromised, modified, and integrated through innumerable iterations. Each nut, bolt, washer, and rivet is analyzed and examined to ensure that critical load paths at worst case conditions exhibit satisfactory margins of safety under static and dynamic loadings. Figure 12.1 depicts a simplification of this process before any aluminum is formed, composite is wound, or fastener installed. The airframe design process, from an aerodynamic viewpoint, must also contain sufficient structure to permit landing and taxi loads.

Once the basic analyses have been completed and preliminary design has given way to initial fabrication, mock-ups are used as a tool to determine actual form and fit of hardware, avionics, control systems, oxygen and pressurization systems, ducting, hydraulics, and electrical routings. As this sizing progresses, structural components undergo load testing to determine the accuracy and fidelity of analyses and to update simulations. Fabrication leads to installation and integration, yielding structures that finally begin to look and feel like aircraft. Selection of materials is covered elsewhere in the chapter, but is a continuing process in design in an attempt to provide required shape, strength, size, and airflows at minimum weight. The design process continues through flight testing the entire system, improving on previous attempts to upgrade performance with minimum cost and weight.

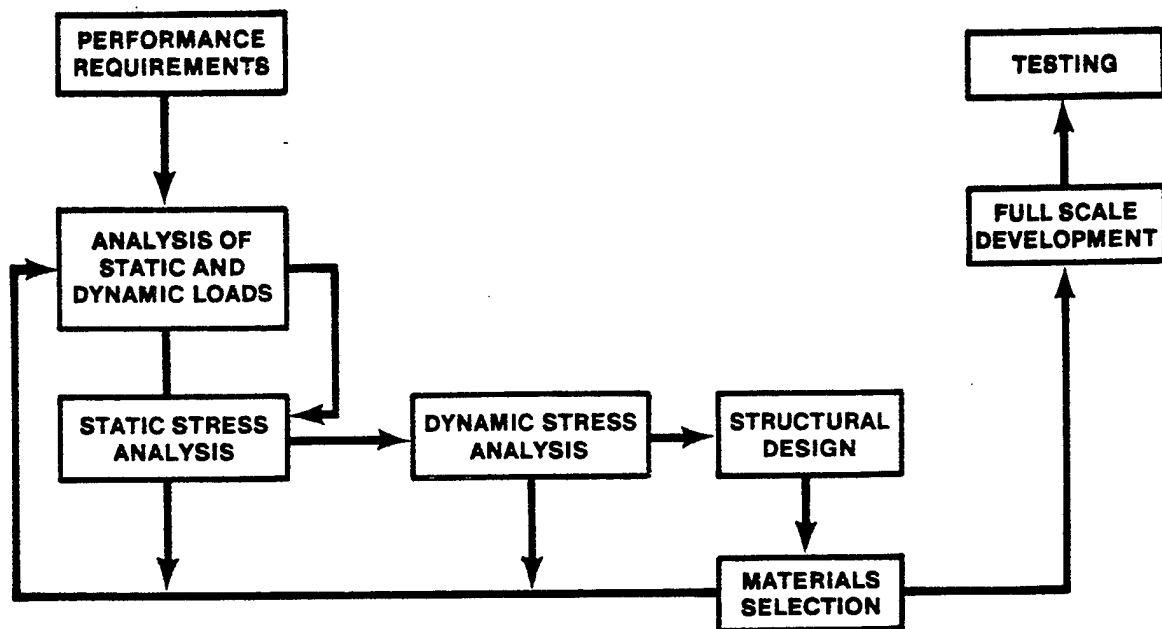


FIGURE 12.1. DESIGN PROCESS

12.3.3 Material Properties

The value of an engineering material is highly relative depending on the specific circumstances under which it is to be used. There are as many different materials suitable for a given design as there are different designs to accomplish a certain design goal. However, there is a "best" material for a certain design when a sufficient number of conditions are set for the material to meet.

There are a number of material properties that are basic in almost all engineering designs. For some applications, more than one property may be needed, such as high strength associated with good electrical conductivity and corrosion resistance. As more conditions are introduced, the selection narrows down. Obviously, an infinite number of conditions such as the three above can be set to finally limit the choice of available materials. Unfortunately, the ideal material for a particular application having a combination of optimum values for various properties does not always exist and a compromise is necessary at this stage to reach a definite decision. This is

only possible by understanding the properties which describe the character of the material.

Some of these properties will be discussed in more detail on the following pages. These properties are: mechanical, physical, chemical, thermal, electrical, and optical. In addition, availability, cost, fabrication techniques, reliability, and maintainability must be considered. Though not often thought of as material properties, they are usually based on a combination of properties, design, and economics.

12.3.3.1 Mechanical Properties. The mechanical properties of most concern at present are stiffness, strength, toughness, ductility, hardness, and fracture toughness. This discussion will treat only tensile loads, but the same analysis could be made for compressive and shear loads.

Stiffness. When stiffness is considered, there are two definitions that must be understood. The first is stiffness as it refers to the ratio of stress (σ) to strain (ϵ) in the elastic region of the stress-strain diagram shown in Figure 12.2. Stiffness in this sense is Young's Modulus (E); in torsion the analogous parameter is G , modulus of rigidity.

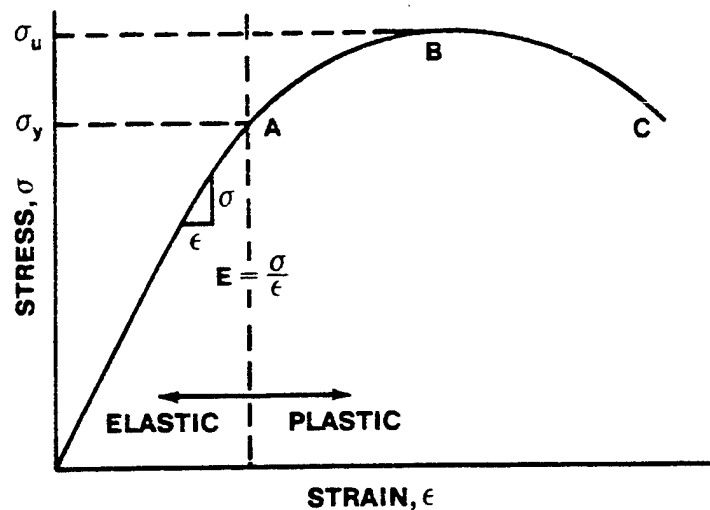


FIGURE 12.2. TYPICAL STRESS-STRAIN DIAGRAM

Stiffness (E) is closely related to the bonding between atoms in metals and ceramics and the bonding (number or type) between chains in polymers. For a given metal or ceramic, there is little that can be done to significantly change the value of E for the material. In the case of polymers, the value of E can be changed because interchain bonding can be varied.

Stiffness (E) is not necessarily related to the strength of a material which will be seen when strength is considered. Figure 12.3 shows what is meant by this statement. Material A has the highest E but the yield strength is less than for Material B which has a lower E . The meaning of yield strength will be discussed in the next section.

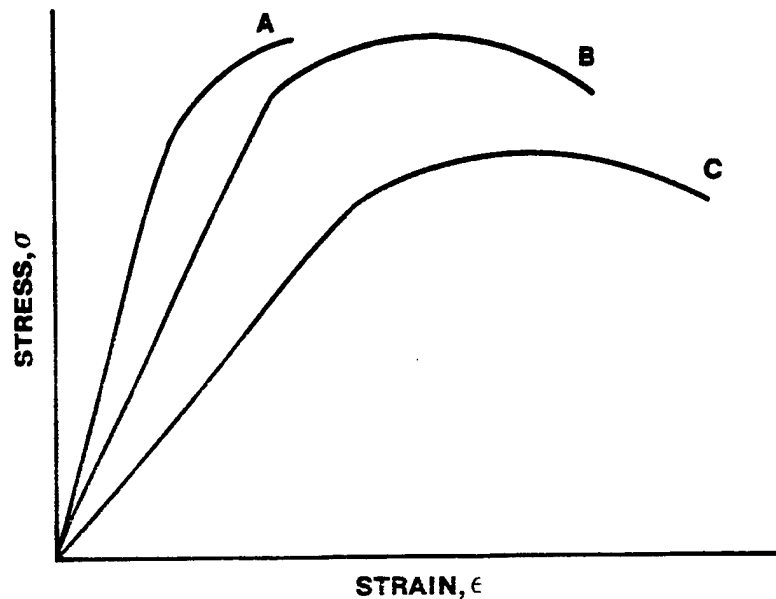


FIGURE 12.3. STRESS-STRAIN DIAGRAM, DIFFERENT MATERIALS

Strength. The strength of a material is a mechanical property of the material. It also depends on what the failure criteria are defined to be. There are several "strengths" depending on what constitutes failure: (1) yield strength (σ_y); (2) ultimate strength (σ_u); and (3) rupture or breaking strength. The common failure criteria are:

1. Excessive elastic deformation - related to σ_y since when stress is equal to σ_y , plastic deformation begins.

2. Excessive plastic deformation - an example of this is creep in jet engine turbine blades.
3. Fracture - separation of the material due to ductile or brittle fracture, fatigue, or creep. There are other failure criteria such as loss of appearance, which often must be considered. The three listed above are of major concern and will be developed further.

Strength data for a given material are usually obtained from simple tensile tests of standard specimens and are displayed on a stress-strain diagram as shown in Figure 12.2. Normally, materials display a region of elastic response and one of plastic response. The response is taken to be elastic (completely recoverable under ideal conditions) up to the yield strength (σ_y). Thereafter, the response is plastic, and the deformation is not completely recoverable when the load is removed - some permanent set being retained. The ultimate strength (σ_u) at Point B represents the ratio of the maximum load applied to the specimen to the original specimen's cross-sectional area (A_0). From Point B to C, the specimen continues to be loaded. However, the load is decreasing in magnitude and the cross-sectional area is decreasing. Consequently, the σ/ϵ curve decreases. Point C represents the complete separation of the material (fracture).

Figure 12.2 showed an engineering σ/ϵ curve in which all loads were divided by A_0 . Engineering stress (σ_{ENG}) is

$$\sigma_{ENG} = \frac{P}{A_0} \quad (12.1)$$

and engineering strain (ϵ_{ENG}) is given by

$$\epsilon_{ENG} = \frac{\delta}{l_0} = \frac{l_f - l_0}{l_0} \quad (12.2)$$

However, during the test, the cross-sectional area clearly decreases and the length increases. If instantaneous values of cross-sectional area (A_i) and length are used rather than the original values, true stress and strain (σ_{TR} , ϵ_{TR}) are obtained. These equations are

$$\sigma_{TR} = \frac{P}{A_i} \quad (12.3)$$

and

$$\epsilon_{TR} = \int_{l_0}^{l_f} \frac{dl}{l} = \ln \left(\frac{l_f}{l_0} \right) \quad (12.4)$$

but

$$l_f = l_0 + \delta,$$

so ϵ_{ENG} and ϵ_{TR} can be related by

$$\epsilon_{TR} = \ln (1 + \epsilon_{ENG})$$

Figure 12.4 shows a comparison of true and engineering stress-strain diagrams. The true σ/ϵ curve continues to increase even after the load decreases because the instantaneous cross-sectional area (A_i) is decreasing at a faster rate due to necking of the specimen. This discussion will consider engineering stress and strain since the engineer is concerned with the original areas, lengths, etc., in the design phase.

Materials are often characterized as ductile or brittle depending on the extent of their plastic behavior. Figure 12.5 shows hypothetical materials of varying ductility. Material A is entirely brittle and fractures while still responding elastically. Ceramics display this type of behavior. Material B undergoes some plastic deformation before fracture and is characterized as being ductile. The strain in the plastic region of the σ/ϵ curve is a measure of the ductility of the material. If the material is greatly strained before fracture, the material is considered to be ductile. Ductile and brittle are relative terms; thus, Material B is ductile relative to Material A and brittle relative to Material C. There are three additional mechanical properties of great concern that are related to ductility: hardness, toughness, and fracture toughness.

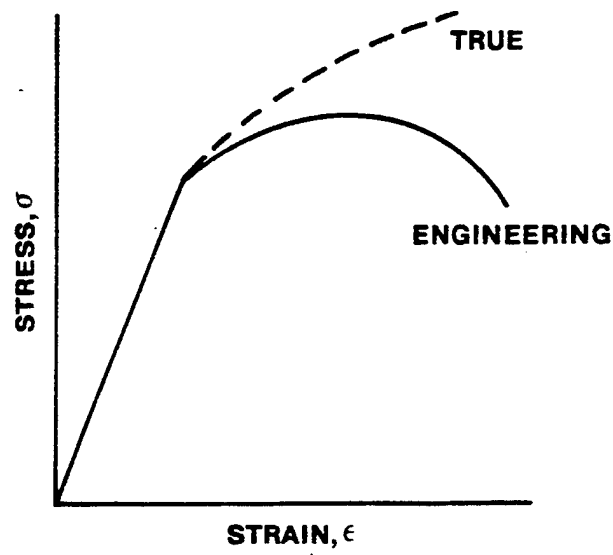


FIGURE 12.4. COMPARISON OF TRUE AND ENGINEERING STRESS-STRAIN DIAGRAM

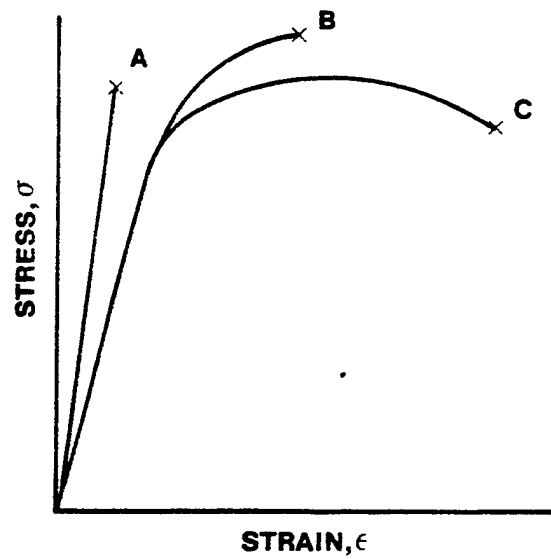


FIGURE 12.5. EFFECT OF DUCTILITY ON STRESS-STRAIN CHARACTERISTICS

Hardness. There are a number of ways to measure the hardness of a material: abrasion, rebound, cutting, indentation, etc. The most common method for metals is by indentation. Penetrators of specified geometry and material are forced into the metal by known loads and the depth of penetration measured. The depth of penetration is then a measure of the metal's hardness. Since the penetrator is forced into the metal, the metal is plastically deformed indicating that hardness and ductility are directly related. If the material is ductile, it can be easily deformed plastically and consequently is soft. If the material is brittle, it cannot be easily deformed plastically and is therefore a hard material. Hardness, then, is a measure of the resistance of a material to indentation.

For many metals (particularly steels), there is a direct relationship between the hardness and the ultimate or tensile strength of the material. The approximate relationship for carbon and low alloy steels is

$$\sigma_u = 480 \text{ (BHN)} \quad (12.6)$$

where BHN is the Brinell Hardness Number - the result of a Brinell Hardness Test. Other hardness numbers could be obtained from Rockwell or Vickers Hardness Tests and then related to the BHN.

Toughness. Toughness is a measure of the ability of a material to absorb energy in the plastic range. One way to measure toughness would be by using the area under the σ/ϵ diagram. Thus, in Figure 12.5, Material C would have to be the toughest and Material A the least tough.

In the elastic range, there is a property related to toughness which is called resilience. Resilience is a measure of the capacity to absorb energy in the elastic range and is the area under the elastic portion of the σ/ϵ curve. Resilience is important when considering such things as leaf springs for automobiles. The material must always operate within the elastic range and absorb energy in that range.

There are other properties of importance such as electrical, thermal, magnetic, optical, chemical, and physical. Only electrical, thermal, and chemical properties will be briefly mentioned here.

12.3.3.2 Electrical. Some materials are conductors and others insulators; semiconductors fall in between. The electrical conductivity of a material

depends on the type of bonding. If the valence electrons are bound as they are in ionic and covalent bonding, then the material is an insulator. If the valence electrons are free to move as in the metallic bond, the material is a conductor. At very high temperatures the ions in ceramics may become electrical conductors.

12.3.3.3 Thermal. Thermal conductivity and the coefficient of thermal expansion are also related to bonding. Thermal conductivity requires that electrons be free to move so the same materials that conduct electricity are normally thermal conductors. Those that are electrical insulators are thermal insulators. The coefficient of thermal expansion (α) is inversely related to the strength of the atomic bonds. Therefore, as bond strength increases, α decreases. Many designs are subjected to a thermal environment, and thermal stresses are set up that result in failure of the part. Another thermal effect is creep or accelerated plastic deformation that only becomes a problem at about one-half the material's melting point on an absolute scale.

12.3.3.4 Chemical. Chemical properties, as used here, refer to the corrosion and oxidation properties of the material.

12.3.4 Conclusion

The design process is a rather long and exhaustive process because of the great number of factors to be considered and the interplay of mechanics and materials. Good design is possible only if the designer is familiar with materials and every materials engineer is familiar with the design process.

12.3.5 Composite Materials

12.3.5.1 Introduction to Composite Materials. Early man had a variety of natural materials such as wood, clay, stone, copper, and iron available. Although he did not understand the basis for a material's behavior, he selected materials that met his needs. The early Egyptians are an example of men who, not having a natural material available to meet their needs, combined two materials to form a composite that overcame their limitations. They combined mud with straw to produce reinforced bricks which they used to build their cities.

This cycle continues and even more so in today's highly technological world. Design ideas limited by materials lead to the development of new, more advanced materials. The need for higher performance materials to overcome present design limitations has created a new class of materials called composites. A composite material is a combination of two or more constituents from the three general classifications of materials: metals, ceramics and/or polymers. Composite materials were created to provide materials with improved mechanical properties such as stiffness, strength, and high temperature stability. The development of composite materials is a revolutionary advancement in materials technology. Until recently, materials selection was a substitution affair where the question was, "What material can I use in place of alloy X?" The material selection was often a secondary decision that did not influence the design. A composite material allows the materials engineer to incorporate the required properties which greatly affect the design and should be considered early in the preliminary design phase.

The importance of composites becomes clear if one examines material properties on a density-corrected basis. Table 12.1 illustrates this fact by comparing mechanical properties (density corrected) to show the specific properties. It is apparent that very little flexibility in material selection actually exists for conventional materials. Composite materials combine a reinforcing material with high specific strength and specific stiffness with a low density matrix material that results in a system that is synergistic (properties of the whole are greater than the sum of the individual constituents).

These materials are especially useful in aerospace applications where weight is an extremely important and driving design parameter. Development of composites has been primarily financed by research and development in the aerospace industry conducted by both private industry and government. A large variety of laminated composite structures have been designed and flight tested. A large number of materials can be classified as composite materials; however, this chapter will be confined to the more advanced fiber reinforced composites that utilize continuous and discontinuous fibers as the reinforcement material.

TABLE 12.1

MECHANICAL PROPERTIES

<u>Materials</u>	<u>ρ (lb/in³)</u>	<u>E (psix10⁶)</u>	<u>E/ρ (inx10³)</u>	<u>TS (psix10³)</u>	<u>Ductility %</u>
Steel (Hot Rolled) (Metal)	.283	30	105	65	30
Steel (Cold Rolled) (Metal)	.283	30	105	85	20
Aluminum (Metal)	.100	10	100	63	7
Titanium (Metal)	.165	17	103	165	15
Beryllium (Metal)	.067	42	625	83	16
Pine Wood (Polymar)	.0145	1.3	90	7	--
Silica Glass (Ceramic)	.079	10	126	--	--
Graphite Whiskers	.060	102	1700	2845	--
Boron/w Wire	.095	55	580	400	--
Boron Epoxy (Composite)	.075	20	270	133	--

12.3.5.2 Continuous Fiber Reinforcement Materials. A composite material is composed of two basic components - a reinforcing fiber which is surrounded by a soft light-weight matrix. The majority of advanced composite materials utilize continuous fiber reinforced materials fabricated from ceramics and metals. The fiber must have a high specific strength to carry the load in the composite structure and a high specific stiffness to supply the required structural rigidity. Designs require the fibers to be uniformly aligned to maximize the contribution of fiber strength properties to the composite structure. Ideally, the fiber axis should be aligned parallel to the maximum

loading axis of the structure. Since a single row of fibers is called a lamina (Figure 12.6) and one must stack up lamina in a sequence to form a laminated structure (Figure 12.7) where the fiber orientation can be varied, the materials engineer can design in a wide variety of material properties. Another benefit the fiber offers is that it will prevent crack propagation through the matrix.

The strength and stiffness requirements for fibers limits the material selection primarily to ceramics and metals. Table 12.2 shows the primary materials being investigated; for metals, boron, tungsten and steel are the most promising. For ceramics, graphite, glass and silicon carbide hold great promise. Boron fibers are the most versatile metal fibers. Research and development have concentrated on these fibers. Tungsten and steel are of interest for high temperature applications. Graphite is the most attractive ceramic fiber and it can be made into a variety of fiber shapes and lengths. Its primary disadvantage is cost. Glass is cheaper by comparison and does have some very attractive properties; however, it requires special surface coating protections called sizes to protect the fiber from degradation by the environment and from handling during manufacture. Ceramic fibers exhibit the greatest strengths and are very stable, but they can be difficult to bond and usually require a coating to promote better interfacial bonding. The metals tend to exhibit lower strengths but are easier to bond. However, interfacial reactions can degrade the fiber properties.

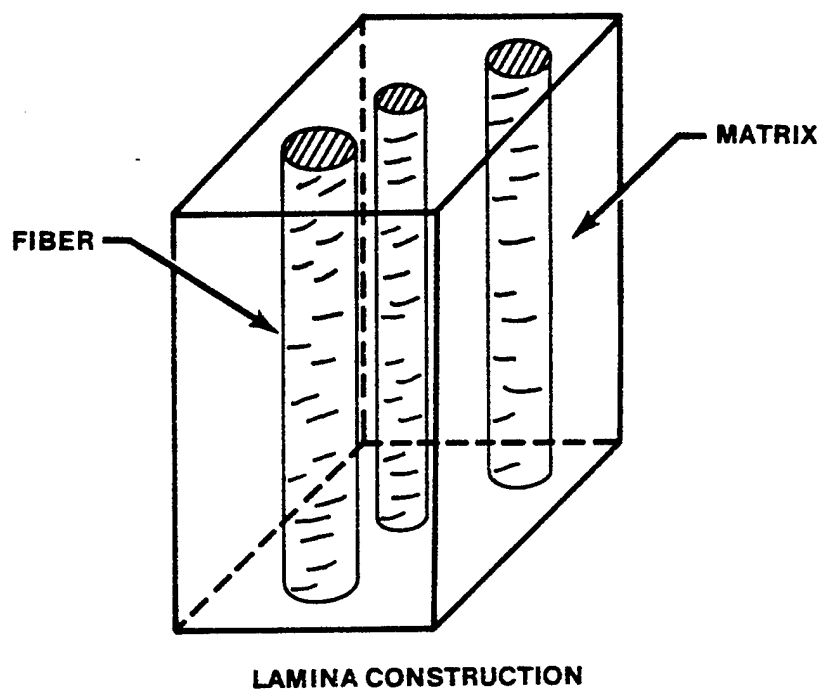


FIGURE 12.6.

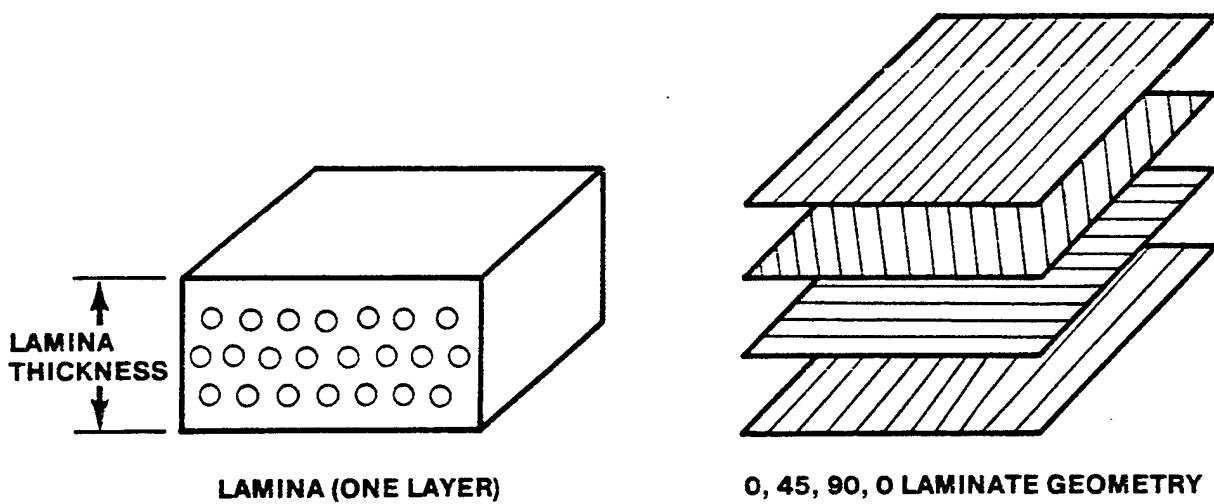


FIGURE 12.7. LAMINATED STRUCTURE

TABLE 12.2

PROPERTIES OF FIBER AND MATRIX MATERIALS

	<u>Melt Point</u>	<u>Density</u>	<u>Tensile St.</u>	<u>Strength</u>	<u>E</u>	<u>Modulus</u>
	(°F)	(lb/in ³)	(Ksi)	Density (x10 ⁶)	(x10 ⁶ Psi)	Density (x10 ⁷ in)
AMORPHOUS FIBERS						
S-Glass	1540	.090	650	7.2	12.6	14.0
SiO ₂	3020	.079	850	10.8	10.5	13.3
DISCONTINUOUS FIBERS (SINGLE CRYSTAL)						
Al ₂ O ₃	3700	.143	3000	21.4	62	43.4
SiC	4870	.116	3000	26.1	70	60.8
Graphite	6600	.060	2845	47.4	102	170
POLYCRYSTALLINE FIBERS						
Al ₂ O ₃	3700	.144	300	2.6	25	21.9
Graphite	6600	.054	200	3.7	30	56.5
Tungsten	6150	.697	580	.8	59	8.5
Steel	2550	.280	600	2.1	29	10.3
MULTIPHASE FIBERS						
Boron/W	4170	.095	400	4.2	55	57.8
SiC/W	4870	.148	300	2.0	70	43.3

Cont.			Tensile	
Use Tem. (°C)	<u>Elongation (%)</u>	<u>Strength (Ksi)</u>	<u>Modulus (x10⁶ Psi)</u>	

MATRIX MATERIALS

Polycarbonate	120	80	9	.34
Polysulfone	150	50	10	.36
Epoxy-BPA	145	4.8	13	.36
Epoxy-CA	150	3.5	19	.78
Phenolic	160	2	9	.45

The fibers can exhibit a variety of crystalline structures which affect their properties. Single crystal discontinuous fibers are of an order of magnitude stronger than all the other fibers; however, they are microscopically small and difficult to fabricate. Polycrystalline fibers have lower strengths due to the imperfections present in the larger fibers. Amorphous fibers are strong but highly susceptible to damage and degradation.

There are a variety of manufacturing processes used to fabricate reinforcement fibers. Glass fibers are typically prepared by making the material molten and then extruding it through small orifices ($\approx .005$ inch) which removes water. The fibers are fired at a temperature to densify. Metal fibers are made using the wire drawing process; however, to reduce the fiber down to .005 inch requires diamond dies which are very expensive. There are other processes such as electromechanical, liquid metal, vapor deposition, and numerous proprietary processes.

The fabrication of boron fibers is very interesting and unique. A tungsten wire .005 inch in diameter is passed through a long glass tube that contains boron gas such as boron trichloride (BCl_3). Pressure is maintained in the tubes to force the boron to deposit on the tungsten filament which is heated electrically. The entire process takes less than two minutes and produces a filament between .003" - .005" in diameter. The time can be adjusted to yield other diameters but .008 inch is presently the upper limit. The fibers are usually produced in continuous lengths of 10,000 feet. The only supplier of boron fibers in quantity is the AVCO Corporation in Lowell, Massachusetts. One advantage of composite fibers is that they can be processed by winding around mandrels. They are then woven into two-dimensional cloths and three-dimensional mats that are then impregnated with the matrix. This process can be a definite advantage in producing complex shapes.

12.3.5.3 Matrix Materials. The second basic component material is the binding or matrix material. The fibers carry load and give structural rigidity. The matrix material bonds the fibers and holds them in a specific alignment. It transfers loads through shear mechanisms to the fibers. The matrix material must be light weight so that the benefits of the specific

strength and specific stiffness are not depleted. Similarly, a soft ductile material will assure full fiber strength is utilized and provide good plastic behavior for transferring load by shear mechanisms. The matrix also serves to protect the fibers from the environment which may tend to attack the fibers and degrade properties. This is especially true of glass fibers. The matrix will arrest crack propagation occurring in fibers since it acts as a foreign material interface and will deflect the cracks. Other properties the matrix can contribute include toughness, fatigue strength, oxidation resistance, corrosion resistance, etc. The matrix material requirements have limited selection to polymers and metals. Polymers such as epoxies, phenolics, and polysulfones, and metals such as titanium and aluminum possess the lower strength/high ductility behavior that is necessary in a matrix. Epoxies and aluminum have been extensively researched and most components that are flying on aircraft or are in the development stages are made from these matrices. The phenolics and titanium are still in their early stages but hold great promise for higher temperature applications. Unlike fibers, these materials can usually be fabricated using conventional techniques already established which reduce costs. The polymers are temperature limited, can be sensitive to humidity, and possess a wide variation in properties such as chemical and corrosion resistance. Important considerations in design are the stresses and life expectancies required of these matrix materials. These polymers also exhibit shrinkage which must be accounted for in the processing since it can be as great as 15%. Typical matrix properties are shown in Table 12.2.

12.3.5.4 Manufacturing of Composite Materials. Careful consideration must be given to the decision concerning which fiber to combine with which matrix to yield the optimum design. All design parameters must be considered in order for the materials engineer to design in the required properties. This further requires that material selection and assessment be made early in the preliminary design phase.

Regardless of the selection of fiber and matrix, they both must be properly bonded together. The bonding surface between fiber and matrix is called the interfacial bond, and it has an enormous effect upon composite material properties and fabrication. The metallurgical reactions that occur

are complicated and difficult to control. Poor bonding at the interface results in premature failures. The fiber shape is also important. The greater the surface area available for bonding, the better the bonding will be. Thus, non-circular cross sections promote superior bonding.

There are a number of techniques employed to control interfacial reaction zones to limit property degradation while promoting good bonding. The ceramics tend to be thermodynamically stable and show smaller reaction zones. They do not, however, bond as well to the matrix and therefore require a coating such as polymeric or metallic coating. These coatings are especially required in metal matrix composites. When boron was initially used, it often had to be coated with silicon carbide to bond it with aluminum and titanium. Advances in composite technology and fiber treatment have eliminated these requirements.

Interface reactions result in the destruction of the fiber. The three most prevalent reactions that occur include diffusion between fiber and matrix which can leave a penetration zone with recrystallization that causes premature failure of the fibers. In addition, precipitation reactions and/or solid solution reactions can produce fracture initiation sites leading to failure.

A variety of manufacturing processes are utilized that allow the designer latitudes which conventional materials do not possess. The fibers can be wound around a mandrel and then impregnated with the resin matrix material or a "prepreg" (partially cured) composite can be wound on a mandrel. The "prepreg" composite is often used to allow forming of lamina into desired shapes and then using a mold under heat and pressure to produce final curing. The metal matrix composites can be handled in this same manner. Often, large sheets of composite material are precut into ply patterns which are hand-assembled and then finish processed. Composites can be woven into two-dimensional and three-dimensional shapes which are then impregnated with the matrix and cured. This type of fabrication gives the designer tremendous capabilities that otherwise would not be available.

12.3.5.5 Design Applications. As composites become more common, it is necessary for engineers accustomed to dealing with metals to become more versatile in their thinking. The various properties of metals are generally

considered to be isotropic - the same in all directions. The design trade-offs mentioned earlier are thus fairly straightforward. It is common when dealing with metals to consider such properties as modulus, E, as constants. This, in fact, is not the case with composite materials. Composites are anisotropic; that is, having different strength, stiffness and thermal properties in the various directions. This produces an added complexity for the designer but also provides him with more flexibility and a chance to truly optimize a structure. If the designer fully understands the anisotropic nature of a material, he is able to design the material to meet the specific design requirements (strength, stiffness, etc.) of his structure in its specific directions. This, of course, forces the designer to analyze the strengths and stiffnesses required in his structure based upon such factors as the expected loads and allowable deflections. Since structures are often loaded in only one or two directions, a composite can be made strong in those directions. This can be compared with fabricating steel or aluminum where, in order to meet a maximum strength requirement in one direction, the material, because of its basic nature, is equally strong in other directions. It can thus be seen that a composite can be used more efficiently and produce a second weight savings in addition to the one inherent in its high strength-to-weight or stiffness-to-weight ratios.

12.3.5.6 Economic Factors. Composite materials have gained a reputation for being expensive. To some extent, this reputation is deserved. As graphite and boron filaments were first being developed in the 1960's, costs of \$600 per pound and \$400 per pound, respectively, were common. With increased production, these costs are now on the order of \$100 per pound for boron and \$50 per pound for graphite, which still does not favorably compare with a few dollars per pound for steel. However, the cost to be considered is not the material cost but the cost of the finished product or the dollars per payload of the final system.

The cost of compositing includes the tape fabrication, laying the tape into layers and the final assembly of the part including its joining to other parts of the structure. Metal parts, of course, have forming and machine costs associated with them. The Navy built a composite wing for a Target Drone using graphite epoxy. While the material costs were higher than the

aluminum it replaced, the manufacturing steps in fabricating the wing were reduced from approximately 50 for the aluminum to 3 for the graphite. The savings resulting from this are quite obvious.

C.E. Cataldo, in an article on the use of composites for the space shuttle, estimates that composites can save 5-9% of the structural weight of approximately 200,000 pounds. This savings of 10,000-18,000 pounds, when compared to the original payload of 25,000-65,000 pounds, produces a payload increase of up to 40%. The cost savings resulting from this are so huge that they overshadow any material costs.

12.3.5.7 Analysis of Composite Materials. A technique used to determine the properties of a composite is based upon the volume fraction of its constituents. This rule of mixtures is illustrated in the following paragraphs.

If we stipulate that the fibers are uniformly aligned, as shown in Figure 12.7, and that a perfect bond exists between the fiber and matrix, then the strain is the same for the composite, the matrix, and the fiber

$$\epsilon_c = \epsilon_f = \epsilon_m$$

The total load in the composite will be the sum of the loads carried by the fiber and the matrix.

$$P_c = P_f + P_m$$

Utilizing the axial stress relationship and solving for P, the equation can be rearranged as follows

$$\sigma = \frac{P}{A} \quad \therefore P = \sigma A$$

$$\sigma_c A_c = \sigma_f A_f + \sigma_m A_m$$

Dividing by the area of the composite and noting it is equivalent to the sum of the areas of the fiber and matrix yields

$$\sigma_c = V_f \sigma_f + V_m \sigma_m \quad (12.7)$$

where V_f and V_m are volume fractions. Note $V_f + V_m = 1$. Dividing by the strain yields

$$E_c = V_f E_f + V_m E_m \quad (12.8)$$

EXAMPLE: Design a composite material with a modulus of elasticity of 11 GPa and a yield strength of 160 MPa. The properties of the fiber and matrix are shown below and have been measured for the limiting strain.

$$E_f = 14. \text{ GPa}$$

$$E_m = 7. \text{ GPa}$$

$$\sigma_f = 210. \text{ MPa}$$

$$\sigma_m = 105. \text{ MPa}$$

$$@ \epsilon_f = .015 \text{ m/m}$$

$$@ \epsilon_m = .015 \text{ m/m}$$

Consider both equations

$$a. \quad \sigma_c = V_f \sigma_f + V_m \sigma_m$$

$$b. \quad E_c = V_f E_f + V_m E_m$$

$$160 = 210 (V_f) + 150 (V_m)$$

$$11 = 14 (V_f) + 7 (V_m)$$

$$\text{Note: } V_m = 1 - V_f$$

$$160 = 210 (V_f) + 150 (1 - V_f)$$

$$11 = 14 (V_f) + 7 (1 - V_f)$$

$$V_{f_\sigma} = 0.524$$

$$V_{f_\sigma} = 0.571$$

Notice there are two answers and in order to meet both design requirements you must choose the largest value where the volume fraction of fibers would be 57.1%.

This type of analysis is often applied to composites and is adequate for properties such as density and certain mechanical properties such as the longitudinal stiffness. Note, however, that this relation says that the properties of a composite are bounded by those of its constituents.

As mentioned earlier, a simple analysis such as the rule of mixtures or ideas that one might be comfortable with in dealing with metals is not adequate in the analysis and design of composite structures. Since the mathematics of anisotropic elasticity and of composite laminate analysis are beyond the level of this course, this chapter will simply present an overview of some of the techniques used.

There are more steps with more complexity in the design of a structural composite than exist in the design of metal structures. The design cycle starting with the fiber and matrix constituents are illustrated in Figure 12.8. Note that this cycle is continuous. This implies that the material's design must be simultaneous with the structure's design. The final objective of the design process is, of course, to achieve an optimum structure. This can often be translated into minimum weight.

The design cycle shown in Figure 12.8 combines two basic approaches which have been labeled microscopic and macroscopic. The microscopic approach considers the mechanical and physical characteristics of possible fiber and matrix materials. These properties are normally considered to be isotropic; however, the structure as a whole is heterogeneous (non-homogeneous). Using various assumptions concerning the state of stress and strain between the fiber and matrix, the designer must select the proper constituent materials and decide upon the packing arrangement of the fibers and their proper volume fraction. As seen in Figure 12.9, the properties of the unidirectional laminate depend upon this microscopic analysis of the constituents. The reason the laminate or single layer of composite is made of fibers all oriented in one direction is that this allows ease of manufacture and analysis.

The next step is to determine the mechanical and physical characteristics of the building block laminate. This involves what is called a macroscopic

analysis. Here, the matrix and fiber are considered smeared together to form a homogenous but anisotropic material for analysis purposes. Such a procedure is advantageous since existing plate and shell theories can be applied to the analysis of these thin homogeneous anisotropic laminatae.

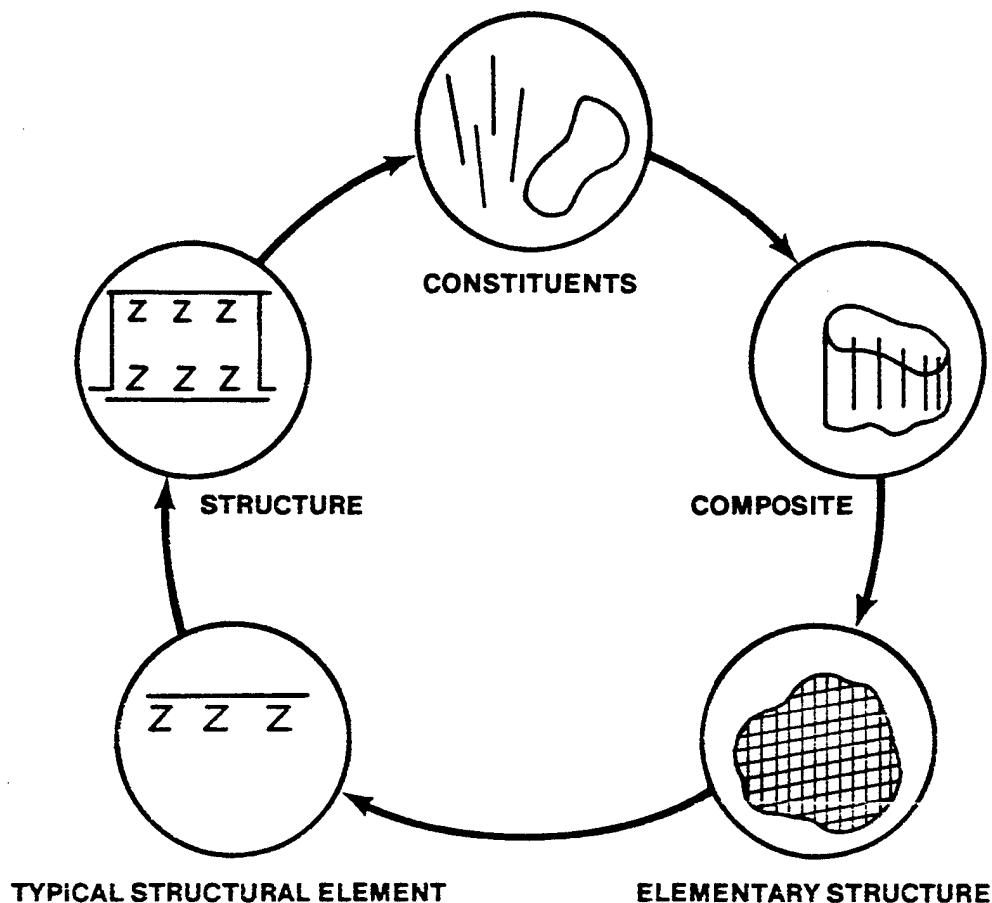


FIGURE 12.8. COMPOSITE STRUCTURAL DESIGN AND ANALYSIS CYCLE

Laminate analysis involves determining the optimum number and orientation of the lamina necessary to provide the desired properties. Presently there is not a unique mathematical solution to this problem and the combination of computer iteration and experience guides the designer to a final laminate arrangement. An arrangement of 0, 45, 90, 0 for a four-ply structure is illustrated in Figure 12.7. Usually the optimization procedure produces

angles which might be difficult to manufacture; thus, it is common to change a calculated 0, 39, 87, +5 arrangement to the 0, 45, 90, 0 mentioned earlier for ease and economy of manufacture.

The final result of this analysis is a structure of lower cost, improved maintainability and increased performance. Table 12.3 shows some of the current applications of composites. During development, the aerospace industry tested composites in non-critical structures such as doors in the F-111 and in the wing of a Navy Target Drone. The use of materials and fabrication techniques previously untried was often done to the reluctance of both designers and users. Today, however, such materials are seeing use in primary aircraft structures such as the longitudinal spine of the B-1 and horizontal and vertical stabilizer sections of the F-15.

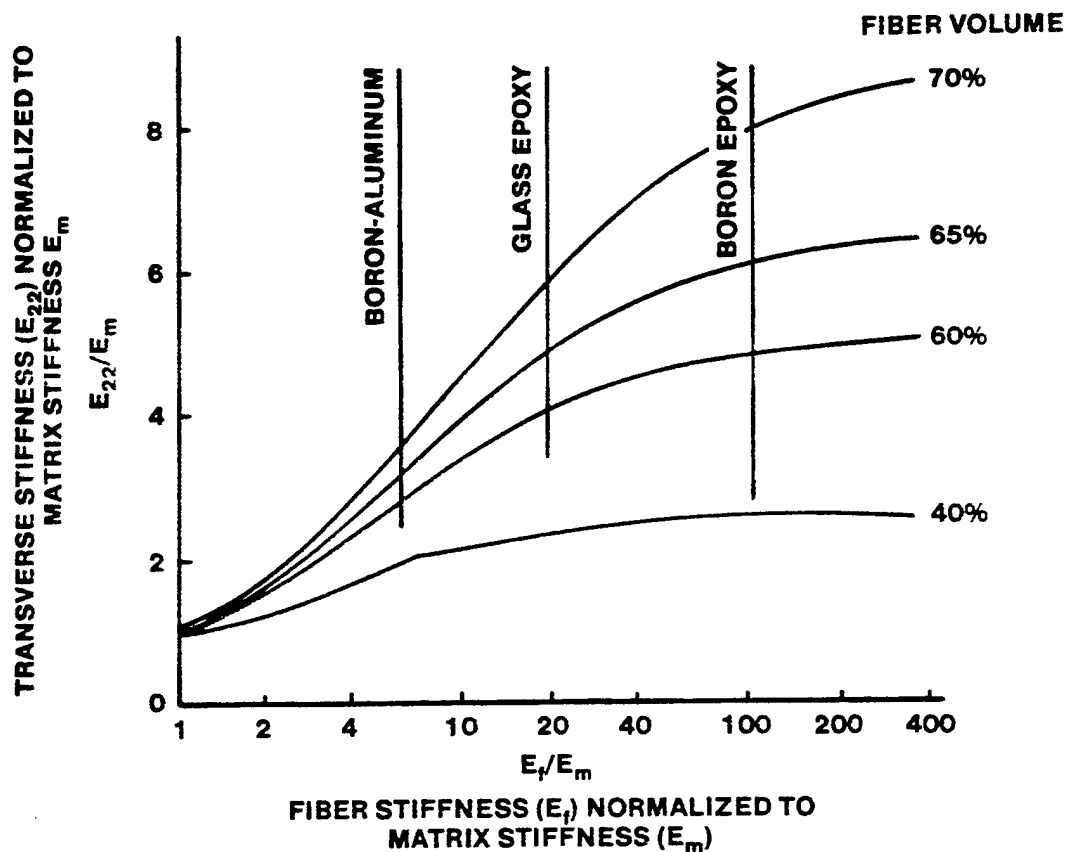


FIGURE 12.9. TRANSVERSE STIFFNESS IN UNIDIRECTIONAL LAMINATE

12.3.5.8 Discontinuous Fiber Reinforcement Materials. There are various types of discontinuous fiber reinforcement materials. In this paragraph, glass, whisker formation, and binary eutectic fiber reinforced composites will

be discussed. The discontinuous glass fiber reinforced composites are the most widely used composites in industry today. The primary advantages of these composite systems are in their manufacture. They utilize the technology applied to the polymeric and textile industries. This eliminates the need to make large capital investments in exotic manufacturing equipment. In addition, the fabrication of the glass fibers and polymeric matrices are well established and inexpensive. The glass can be chopped into fibers and randomly distributed throughout the matrix giving three-dimensional stiffening and strengthening. The procedure consists of mixing a polymeric with glass fibers and using conventional injection molding techniques to produce fiberglass types of structures. The fibers can be chopped up and blown into a meshed structure with a matrix added to form a "prepreg" that can be final cured into a finished product. The glass fibers can be woven into mats and impregnated with resin to form a continuous fiber reinforced composite. There are many epoxy and phenolic resins that can be used with the chopped fibers but these composites do not exhibit high strength levels. They are used for corrosion resistance, light weight, low cost manufacturing, optical properties, etc.

It is obvious from Table 12.2 that the single crystal whiskers possess an order of magnitude greater properties over the polycrystalline, amorphous and multiphase fibers. These whiskers are free from defects and dislocations, and their properties approach theoretical values. The obvious question is, "Why aren't these composite fibers being used throughout the industry?" The answer is technically complicated but economically simple. The whiskers are only 100-200 microns long which is the reason they can be fabricated defect-free. But they are also difficult to bond to the matrix and infinitely more difficult to align. The handling and fabrication of these whiskers requires expensive and sophisticated equipment. Economically they are impractical. A typical example is silicon carbide whiskers. They are grown using a sublimation technique that involves the prolysis of organosilanes, silicon compounds, and hydrocarbons in a hydrogen atmosphere at 1500-2000°C. Graphite can be formed into scroll-type fibers by combining sublimation techniques with DC arcing under high pressure in an inert atmosphere. Other techniques use evaporation and vapor-liquid-solid deposition processes, but all are prohibitively expensive.

TABLE 12.3

COMPOSITE APPLICATIONS AND DEVELOPMENT

SPACE SHUTTLE APPLICATIONS

<u>Thrust Structure</u>	<u>Fuselage</u>	<u>Bulkheads</u>	<u>Tanks</u>	<u>Hot Structure</u>	<u>Shrouds</u>
<u>SKINS</u>					
Boron-Epoxy	Ring Frames Longerons Stringers Skins Beams Fittings	Glass-Epoxy	Glass-Filament Wound with Liners	Carbon-Carbon	Boron-Epoxy
Boron-Alum.		Graphite Epoxy		Graphite Coated	Boron-Alum.
Graphite-Epoxy					Graphite Epoxy
					Glass-Honeycomb
<u>BEAMS</u>			Graphite-Epoxy for small tanks	Boron-Polyimide 650°	
Same				Graphite-Polyimide 650°	
	Boron-Epoxy			Boron-Alum. 600°	
	Boron-Alum				
<u>STRUTS</u>	Graphite-Epoxy			Metal-Metal 2000-2500°	
Same	Glass-Epoxy				
				Borsic-Ti 800°	

TABLE 12.3 (continued)
COMPOSITE APPLICATIONS AND DEVELOPMENT

DEVELOPMENT STATUS

<u>Current Developments</u> (Near Term Payoff)	<u>Advanced Development</u> (Long-Term Payoff)	<u>Future Development</u> (New Concepts-New Materials)
Boron-Epoxy	Boron-Polyimide Graphite-Polyimide	In-Situ Reinforcements
Graphite-Epoxy	Wire Reinforced Metals	
Boron-Aluminum	Graphite-Aluminum	High Temperature Polymers
Carbon-Carbon	Beryllium Composites	Low Cost High Speed Production
	Hybrids	Advanced Hybrids

COMPOSITE TEMPERATURE CAPABILITIES

Maximum Temperature Capabilities

<u>Polymer Matrices</u>	<u>Temperature (⁰F)</u>	<u>Metal Matrices</u>
S-Glass/Epoxy		
Boron/Epoxy	350*	
Graphite/Epoxy		
Graphite/Polyimide	600	Boron/Aluminum
	650	Graphite/Aluminum
	700	
	800	Borsic/Titanium
Carbon/Carbon	1000	Beryllium/Titanium
Carbon/Carbon (Uncoated)	1800	Borsic/Nickel
		Wire/Superalloys
Carbon/Carbon (Anti-Oxidant)	2400	Molybdenum/Columbium Tantalum

* Assuming Stable Core

The binary eutectic system offers the only real viable alternative to this problem which is available with today's technology. A binary eutectic occurs when a liquid transforms into a two-phase solid at constant temperature. The reaction is invariant and occurs only at a specific composition and a specific temperature. It is a specific point on the phase diagram. It should be noted that not all binary systems will exhibit this phenomenon and of those that do, not all can be controlled to produce an aligned microstructure.

The directional solidification (DS) of the eutectic is the key processing parameter. It is the directional cooling which permits the alignment of the whisker fibers within the matrix material. Controlling the cooling gradient by slowly withdrawing molten material from the furnace orients the fiber growth direction parallel to the uniaxial heat flow. The fiber and matrix materials freeze into a solid solution forming a discontinuous fiber reinforced composite material in one step. The growth rates, however, are only about a quarter of an inch per hour which means the manufacturing costs are quite high. The primary application of interest is in the turbine of an aircraft engine. The enormous property increases gained and the potential engine performance improvements justify the high manufacturing costs. The eutectic system receiving the most attention is the tantalum carbide fiber in a nickel base super alloy or cobalt based alloy. There are many shapes the fiber can take; however, it has been shown that rods or platelets give the best properties. These alloys are very stable. They compete with conventional alloys at room temperature but are vastly superior at high temperatures. Their properties do not degrade even at levels close to their melting point. Since the whiskers grow naturally within the matrix, there are no bonding problems. Experiments conducted on the interfacial bond strength show it is stronger than the fiber itself. This is probably due to the unique matching of preferred crystallographic planes that occur during processing. Figure 12.10 center shows a DS turbine blade. The DS blade's composite structure is compared to other forming techniques -- a conventional casting left and a single crystal turbine blade right.

A low volume fraction of fiber will give a rod-like reinforcement structure, whereas near equal fractions of matrix and fibers produce a

platelet structure. The rod fibers are superior and more predictable; however, they only supply uniaxial strengthening. The platelets have a two-dimensional strengthening effect. In addition, studies on solute atoms, dislocation mobility, temperature, strength and plastic properties show that intermetallic compounds make better fibers than do ceramics or metals. These materials offer great advancements to aircraft and engine performance.

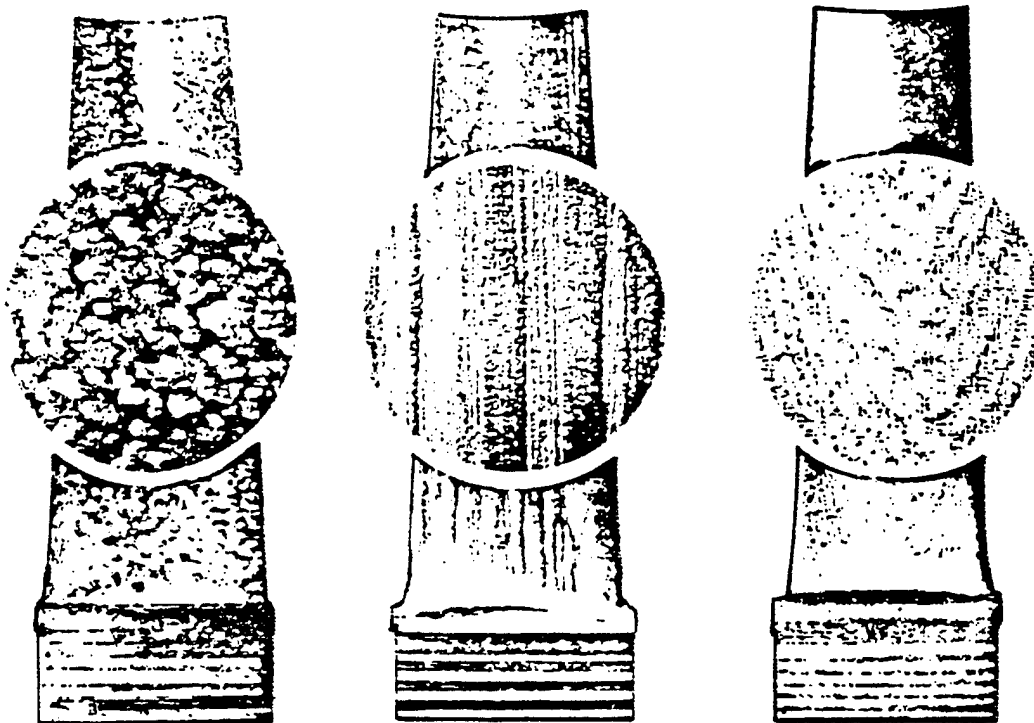


FIGURE 12.10. MICROSTRUCTURE OF CONVENTIONALLY CAST (LEFT),
DIRECTIONALLY SOLIDIFIED (CENTER) AND SINGLE
CRYSTAL (RIGHT) TURBINE BLADES

12.3.5.9 GLOSSARY

Fiber - Reinforcing component of the composite that supplies the strength and stiffness properties.

Matrix - Soft light-weight bonding component of the composite that holds the fibers.

Lamina - A single layer of fibers surrounded by matrix material.

Laminate - A structure build up using lamina at various orientations to yield a structural element.

Prepreg - A partially cured composite laminate that is pliable and can be shaped and then finish cured.

Interfacial Bond - Surface bond between the fiber and the matrix.

Eutectic Composite - A two-phase solid where one phase acts as fiber reinforcement and the second phase is the matrix.

Whisker - A small single crystal fiber that is defect free (length is 100-200 microns).

12.4 FUNDAMENTALS OF STRUCTURES

This section on the fundamentals of structures has been prepared to provide a practical combination of theory and application to the operational problems of aircraft, missiles, and space craft. For this reason only the minimum mathematical relationships are provided.

There are three fundamental objectives that will be addressed:

- (1) Acquaint the reader with the basic properties of structural materials and the particular qualities of these materials that make them suitable in particular structures.
- (2) Furnish the reader the fundamental reasons for operating strength limitations and good maintenance practices.
- (3) Equip the reader with the ability to recognize and diagnose the causes of structural and mechanical failures.

These objectives are first served by describing the principal requirements of any aircraft, missile, or space craft structure. The most important basic requirement is that the primary structure should be of the lowest possible weight. All of the basic items of performance and efficiency of a configuration are seriously affected by the structural weight. This is especially true when the extremes of performance are demanded of a configuration. For example, during preliminary design of a long range jet aircraft, a configuration weight growth factor of twenty may be typical. In other words, if the weight of any single item, e.g., landing gear structure, were to increase one pound, the gross weight of the aircraft must increase twenty pounds to maintain the same performance. Any additional weight would require more fuel, more thrust, larger engines, greater wing area, larger landing gear, heavier structure, more fuel, etc., until the aircraft gross weight had increased twenty times the original weight change.

Long range missiles and space craft usually encounter a design growth factor which is considerably in excess of any typical aircraft. Some typical long range ballistic missiles have demonstrated preliminary design growth factors on the order of 80 to 200. Of course, such configurations

represent an extreme of performance but serve notice of the great significance of structural weight. A limiting situation can exist when the demands for performance exceed the "state-of-the-art". If performance demands are extreme and basic powerplant capabilities are relatively low, the growth factors approach infinite values and impractical gross weights result for the configuration.

While the structure must be of the lowest possible weight, it must also be easily accessible for repair, inspection, and maintenance. There must be adequate protection from the environment to prevent corrosion, ionizing radiation, etc. In many instances, the accommodation for easy access for simple maintenance must be forsaken simply to obtain reduced structural weight.

The primary structure must be the minimum weight structure which can safely sustain the loads typical of operation. The actual nature of the most critical loads will depend to a great extent upon the design mission of the vehicle. During design and development, the mission must be thoroughly analyzed to define the most critical loads that will determine the minimum necessary (size and weight) of the structural elements. From an apparent infinite number of possible situations, the most critical conditions must be defined. Generally, there are three important areas of structural design, any one of which (or combination) could provide the most critical requirements of the structure.

12.4.1 Static Strength Considerations

Static loads refer to those loads which are gradually applied to the structure. The effects of the onset of loading or the repetition of loading deserve separate consideration. Throughout the operation of its mission, a vehicle structure encounters loads of all sorts and magnitudes. Various loads may originate during manufacture, transport, erection, launch, flight gusts and maneuvers, landing, etc. These various conditions may be encountered at various gross weights, e.g., positions, altitudes, pressurization, etc. If particular elements of the structure are separated for study, it is appreciated that these elements are subject to a great spectrum of varying loads.

For the considerations of static strength, it is important that this spectrum be analyzed to select the maximum of all loads encountered during

normal (or intended) operation. This maximum of all normal service loads is given special significance by assigning the nomenclature of "limit" load. The specific requirement of the structure is that it must be able to withstand "limit" load without ill effect. Most certainly the structure must withstand limit load without objectionable permanent deformation.

Specific requirements are different for various structural applications, and, in some cases, a "yield" factor of safety of 1.15 must be incorporated. This requirement would demand that the primary structure be capable of withstanding a load 15% greater than limit without "yielding" or deforming some objectionable amount. If such requirements were specified for a fighter aircraft, the aircraft could be safely maneuvered to limit "G" without causing the aircraft to be permanently deformed. If such requirements were specified for a typical missile, the missile could be fueled and static tested without causing the structure to be permanently deformed. Of course, the number of times this action could be repeated without ill effect would not be part of the static strength consideration.

A separate provision must be made to account for the possibility of a one-time application of some severe load greater than limit. For example, the previously mentioned fighter aircraft may require some flight maneuver load greater than limit in order to avert a disaster of collision. The same idea applies to the missile where malfunction of equipment may cause higher than normal tank pressurization. In either of these examples, some load greater than limit is always a (remote) possibility and, within reasonable limits, should not cause a catastrophic failure of the primary structure. There must be some provision for the possibility of a single critical load greater than limit.

Experience with piloted aircraft has shown that an "ultimate" factor of safety of 1.5 is satisfactory. Thus, a primary structural element should be capable of withstanding one load 50% greater than limit without failure. Of course, loads which generate stresses greater than the "yield" point will cause objectionable permanent deformation of the structure and render it unsuitable for continued operation. The principal concern is that the primary structure withstand the "ultimate" load without failure. To be sure, the ultimate load can be resisted only by a sound structure, i.e., no cracks, corrosion, eccentricity, etc.

In the previous discussion the yield factor of safety of 1.15 and ultimate factor of safety of 1.5 have been selected for example since these values are representative of piloted aircraft. On the other hand, certain missile configurations may have factors of safety well below that of piloted aircraft, e.g., yield factor of safety of 1.0, ultimate factor of safety of 1.2. In order to complete the picture, some ground support equipment may have an ultimate factor of safety of five or six, and a typical bridge structure may have an ultimate factor of safety of twenty. The factors of safety for airborne vehicles must be as low as is consistent with the safety and integrity of the structure.

When specific limit loads, yield and ultimate factors of safety are defined, there will be no deliberate addition of strength above these specified minimums. The reason is simple: undesirable structural weight would be added. However, the normal variation of material strength properties must be accounted for by designing to minimum guaranteed strength or specific levels of probability. In either case, it is possible that a considerable percentage of the structures will exceed the strength requirements by slight margins. This is an expected result when the structure is required to meet or exceed the minimum specified values.

As a result of these static strength considerations, the primary structure must withstand limit load without objectionable permanent deformation and ultimate load without failure. Because of the yield factor of safety and certain material characteristics, objectionable permanent deformation does not necessarily take place immediately above limit load. This could lead to difficulty in appreciating over-stress conditions since objectionable permanent deformation does not necessarily occur just beyond limit load. However, at ultimate load, failure is imminent.

12.4.2 Rigidity and Stiffness Considerations.

"Strength" could be defined as the resistance to applied loads. On the other hand, "stiffness" could be defined as the resistance to applied deflections. This particular distinction between strength and stiffness is a necessary consideration since the development of adequate strength does not ensure the attainment of adequate stiffness and rigidity. In fact, the

particular requirements of stiffness must be given consideration which is separate (but not completely independent) from the basic strength considerations.

The stiffness characteristics of a structure are very important in defining the response of the structure to dynamic loads. In order to distinguish a dynamic load from the ordinary static load, inspect Figure 12.11 where a weight, W , is suspended by a spring which has a stiffness, K .

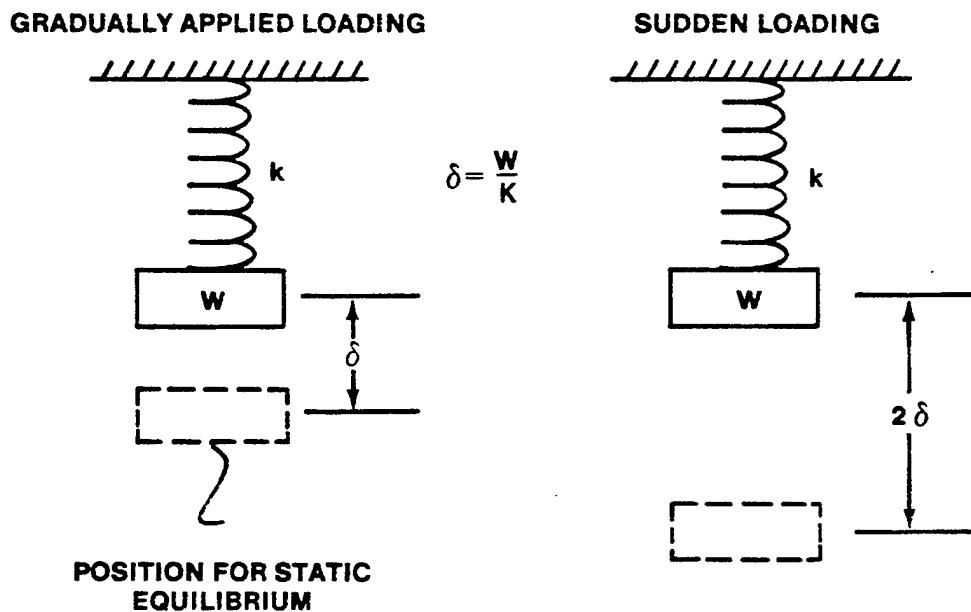


FIGURE 12.11. TIME DEPENDENCE OF LOAD APPLICATION

If the weight were lowered slowly and the force gradually applied to the spring, the spring would deflect slowly until the spring supports the entire weight with an equilibrium deflection of $\delta = W/K$. Alternatively, if the weight is suddenly dropped onto the spring, the input energy of the sudden loading will cause the spring to deflect twice as greatly, 2δ . Then the weight will oscillate back and forth, finally coming to rest at the same equilibrium deflection as for the gradually applied load. During the first plunge when the spring is deflected 2δ , the spring is subject to an instantaneous load which is twice the weight. Under the dynamic loading illustrated, the dynamic load is twice as great as the static load. Of

course, if the weight had been projected downward onto the spring with an initial velocity, the input energy would be greater and the dynamic amplification of load would be increased considerably.

The previous example serves only to point out the serious nature of dynamic loads. In a more typical (and complex) aircraft or missile structure, many degrees of freedom exist and the response may show the coupling between various possible modes of oscillation. In any case, the energy of load input, the rate of onset, and the characteristic response of the structure must be examined to determine the critical amplification of loads. The stiffness characteristics and the existence of damping, either natural or synthetic, must be tailored - if possible - to minimize critical amplification of loads.

Vibration of structures may provide critical situations and create a source of damaging loads. The fundamental nature of a vibrating system is best illustrated by the simple spring-mass system of Figure 12.12. If a weight, W , is suspended on a spring of stiffness, K , a small disturbance of the system will cause the weight to oscillate at some frequency which is dependent on spring stiffness and weight.

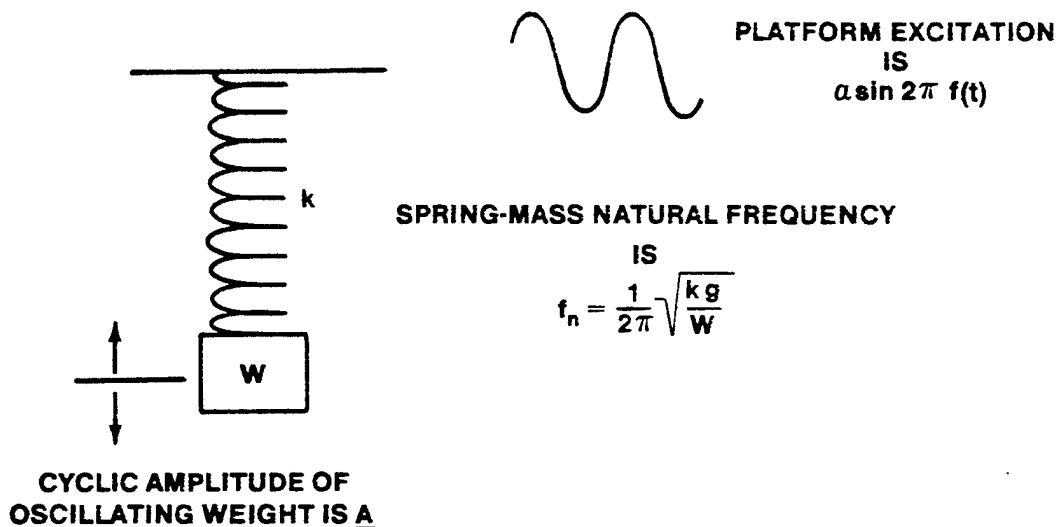


FIGURE 12.12. FUNDAMENTAL NATURE OF A VIBRATING SYSTEM

This "natural" frequency is related by Equation 12.9.

$$f_n = \frac{1}{2\pi} \sqrt{\frac{Kg}{W}} \quad (12.9)$$

where f_n = natural frequency, cps

K = spring stiffness, lbs/w.

g = acceleration due to gravity, 386

W = weight, lbs.

In order to consider the possibility of a forced vibration of this system, suppose the platform is moved back and forth with a sinusoidal motion, $a \sin 2 \pi f(t)$, where f is the frequency of excitation and a is the amplitude of excitation. The cyclic motion of the platform will induce a cyclic motion of suspended weight. The amplitude of motion of the weight, A , is related to the platform excitation and the natural frequency of the spring-mass system. Equation 12.10 defines this relationship:

$$A = \frac{a}{1 - (f/f_n)^2} \quad (12.10)$$

where A = amplitude of weight motion

a = amplitude of platform motion

f = excitation frequency of platform

f_n = natural frequency of spring-mass system

A careful inspection of Equation 12.10 points out one of the undesirable possibilities of a forced vibration of a structure. As the excitation frequency of the platform equals the natural frequency of the system ($f/f_n=1$), a resonant condition develops and the amplitude of weight motion approaches an infinite value. Of course, this resonant condition could cause sudden failure of the spring.

If the platform is subjected to an excitation frequency which is well below the natural frequency, the weight amplitude is very nearly the same as

the platform amplitude. The weight would move along with the platform with only slightly greater than static deflection of the spring. When the excitation frequency is considerably greater than the natural frequency, the weight is essentially isolated while the platform oscillates. The cyclic deflection of the spring would approach the cyclic displacement of the oscillating platform. If damping, or resistance to motion, is introduced into the system, the resonant condition will simply produce less than infinite motion of the oscillating weight. Above and below the resonant condition, damping will alter the motion depending on the amount of damping present in the system.

While the simple system illustrated does not portray the behavior of complex structures, the fundamental relationships are the same. During design of a structure the stiffness and mass distribution must be tailored to ensure that the ordinary environment of vibration does not allow any approach to resonant conditions and produce damaging loads.

Aeroelastic problems are encountered due to the interaction of aerodynamic forces and elastic deflection of the structures. Since elastic deflections are involved, the inherent stiffness and rigidity of the structure is a principal quality determining the extent of aeroelastic problems.

Static aeroelastic problems involve only the relationship of the aerodynamic forces and elastic deflections without the generation of inertia forces. A typical static aeroelastic problem encountered in aircraft is the phenomenon of "aileron reversal". Deflection of an aileron produces a section pitching moment tending to twist the wing in torsion. Thus, if an aileron is deflected down at high speed, the wing may develop such significant twisting deflection that the aircraft may roll opposite to the direction desired. Of course, sufficient stiffness must be provided in the structure to prevent aileron reversal or any significant loss of control effectiveness within the intended range of flight speeds.

A more disastrous sort of aeroelastic problem is referred to as "divergence." Suppose that a surface is subjected to a slight up gust when at very high speed. If the change in lift occurs forward of the elastic center, the surface will tend to twist leading edge up as well as bend up. The twist represents additional angle of attack, more lift, more bend, more twist, etc., until a sudden failure results. Such a failure is sudden and catastrophic

without warning. It is obvious that divergence could not be tolerated and sufficient stiffness must be present to prevent divergence within the anticipated flight range. In addition, below the divergence speed there must be sufficient stiffness to ensure no serious change in load distribution due to this sort of interaction between aerodynamic forces and elastic deflections.

All of the static aeroelastic problems are specific to the stiffness qualities of the structure and the dynamic pressure of flight. Thus, any specific operating limitation imposed will be relative to a certain dynamic pressure hence, indicated, calibrated, or equivalent airspeed.

The dynamic or oscillatory aeroelastic problems introduce an additional variable: inertia forces. Thus, dynamic aeroelastic problems involve some combination of aerodynamic forces, elastic deflections, and inertia forces. "Flutter" is one such problem. If a surface with particular mass and stiffness distribution were exposed to an airstream, the oscillatory aerodynamic forces may combine with the various natural oscillatory modes of the surface to produce an unstable motion. Flutter is essentially an aerodynamically excited oscillation in which airstream energy is extracted to amplify the energy of the structural oscillation.

Flutter is not necessarily limited to control surfaces or wing surfaces. Structural panels may encounter flutter conditions which are just as critical and damaging.

During design, the review and analysis of possible flutter behavior constitutes one of the most highly complex studies. The mass and stiffness distribution must be arranged to prevent flutter from occurring during normal operation. There is the implication that any alteration of stiffness or mass distribution due to service operation could cause a possible dangerous reduction of the speed at which flutter would occur.

This fact is important with respect to all of the conditions requiring adequate stiffness of the primary structure. Any alteration of stiffness may produce a dangerous change in dynamic response, vibration, or aeroelastic behavior.

12.4.3 Service Life Considerations

When considering the service life of a structure, the entire gamut of loads must be taken into account. To achieve satisfactory performance during

service operation, a structure must withstand the cumulative effect of all varieties of load that are typical of normal use. Normal periods of overhaul, inspection, and maintenance must be anticipated.

Creep is the continued plastic straining of a part subjected to stress. Of course, creep is of a particularly serious nature when the part is subject to stress at high temperature since elevated temperatures reduce the resistance to plastic flow. Gas turbine components, reentry configurations, rocket combustion chambers and nozzles represent some of the typical structures in which creep is important.

If a part is exposed to stress at high temperature, the part will continue to strain at a constant stress. If the exposure time is increased to some critical point, the creep rate will suddenly increase and failure will occur. Such failures due to creep can take place at well below the static ultimate strength of the material. Of course, the creep stress must be supplied for sufficient time to generate the condition of failure. It is typical of all metals that any increase in applied stress or temperature will increase the creep rate and reduce the time required to cause failure.

The creep damage is accumulated throughout the life of a structure, with the times at high stress and temperature causing the most rapid rate of accumulation. In order for a structure to perform satisfactorily in service, the spectrum of varying loads and temperatures must not cause a critical accumulation of creep damage. In other words, service use should not cause either creep deformation sufficient to prevent operation or creep failure by fracture or buckling. In some applications of turbines, machinery and mechanism, the limit of creep deformation may be the appropriate design consideration. The primary airframe structure may not be adversely affected by such creep deformations and the final failure by fracture or buckling may be the critical consideration.

In special high temperature structures the anticipated service life has distinct limitations. For example, gas turbine powerplants may have turbine structural elements which must be replaced at regular intervals while the shaft, case, and compressor withstand only ordinary inspection. If certain turbine elements were required to demonstrate the same time life as less highly stressed or heated parts, such life may not be at all possible. As a result the design service life of such high temperature, high stress parts may be set by design limitations rather than arbitrary desirable values.

Fatigue is the result of repeated or cyclic loads. If a metal part is subjected to cyclic stress of sufficient magnitude, a crack will eventually form and propagate into the cross-section. When the remaining cross-section cannot withstand the existing loads, a final rupture occurs as if by static load. The most important aspect of fatigue is that the failure is progressive by the accumulation of fatigue damage. When a critical level of damage is accumulated, a crack forms and propagates until final failure takes place. When a part is exposed to the variety of repeated loads during service operation, the cumulative fatigue must be limited so that failure does not occur within the anticipated service life.

In order to prevent fatigue failures, the structural design must bring into consideration many important factors. First, a reasonable estimate of the service life must be made and the typical spectrum of service loads must be defined. Then the fatigue characteristics of the materials must be determined by laboratory test of specimens. The effect of stress concentrations, corrosion environment, residual stresses, and manufacturing quality control must be analyzed. With these factors known, the concept of cumulative damage can be applied to determine the dimensions of the part necessary to prevent fatigue failure during the anticipated service life.

The normal scatter and variation in material properties encountered in fatigue tests will not allow prediction of the specific life of individual parts. A more appropriate consideration would be to account for the variability of material characteristics and load spectrum by the definition of failure probability. In other words, as parts in service approach the design service life, the probability of fatigue failure increases. If parts are exposed to service well beyond the design service life, failure probability will be quite high and the incidence of failures and malfunction of equipment will increase.

The use of periodic inspection and maintenance is very unnecessary to ensure failure free operation. Regular inspection must guarantee that parts do not incur excessive deformation or cracks during exposure to fatigue and creep conditions. There is always the possibility of short periods of high stress or temperature which could cause acceleration of creep or fatigue damage and precipitate a premature failure. This is a very important obligation of the maintenance facility.

The various considerations of static strength, stiffness, and service life will all contribute specific demands on a structure. Just which of these considerations predominate will depend upon the exact nature of the structure. An aircraft may show that any one of the static strength, service life, or stiffness requirements may predominate. In the design of most powerplant systems, the service life considerations of creep and fatigue usually predominate. Very short life missile structures may show that the static strength considerations prevail during design. However, if the missile must withstand considerable transportation, handling, and continuous functional checks, service life considerations may be important.

12.4.4 Load and Stress Distribution

Fundamentally, there are two types of loads which can be applied to an element of structure. There are "axial loads" which are applied along the axis of the part (Figure 12.13) and there are "transverse" loads - often referred to as "shear loads" - which are applied normal or perpendicular to the axis of the part (Figure 12.14). Any complicated load condition to which a structure is subjected can be resolved to the various axial or transverse loads acting on a particular part. Since the inherent strength properties of a structural material are based upon the element strengths of its crystals and grains, a more appropriate definition of load condition on a part is the amount of load per unit of cross section area. Thus load per unit area is referred to as "stress" and all basic properties of structural materials are based upon stress or load per unit of cross section area. Of course, as there are two basic types of loads -- axial and transverse -- there are two basic types of stress which result from these loads -- axial or "normal" stresses of tension and compression and the transverse or "shear" stresses.

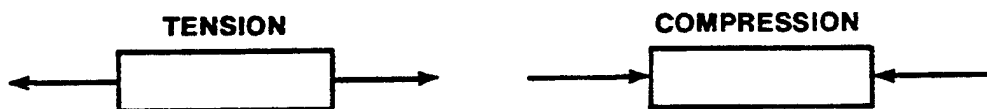


FIGURE 12.13. AXIAL LOADS

Axial tension applied to a material will produce certain types of effects and certain types of failures, while axial compression in the same type of material will produce completely different effects in different types of failures.

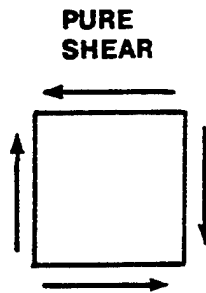


FIGURE 12.14. TRANSVERSE LOADING

A shear stress applied to a particular material results in a somewhat unusual pattern. If a shear is applied to an element of material in a vertical direction, that element will experience balancing shears in a horizontal direction of an equal magnitude. This must be so in order that the element be in equilibrium in rotation.

In any case in which the basic loads -- either axial or transverse -- are resolved on a cross-section of a part, the stresses are then computed for each element of the part as the amount of load per unit of area.

For normal stress,

$$\sigma = P/A$$

σ = normal stress, psi

P = loads in lbs

A = area, in²

For shear stress,

$$\sigma_s = P/A$$

σ_s = shear stress (12.11)

P = loads in lbs

A = area, in²

As an example of the typical stress distribution in a loaded structure, the following example problem is provided. This example will best furnish an

interpretation of the idea of stress and the function of certain structural components.

Figure 12.15 illustrates a typical beam structure. In this case there is a simplified spar or beam subjected to a concentrated load at the right end. The left end is mounted or fixed to a rigid wall surface. For simplicity, it is assumed that the spar (or beam) is the entire effective structure and that all loads will be resisted by this part. The problem will be to investigate the stresses at Points A and B in this spar structure which result from the application of the shear load at Point C. The beam has a constant cross-section throughout the span as shown in Figure 12.15. The spar flanges of this type structure furnish the primary bending resistance, while the spar web connecting the spar flanges provides the primary resistance to shear loads. The rivets attach the spar web to the spar flange, and there are vertical stiffeners attached to the web to maintain the form, shape, and stability of the structure. The distribution of stress at Point A in the beam is best visualized by taking a section through the beam at Point A and supplying the internal loads at the Section A which are necessary to resist the applied external shear load at C, thus maintaining equilibrium of the structure. This is shown in Figure 12.16.

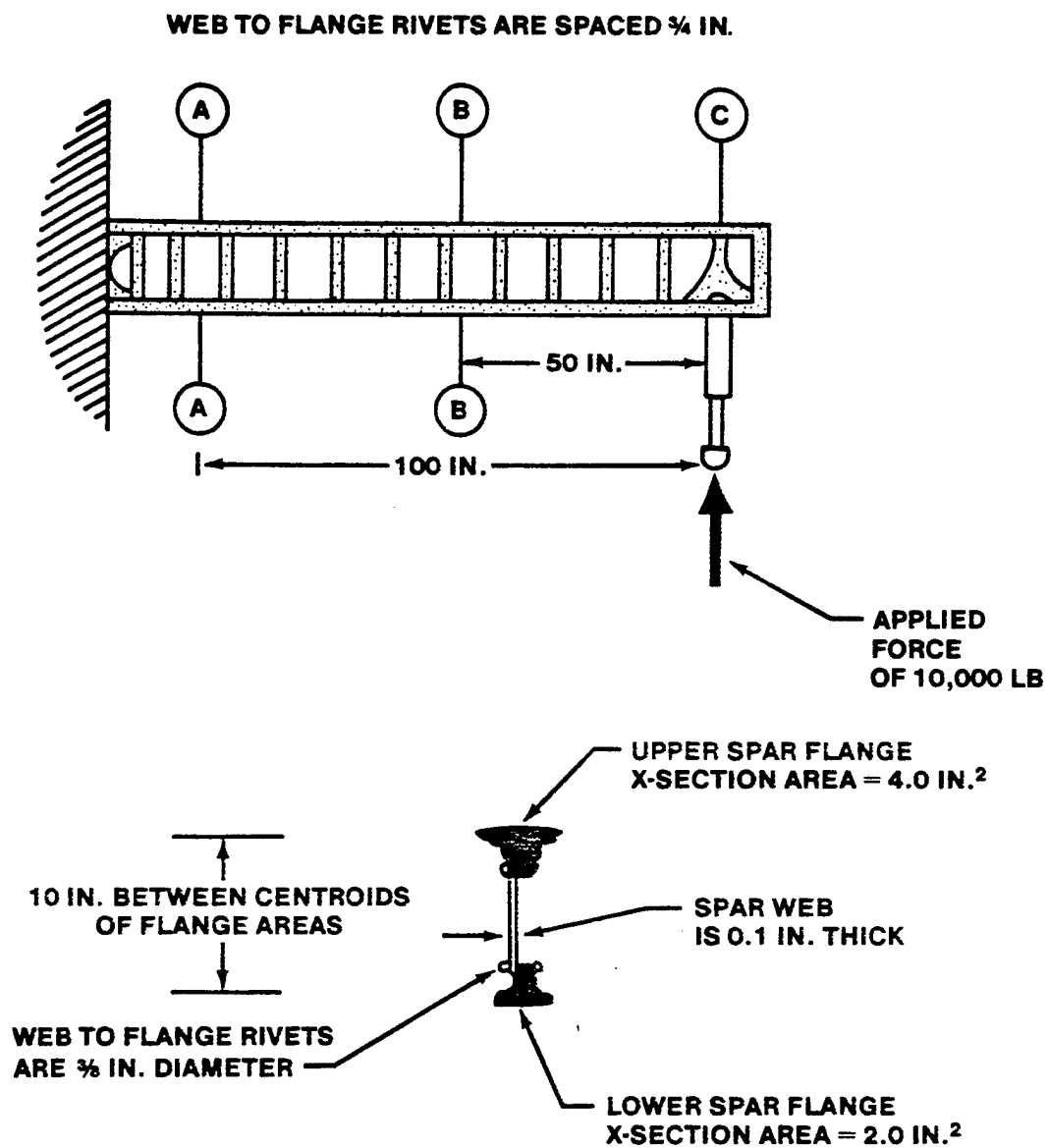


FIGURE 12.15. TYPICAL BEAM STRUCTURE

First, to maintain an equilibrium in a vertical direction, there must be a resisting shear load on Section A of 10,000 lbs in a vertical direction down, which resists the applied shear load up at Point C. Due to the lever arm of force at Point C, there is a bending moment produced in the structure at Point A. The magnitude of this bending moment is the product of the force and the lever arm, i.e., 10,000 lbs times 100 in = 1,000,000 in lbs of moment at Section A. As the spar flanges provide the primary resistance to bending, there will be a compression axial load developed in the upper spar flange and a tension axial load produced in a lower spar flange. These axial loads in the spar flanges for this untapered beam must be equal to maintain equilibrium of a structure in a horizontal direction. These axial forces in the spar flanges will be referred to as "P" pounds of load. These two forces of P, acting as a couple at a distance of 10 in apart (the distance between the centers of gravity of areas of the upper and lower spar flanges) must provide internal balance in the structure to the applied external bending moment of 1,000,000 in-lbs. In other words, $P \times 10$ in must equal 1,000,000 in-lbs. The P pounds of load in a flange is then computed to be 100,000 lbs.

$$P \text{ lb} \times 10" = 1,000,000 \text{ in-lbs}$$

$$P = 100,000 \text{ lbs}$$

To determine the stress in the upper flange, the compression load is distributed over the compression area

$$\sigma_c = P/A = 100,000 \text{ lbs}/4 \text{ sq in} = 25,000 \text{ lbs/in}^2$$

The tension stress in a lower flange is the load divided by the area

$$\sigma_t = P/A = 100,000 \text{ lb}/2 \text{ sq in} = 50,000 \text{ lbs/in}^2$$

Since the spar web furnished primary resistance to shear loads, there is a shear load of 10,000 lbs acting on the effective area of the web. The effective area of this web is the depth times the thickness. In this case, depth is taken as 10 inches and the thickness is 1/10 of an inch which produce

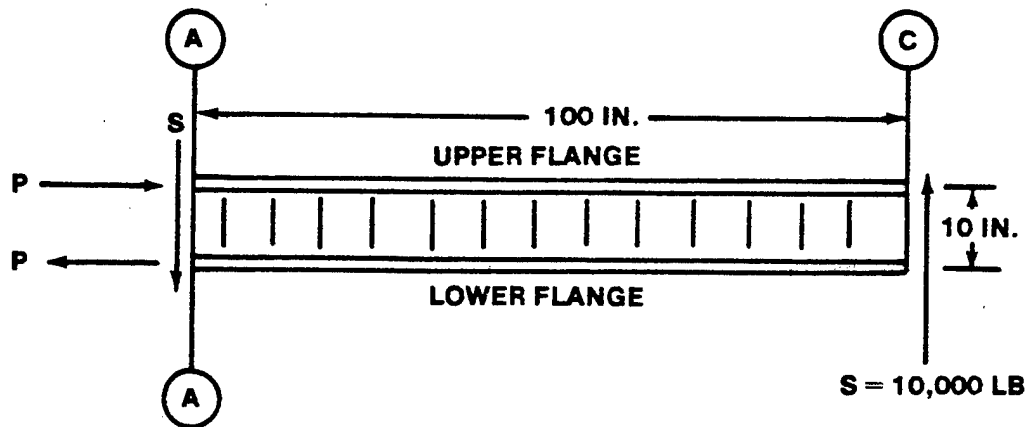


FIGURE 12.16. STATIC STRUCTURAL EQUILIBRIUM

one square inch of cross sectional area. This shear stress in the web is then load divided by area

$$\sigma_s = P/A = 10,000 \text{ lb}/1 \text{ sq. in.} = 10,000 \text{ lbs/in}^2$$

To investigate the stress distribution at Section B, the same fundamental procedure is employed (Figure 12.17). That is, the section at Point B is furnished with the loads on the cross-section necessary to place the structure in equilibrium. The bending moment to be resisted by the spar flanges is the 10,000 lbs of force acting at the 50 inch lever arm. This produces a bending moment of 500,000 in lbs and results in axial loads in the spar flanges of 50,000 lbs each.

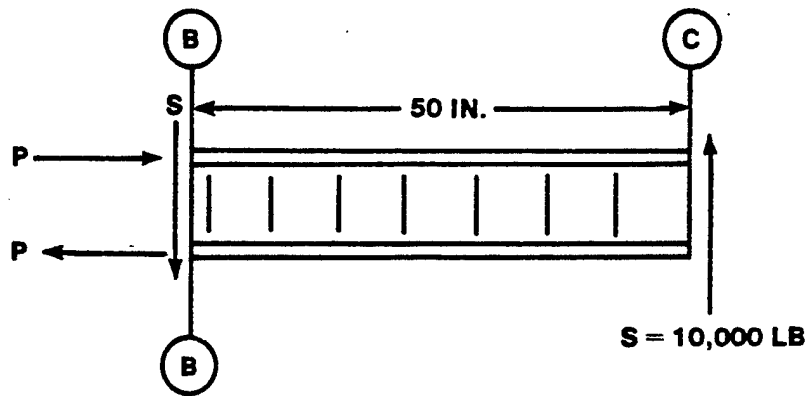


FIGURE 12.17. SHEAR STRESS DISTRIBUTION

The compression stress in the upper flange is then

$$\sigma_c = P/A = 50,000 \text{ lb/ sq in} = 12,500 \text{ lbs/in}^2$$

The tension stress in the lower flange is

$$\sigma_t = P/A = 50,000 \text{ lb/2 sq in} = 25,000 \text{ lbs/in}^2$$

Since the same amount of shear load must be supplied on Section B to provide equilibrium in a vertical direction and resistance to the applied 10,000 lbs shear load, the shear stress in the spar web remains the same 10,000 psi throughout the span of the beam and it does so as long as there is no change in the shear load across the beam.

To determine the stress in the rivets attaching the spar web to the flanges, the function of the rivets must be made clear. The point of load application at Section C on the beam has a vertical load of 10,000 lbs applied. This concentrated load of 10,000 lbs must be appropriately distributed to the web by a fitting. The desired result, as in Figure 12.18, is to distribute the concentrated shear load of 10,000 lbs to the edge of the spar web such that for the 10 inch effective depth of the web there is 1,000 lbs of load for each 1 inch along the edge.

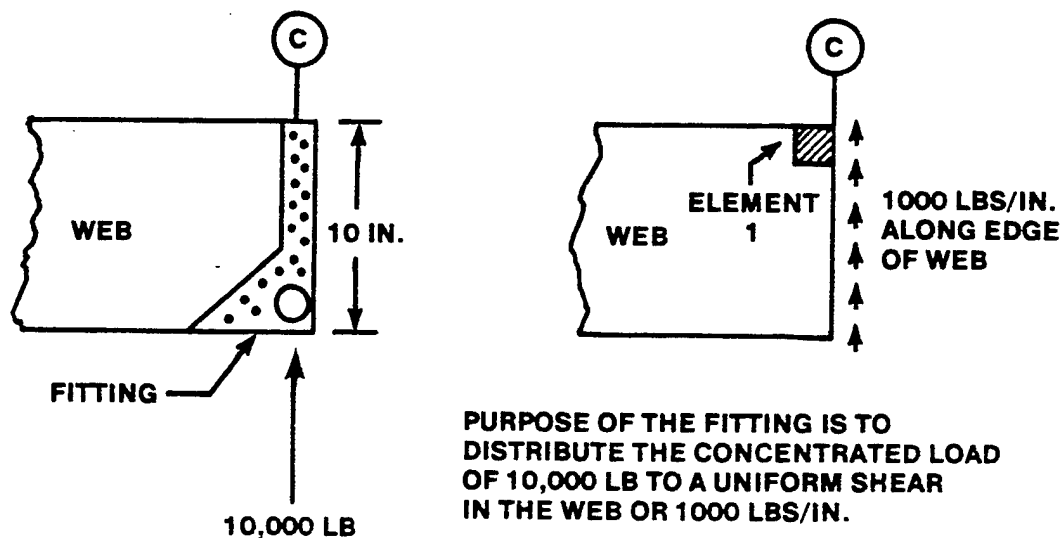


FIGURE 12.18. DISTRIBUTION OF CONCENTRATED SHEAR LOAD

The Element 1 in the upper right hand edge of the web at Section C has applied on its edge 1,000 lbs shear load. Figure 12.19 illustrates the manner in which this 1,000 lbs of load applied to this 1 inch Element 1 is resisted.

At the left hand side, there is a shear load down of 1,000 lbs balancing the applied 1,000 lbs. This shear load on the left hand edge is furnished by the adjacent element of the web to the left of Element 1. Since an element of structure with an applied shear load must also have balancing shears at 90° , there will exist (or must exist) on Element 1 shear loads on the upper and lower edges as shown. The shear load on the upper edge of Element A is supplied by the next piece of structure in contact with the edge of the web. This load must come from the spar flange and is transmitted by the "web-to-flange" rivets. The primary function of the "web-to-flange" rivets is then to provide a continuity of shear and to balance the applied vertical shear load in a horizontal direction. The shear load of the lower side of Element 1 is supplied by the next element immediately underneath Element 1 in the web. If the spacing of rivets attaching the web to the flange is three-quarters of an inch, the load for each rivet in shear will be $3/4$ of 1,000 lbs (rivets spaced $3/4$ inch) or 750 lbs per rivet. With the diameter of the rivet given as $3/8$ of an inch, the rivet stress in shear could then be computed as the

load divided by area:

$$\text{Rivet stress} = \frac{\text{load}}{\text{area}}$$

$$\sigma_s = \frac{750 \text{ lbs}}{(\pi/4) (3/8)^2 \text{ in.}^2}$$

$$\sigma_s = \frac{750 \text{ lbs}}{.1104 \text{ in.}^2}$$

$$\sigma_s = 6800 \text{ psi}$$

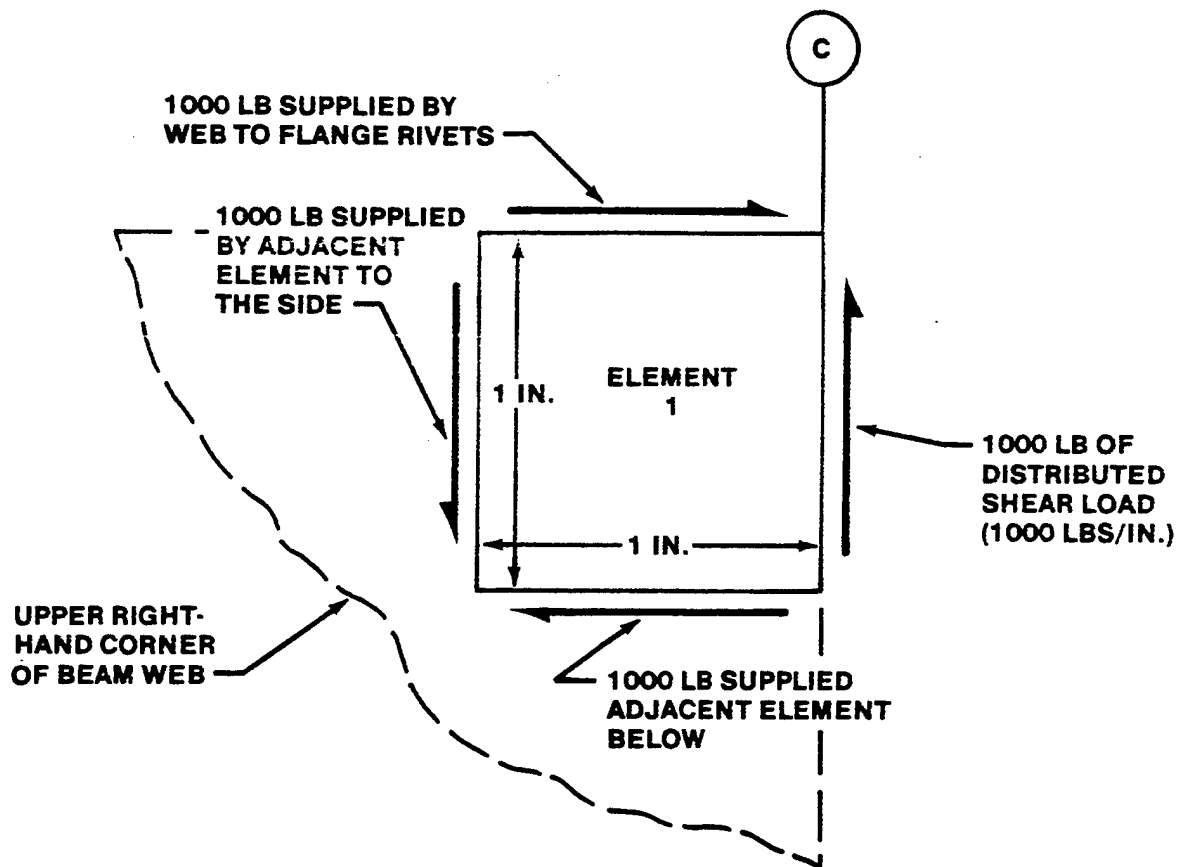


FIGURE 12.19. SHEAR ELEMENT

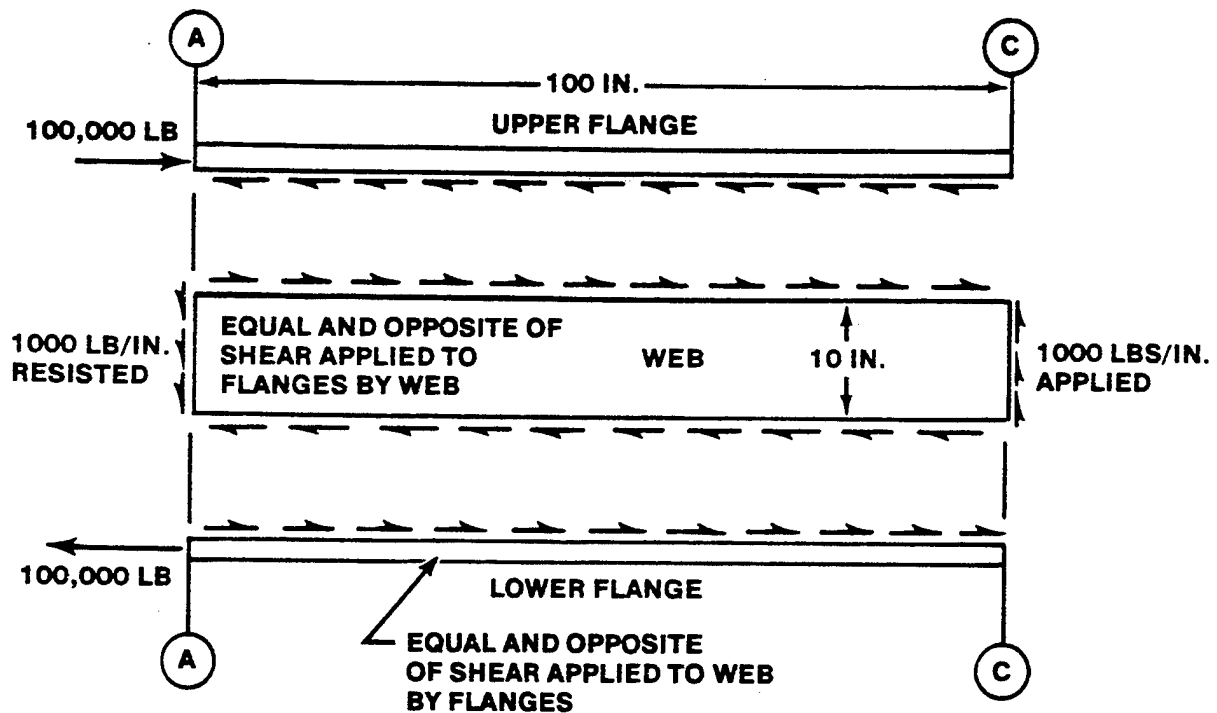


FIGURE 12.20. SPAR FLANGE AND WEB LOADS

Figure 12.20 gives an illustration of the upper and lower spar flange removed from the structure and the loads applied to spar flanges and the web.

The flange loads of 100,000 lbs at Section A are the result of the accumulated axial force from the distributed shear loads of 1,000 lbs per inch for the entire length of 100 inches. This distributed load at Section A (100 inch length) and 50,000 lbs at Section B (50 inch length).

The vertical stiffeners attached to the web have no particular stress -- either compression tension or shear - until the web of the spar begins to buckle. (Figure 12.21)

The primary function of these vertical stiffeners is to maintain the form and stability and to provide support for the web panel, thereby preventing or delaying the shear buckling of the web. When buckling occurs in the web, the

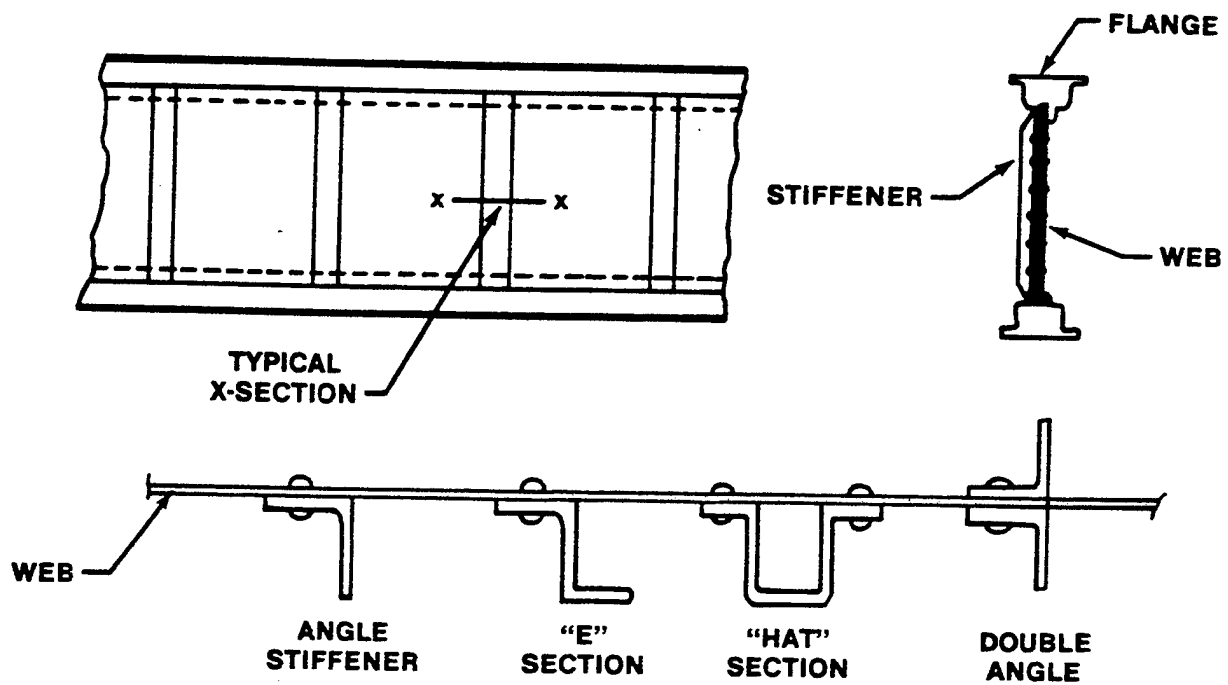
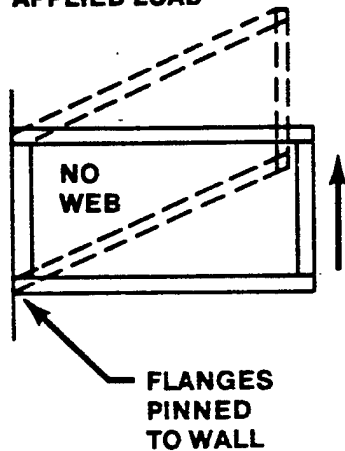


FIGURE 12.21. VERTICAL STIFFENERS

vertical stiffeners must withstand compression loads to prevent collapse of the structure.

The function and importance of the spar web can be best emphasized by two examples shown in Figure 12.22. If there were no web between the pinned flanges and a shear load applied, no resisting loads would be developed in the flanges. The structure would collapse to the shape shown with no resistance to the applied load.

**STRUCTURE OFFERS
NO RESISTANCE TO AN
APPLIED LOAD**



**BENDING OF FLANGES
PRODUCES LITTLE
RESISTANCE TO AN
APPLIED LOAD**

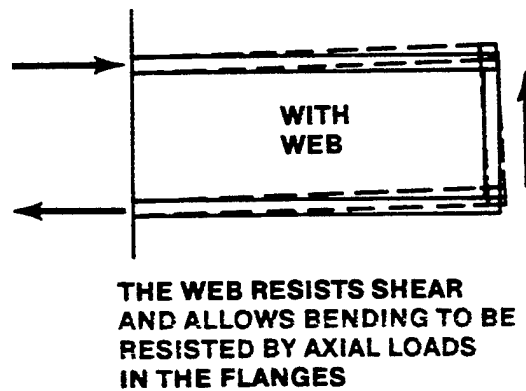
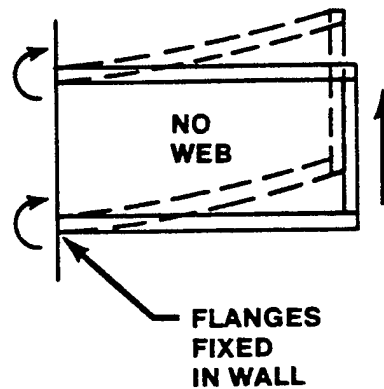


FIGURE 12.22. SPAR WEB FUNCTION

If there were no web between the fixed flanges, a shear load applied would produce "secondary" bending of the flanges. Since the bending resistance of the flanges is quite small, prohibitive stresses and deflections would result. Obviously, the more efficient structure is the web-flange combination which resists shear in the web and bending by axial loads in the flanges.

Actually, there is very rarely such a thing as a "lightening hole" in a shear web. More usually these holes are for access in maintenance and production and are a structural penalty for anything but minimum gage thickness structures (light planes, gliders, airships, etc.).

The previous example problem of the stress distribution in a simplified structure has considered that there were no particular complications to

produce anything other than pure axial and shear stresses. In a more detailed analysis, consideration would be made of the contribution of the web to bending resistance, the complication and magnification of stress due to rivet holes, etc.

There are, of course, examples in which the distribution of stress in a structural element is complicated by the particular manner of loading. There follow certain examples of the particular stress as distributed in typical structures if there is bending, torsion, etc., and the resulting stresses remain in the elastic range of the material characteristics. By "elastic range", it is implied that stresses may be applied, then released, and no permanent deformation of the structure would be incurred.

12.4.5 Pure Bending

Figure 12.23 illustrates the use of a solid, rectangular bar with pure bending moments applied. The stresses at Section A will be distributed as shown with the upper portion of Section A subjected to a compression stress which will be a maximum at the outer surface and the lower surface of Section A subjected to a tensile stress which will be a maximum at the outer surface.

The point at which the stress is zero - neither tension nor compression - is referred to as the "neutral axis". For a symmetrical, rectangular section this point would be midway between the upper and lower surfaces. The neutral axis for a homogenous material subjected to elastic bending is always located at the center of gravity (or "centroid") of cross sectional area.

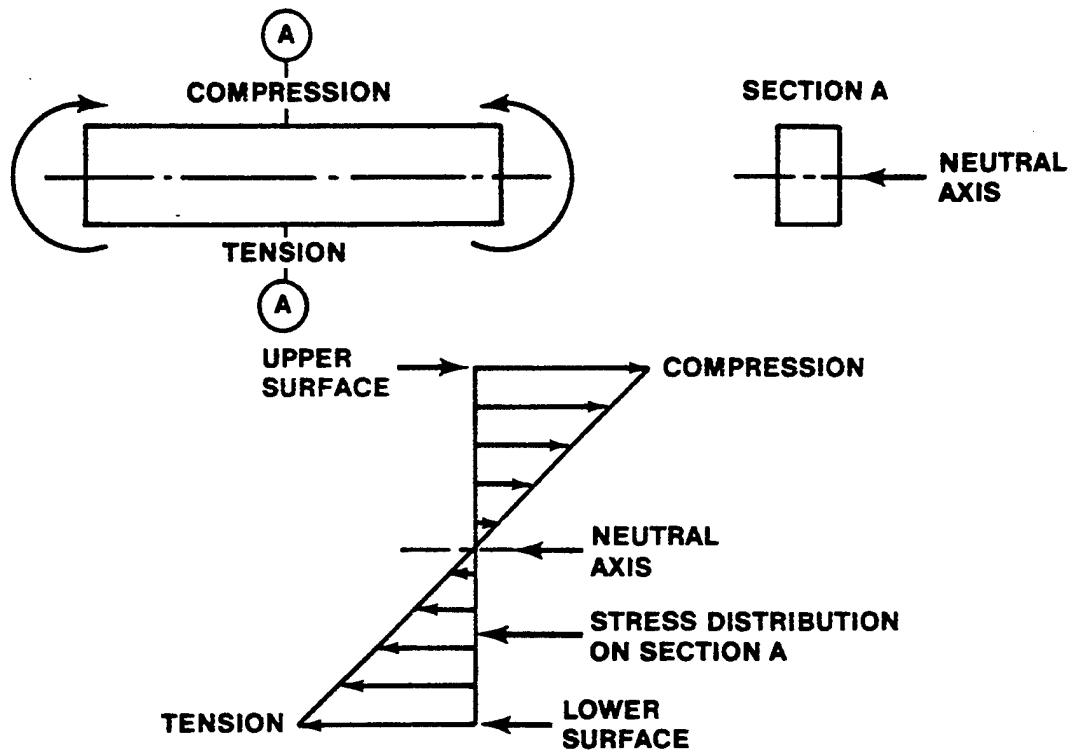


FIGURE 12.23. PURE BENDING OF A SOLID, RECTANGULAR BAR

In Figure 12.24 there is an unsymmetrical cross-section subjected to pure bending. For the cross-section shown, the neutral axis will be closer to the upper surface of the part than the lower surface. The stress distribution illustrated in Figure 12.24 will continue to be a linear variation of stress between the two maximum stresses at the upper and lower surfaces. However, as the neutral axis is closer to the upper surface, the magnitude of compression stress will be smaller than the tensile stress on the lower surface. This must be so, since the compression load produced by the smaller compression stress distributed over the larger area above the neutral axis will be equal to the tension load produced by the higher tensile stress acting over the smaller tensile area below the neutral axis. Thus, equal and opposite compression and tensile loads exist which furnish equilibrium to the cross-section in the horizontal direction.

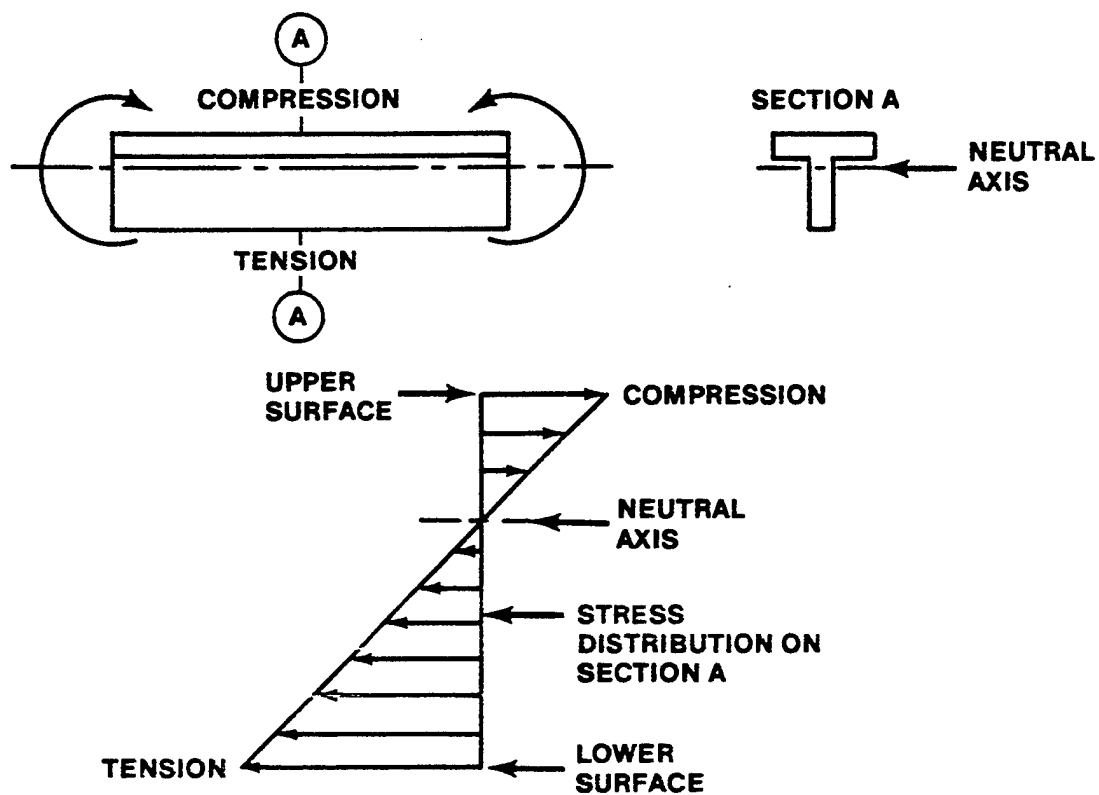


FIGURE 12.24. PURE BENDING OF AN UNSYMMETRICAL CROSS-SECTION

For beams or other structures subjected to bending moments,

$$\sigma_{b_{\max}} = \frac{Mc}{I} \quad (12.12)$$

Where $\sigma_{b_{\max}}$ = maximum bending stress, psi

M = bending moment on cross-section, lb in

c = distance from neutral axis to outermost fiber, in

I = moment of inertia of cross-section, in⁴

If the stress on some other fiber is desired, the equation is simply $\sigma_b = My/I$, where y is the distance from the neutral axis to the fiber under consideration.

The term "moment of inertia" appears in the previous equations. As has been explained, the bending stress in a fiber depends on its distance from the neutral axis. If the material can tolerate a given amount of stress, the largest moment can be resisted when the area resisting it is as far as possible from the neutral axis. The moment of inertia is a quantity which takes the shape of the cross-section into account in determining the amount of bending moment which can be resisted by a given cross-section without exceeding a specified stress. For several cross-section shapes the following apply:

$$I = \frac{1}{12} b h^3 \quad (\text{rectangular})$$

$$I = \frac{1}{36} b h^3 \quad (\text{triangular})$$

$$I = \frac{\pi}{64} D_0^4 \quad (\text{circular})$$

$$I = \frac{\pi}{64} D_0^4 - D_i^4 \quad (\text{doughnut})$$

Where I = moment of inertia about the neutral axis, in⁴

b = rectangle or triangle width, in

h = rectangle or triangle height, in

D₀ = outside diameter, in

D_i = inside diameter, in

12.4.6 Pure Torsion

Figure 12.25 illustrates the condition of pure torsion applied to a solid, circular shaft. With torsion applied to the part, the stress produced on Section A is primarily that of shear - a shear stress which is a maximum at the outer surface and varies linearly to zero at the axis of the part.

For circular shafts subjected to torsion moments,

$$\sigma_{s_{\max}} = \frac{Tc}{J} \quad (12.13)$$

Where $\sigma_{s_{\max}}$ = maximum shearing stress, psi

T = torsional moment or twisting moment, lb in

c = radius from axis to outermost surface, in

J = "polar moment of inertia" of cross-section, in⁴

Use $f = Mr/J$ if the stress at a distance r from the axis is desired.

The polar moment of inertia, J , is used for determining strength of sections subjected to torsion.

Only the circular sections have simple equations for this sort of stress distribution. These are as follows:

$$J = \frac{\pi}{32} D_0^4 \quad (\text{circular})$$

$$J = \frac{\pi}{32} D_0^4 - D_i^4 \quad (\text{doughnut})$$

Where J = polar moment of inertia, in⁴

D_0, D_i = outside and inside diameters, in

For sections other than circular, reference may be made to any of the more standard texts on strength of materials.

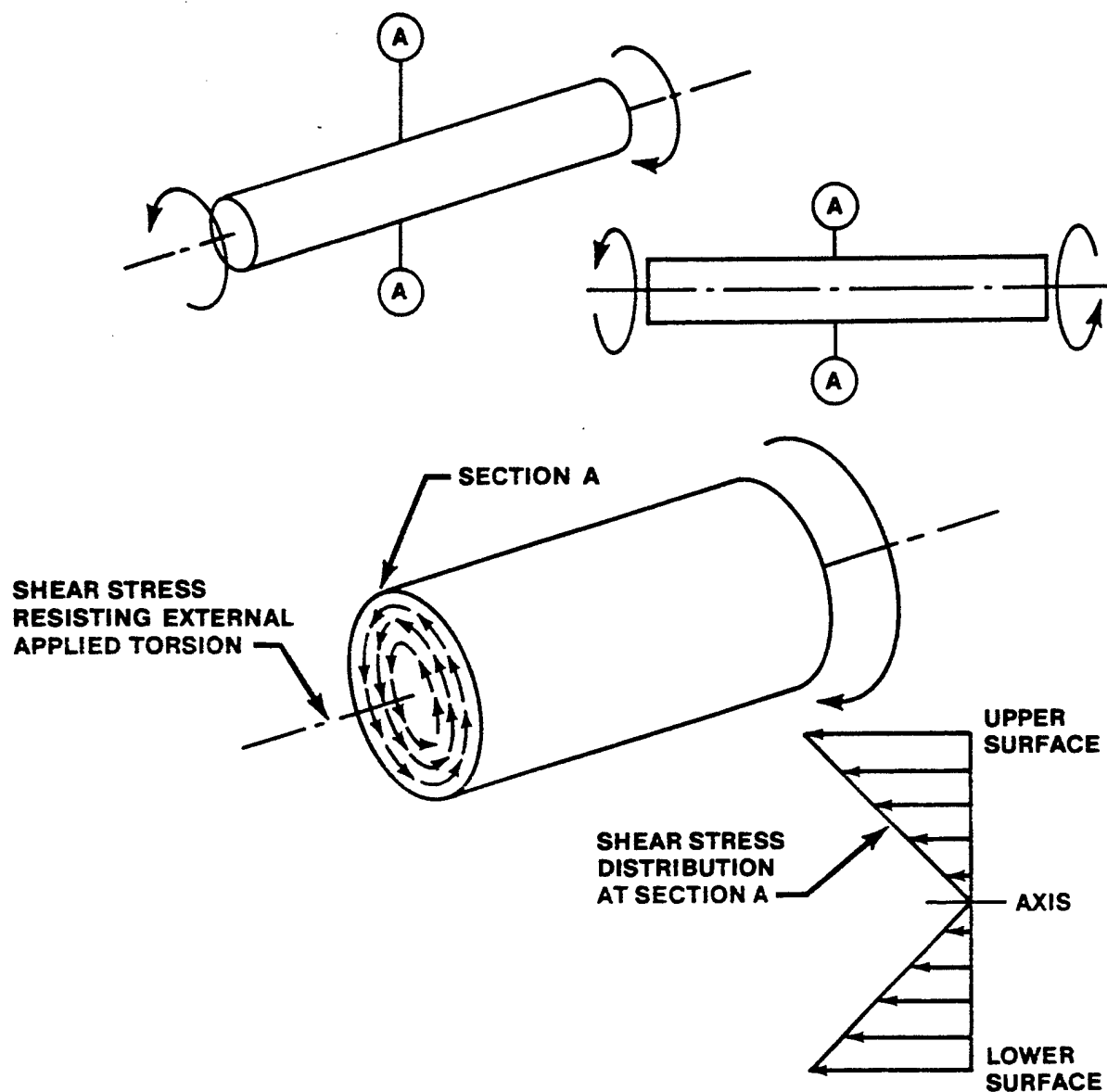


FIGURE 12.25. PURE TORSION OF A SOLID, CIRCULAR SHAFT

Figure 12.26 illustrates the conditions in which a continuous, hollow cross section is subjected to torsion. In this instance, the shear stress is a constant value around the periphery of the cross section. Since the shear load distributed around the periphery must provide an internal resisting moment equal to the external applied moment, the shear stress for this continuous shell structure may be computed by use of the following relationship:

$$\sigma_s = \frac{T}{2At}$$

(12.14)

where σ_s = shear stress, psi

T = applied torque, in-lbs

A = enclosed area of cross-section, sq in

t = shell thickness, in

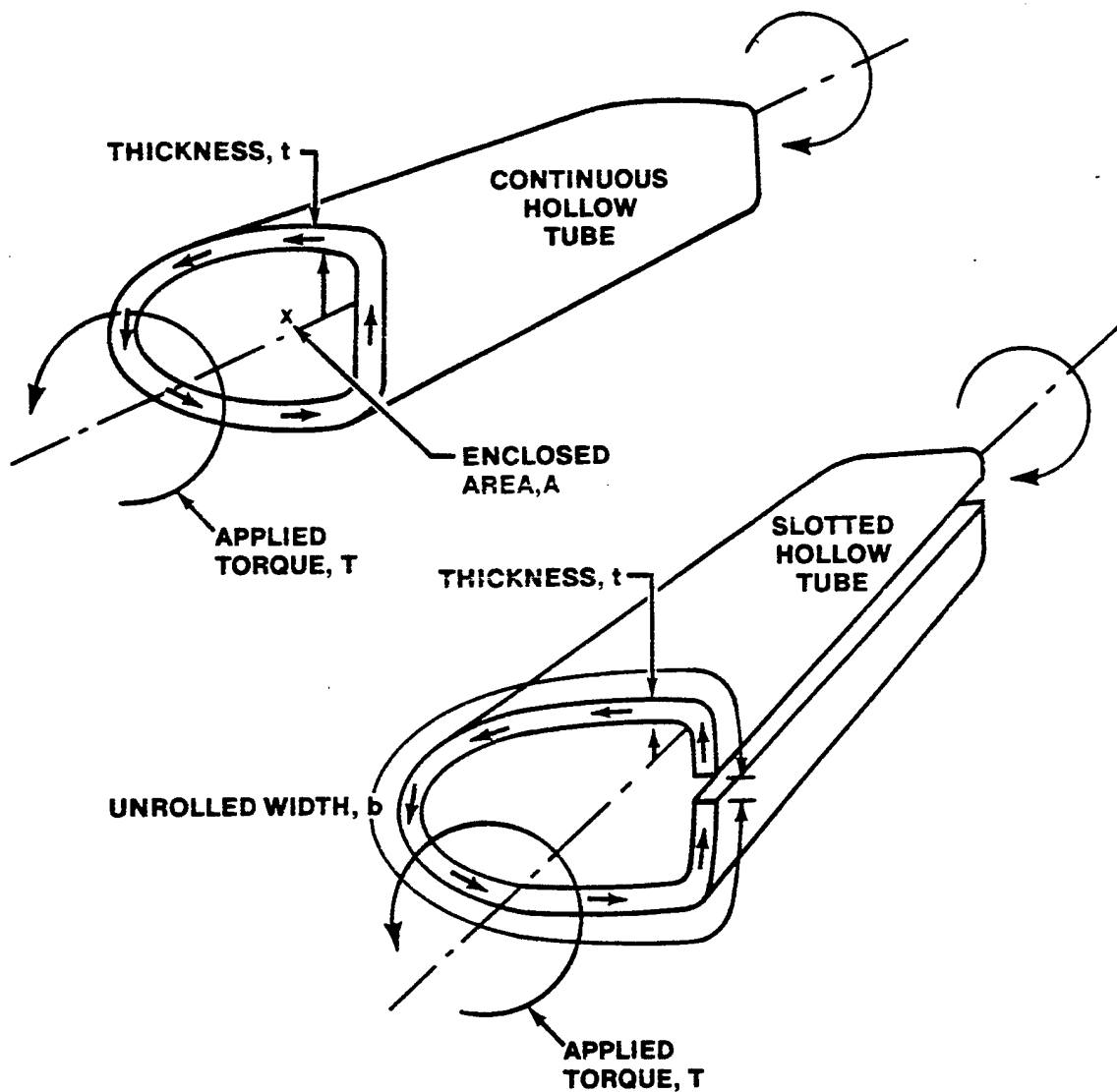


FIGURE 12.26. PURE TORSION OF A HOLLOW TUBE

If this section were slotted in a longitudinal direction, a very large amount of the torsional rigidity would be lost. There would be no continuous shear stress distributed around the periphery of the shell and high local shear stresses with great deflections would be encountered. The maximum shear stress in this case could be calculated by application of the following equation:

$$\sigma_{s_{\max}} = \frac{3T}{bt^2} \quad (12.15)$$

where $\sigma_{s_{\max}}$ = maximum shear stress, psi

T = applied torque, in-lbs

b = unrolled width, in

c = shell thickness, in

Any shell structure subjected to torsional loading which has a cutout or slot will have a tendency to develop much higher stresses and may be excessively flexible.

12.4.7 Bolted or Riveted Joints

Figure 12.27 illustrates a typical type of bolted or riveted joint which is encountered in more conventional structures. In such a joint, the load applied to element A is transferred by the bolt and distributed to elements B and C. This transfer of load by the bolt produces a shear stress on the bolt cross-section. The bolt shear stress is

$$\begin{aligned} \sigma_s &= \frac{\text{load}}{\text{area}} \\ \sigma_s &= \frac{P/2}{\pi/4 d^2} = \frac{2P}{\pi d^2} \end{aligned} \quad (12.16)$$

The tensile load developed in the plate creates a critical tensile stress along section x. The average tension stress at section x is

$$\sigma = \frac{\text{load}}{\text{area}} \quad (12.17)$$

$$\sigma = \frac{P}{(w-d)t}$$

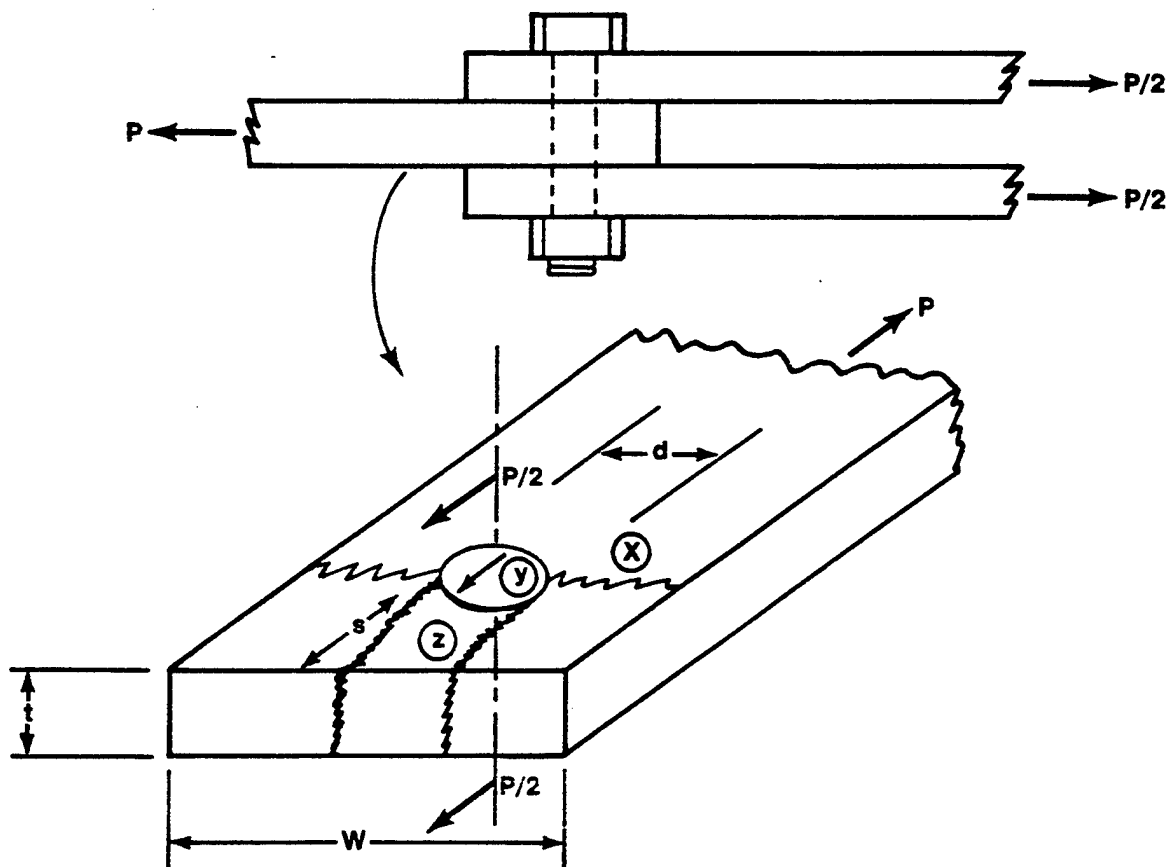


FIGURE 12.27. DOUBLE LAP JOINT, BOLT IN DOUBLE SHEAR

In addition, the bolt bearing on the surface of the hole (surface Y) may create a critical compressive stress. The average bearing stress in the plate at the bolt hole is:

$$\sigma_{br} = \frac{\text{load}}{\text{area}} \quad (12.18)$$

$$\sigma_{br} = \frac{P}{dt}$$

The application of the bearing load creates a shear stress along Sections z which tends to tear out the edge of the plate.

The "edge tear-out" stress is

$$\sigma_s = \frac{\text{load}}{\text{area}}$$

$$\sigma_s = \frac{P}{2ts} \quad (12.19)$$

These simple equations represent only the simple average stresses in order to appreciate some of the fundamental requirements of a joint. There is the obvious possibility that friction between the plates may accomplish part of the shear transfer and the hole may create considerable stress concentration to cause peak stresses well above the computed average.

12.4.8 Pressure Vessels

The use of highly pressurized containers in various aircraft and missiles creates significant structural problems. Some of the more simplified situations are represented by the stresses created in pressurized spherical and cylindrical shells. These vessels are illustrated in Figure 12.28.

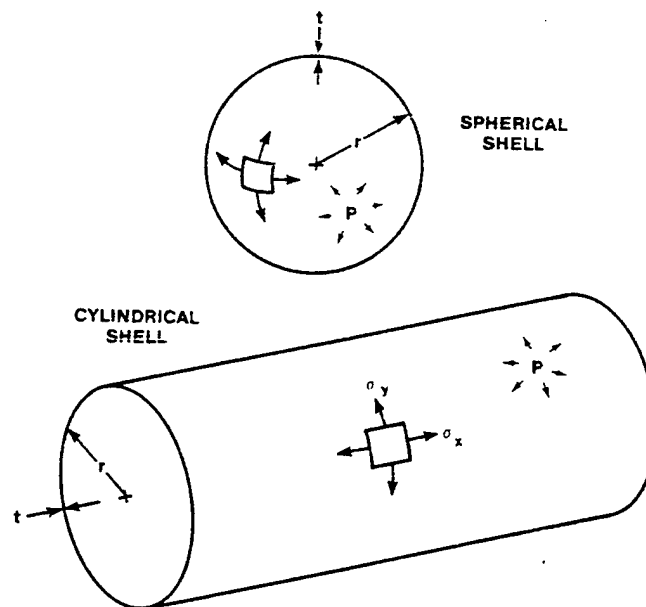


FIGURE 12.28. STRESS IN PRESSURIZED VESSELS

The stress in a pressurized spherical shell is uniform and constant in all directions along the surface. The resulting tensile stress is due to the pressure load being distributed over the effective shell area

$$\sigma = \frac{\text{load}}{\text{area}} \quad (12.20)$$

$$\text{load} = (\text{pressure}) (\text{area})$$

$$= (p) (\pi r^2)$$

$$\text{area} = 2\pi r t$$

$$\sigma = \frac{p\pi r^2}{2\pi r t}$$

$$\sigma = \frac{pr}{2t}$$

In order to consider the stresses in a pressurized cylindrical shell, the existence of two separate stresses must be noted. The longitudinal stress, σ_x is related as follows:

$$\sigma_x = \frac{\text{load}}{\text{area}}$$

$$\sigma_x = \frac{p\pi r^2}{2\pi r t}$$

$$\sigma_x = \frac{pr}{2t} \quad (12.21)$$

This is identical to the relationship developed for the pressurized spherical shell. However, an additional stress, σ_y , is developed which is referred to as the "hoop" stress.

$$\sigma_y = \frac{\text{load}}{\text{area}}$$

$$\text{load per unit length} = 2pr$$

$$\text{area per unit length} = 2t$$

$$\sigma_y = \frac{2pr}{2t}$$

$$\sigma_y = \frac{pr}{t} \quad (12.22)$$

(NOTE: $\sigma_y = 2f_x$)

For this situation the hoop stress incurred is twice the longitudinal stress developed. An important fact is concluded from this relationship: If a failure due to pressure occurs in a uniform cylindrical shell, the hoop stresses will predominate in the mode of failure.

12.4.9 Component and Principal Stresses

Two factors determine the strength and manner of failure of any structural member. One, of course, is the property and character of the structural material. The other is the maximum normal stresses ("principal stresses") and maximum shear stresses which exist in various areas of a part. Whenever there is a normal stress applied to a part there will exist various magnitudes of normal and shear stresses at planes different to the direction of loading. Also, any time a shear stress is applied to a part, there will exist at certain planes various magnitudes of normal and shear stresses. The various components of the applied primary stress must be investigated to determine the influence upon strength and failure type.

A typical example of component stress is illustrated in Figure 12.29. Figure 12.29A shows a specimen of material with a pure axial tension load applied. If a section or cut is made in this specimen at Section X, it is seen that a constant tension stress exists on this plane perpendicular to the direction of loading. Figure 12.29B shows the same specimen subjected to the same pure axial tension load but with a cut made along Section Y. An investigation of the stresses acting on Section Y shows that there still exists a uniform tensile stress across the section. However, the tensile stress which exists on plane Y will have components which are perpendicular and parallel to the surface of the cut. One of these components which is perpendicular to the face of the section will be a normal tensile stress of a smaller magnitude than the tensile stress applied to the cross-section. Along the surface of Section Y will be a component of stress parallel to the surface. This is a shear stress - it is a component of the primary applied tensile stress.

Since the tensile stress component perpendicular to the face of the cut will be of a smaller magnitude than the applied tensile stress, it will have no particular or immediate influence on strength or mode of failure. However, the shear stress component parallel to the face of the section is a stress of an altogether different nature. It may have a decided effect on strength and failure type as some materials are much more critical in shear than in normal stress (particularly ductile metals).

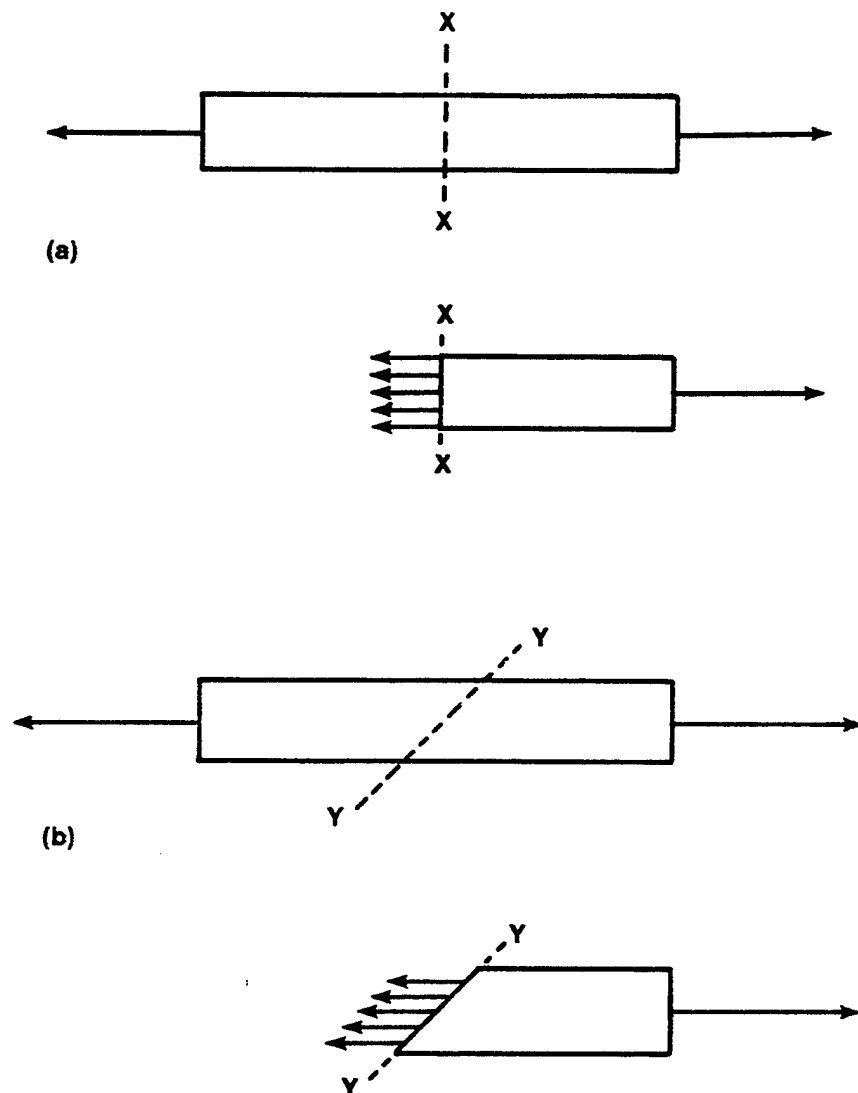


FIGURE 12.29. COMPONENT STRESSES

Figure 12.30A shows a part loaded in tension with a section cut along the direction of applied stress. It is obvious there would be no shear stress

(due to force components) along this Section Z. Since shear stresses do not exist either at a section perpendicular to the direction of applied stress, or at a section parallel to the direction of applied stress, it is reasonable to assume that between these limits the existing shear stress will be a maximum on a section at 45° to the direction of primary load application.

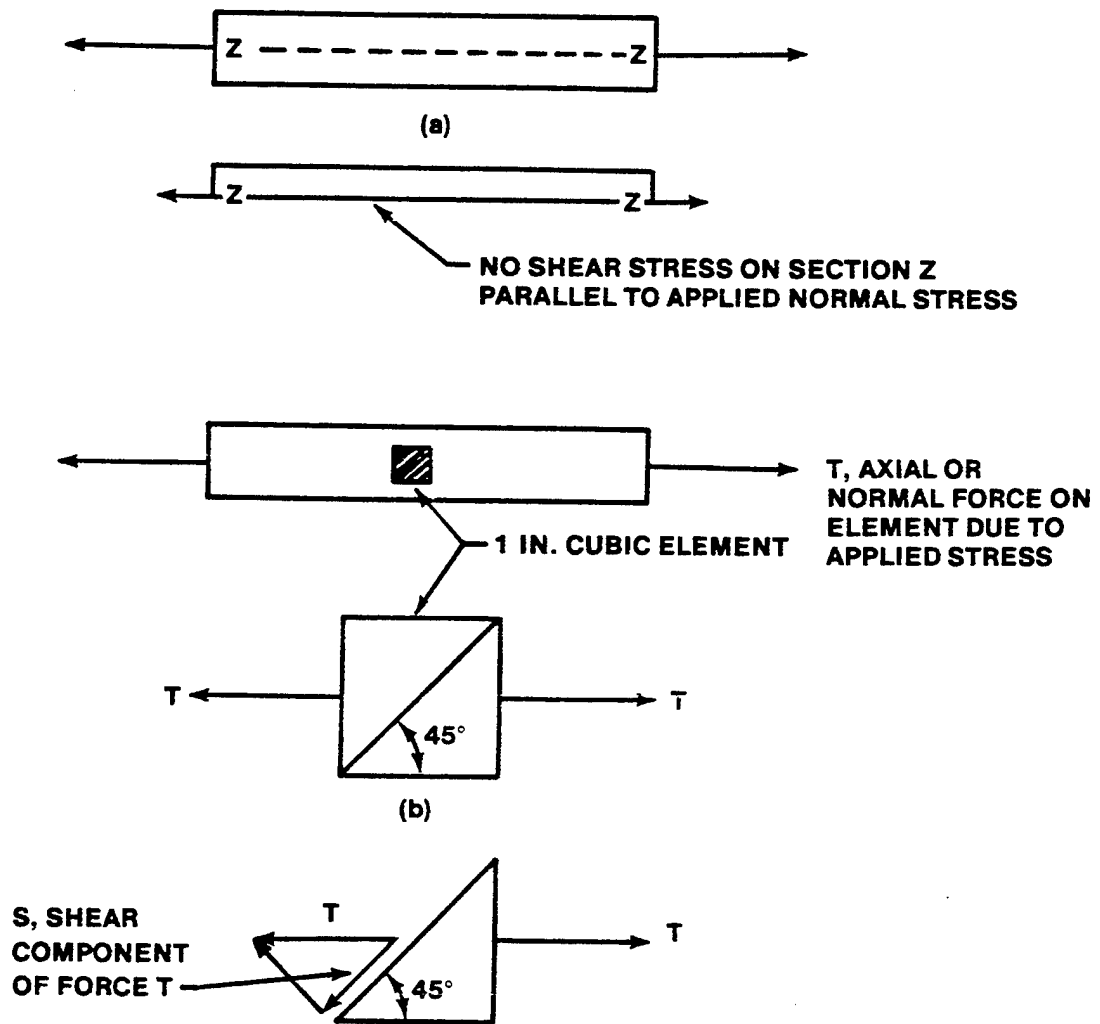


FIGURE 12.30. COMPONENT SHEAR STRESSES

To determine the magnitude of the maximum shear stress, it is best to take a one inch cube of material from the basic specimen and examine the forces existing in this element. There is applied to the sides of this one-

inch element (as in Figure 12.29B) a load which is the tensile stress on the specimen cross-section. Since the section or cut is to be located at 45° to the applied stress, the component of force distributed along the diagonal will be as follows:

$$\begin{aligned} S &= T \sin 45^\circ \\ S &= .707 T \end{aligned}$$

This shear force will be distributed over the diagonal surface which, for the one inch element, will be 1.414 inches. The shear stress is then

$$\begin{aligned} &= \frac{.707 T}{1.414} \\ &= .50 T \end{aligned}$$

Thus, an applied axial stress will produce a maximum component shear stress which is one-half the magnitude of the applied stress. Knowledge of the presence of the component shear stress and its existence as a maximum at 45° is basic to a discrimination between ductile and brittle failure types.

An example of the existence and orientation of the maximum component shear stress is provided in Figure 12.31 where two specimens of metal - one very ductile and one very brittle - are subjected to failing tensile loads. The brittle type material will fracture with a clean break at 90° to the direction of loading. The ductile specimen will exhibit fracture planes at 45° to the direction of the applied tensile stress thus verifying the existence of component shear stresses. This 45° type of fracture from pure tensile loads is referred to as the "ductile" or "shear" type of failure.

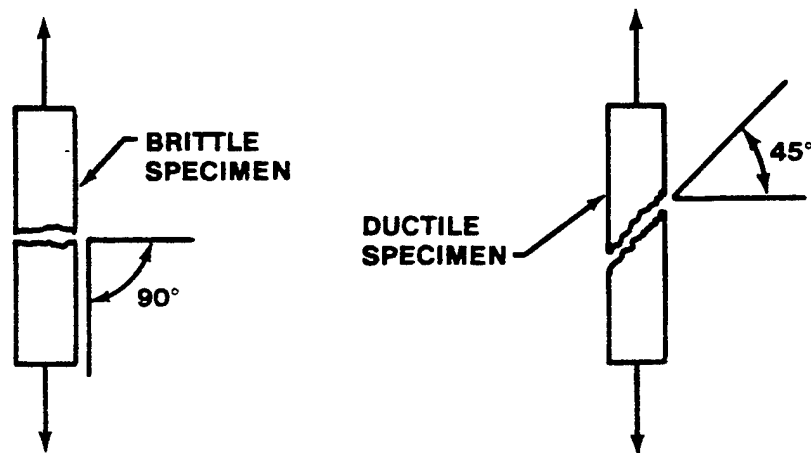


FIGURE 12.31. EFFECT OF DUCTILITY ON FRACTURE

The condition of an applied pure shear presents a different and slightly more complex problem concerning component and principal stresses. Consider a one inch cubic element subjected to pure shear (Figure 12.32).

If a Section A is taken at a diagonal of 45° in one direction, it is apparent that there must be a compression force on the diagonal to statically balance the action of the two shear forces applied along the edges of the element. The two shear forces have components at 45° which are additive and must be balanced.

$$C = S \sin 45^\circ + S \cos 45^\circ$$

$$C = (2) (.707) S$$

$$C = 1.414 S$$

Since the compression force is distributed along the diagonal the compression stress may be found as

$$\text{compression stress} = \frac{1.414 S}{1.414}$$

$$= 1.000 S$$

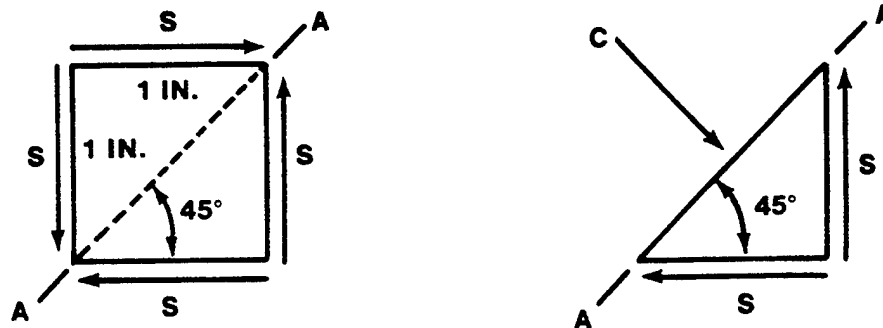


FIGURE 12.32. APPLIED PURE SHEAR - SECTION AA ANALYSIS

Thus, for the case of pure shear applied to an element, there exists at one 45° section a compression stress equal in magnitude to the applied shear stress. The existence of this component compression stress is evident in the failure mode of a thin walled tube subjected to a failing torsion load (torsion, of course, produces a uniform pure shear). If the walls of the tube are sufficiently thin, the tube will fail primarily in buckling due to the principal compression stress existing in the 45° direction.

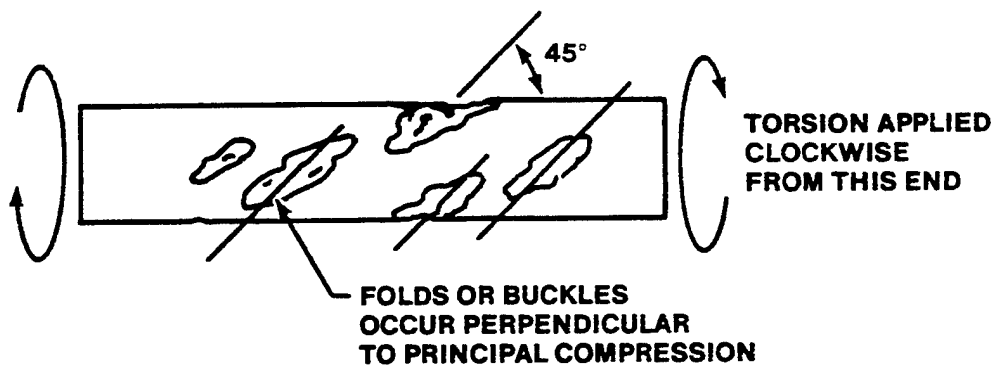


FIGURE 12.33. BUCKLING FAILURE DUE TO TORSION

If the same one-inch element of Figure 12.32 (shown in Figure 12.34) is subjected to the same pure shear condition - but sectioned along Plane B, a different stress situation results. If the element is cut along Section B, it is apparent that a tension force, T , must be sufficient to balance the components of the two shear forces along the edge. This situation will produce a tension stress distributed along the diagonal which is equal in magnitude to the applied shear stress. The presence of this tension stress is verified by the mode of failure of a brittle shaft in torsion (twisting a piece of chalk produces the same result) (Figure 12.35). In this case, a fracture will begin as a 45° spiral surface which is perpendicular to the principal tension stress.

It must be remembered that component stresses may have a definite bearing on the strength and mode of failure of any structure. Any normal or shear stress applied to a part will produce component and principal stress that cannot be neglected.

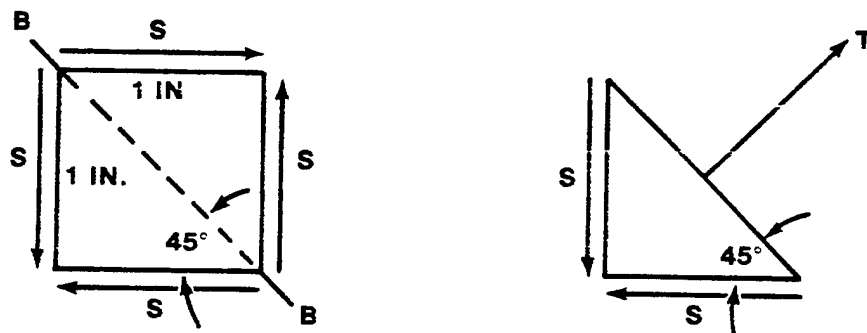


FIGURE 12.34. APPLIED PURE SHEAR - SECTION B-B ANALYSIS

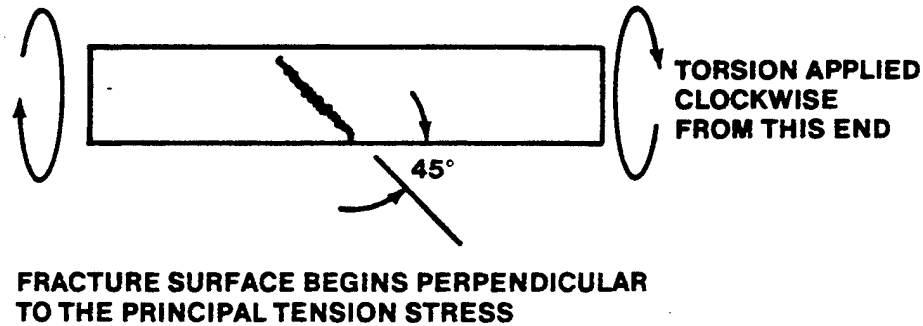


FIGURE 12.35. BRITTLE FAILURE DUE TO TORSION

12.4.10 Strain Resulting from Stress

Any structure which is subjected to stress must deform under load, even though the deformation may not be visible to the naked eye. Recall from the previous sections that stress is the true measure of state for a part subjected to load. Strain is a similar means of measure. In order to fully evaluate the state of being of a stressed material, all deformations must be considered on a unit basis. Strain is thus defined as deformation per unit of length and in most engineering terminology is referred to by "e" or "ε" (epsilon).

Suppose a steel bar 100 inches in length is subjected to a tensile stress of 30,000 psi - as in Figure 12.36. The total change in length throughout the 100-inch length would be about 0.1 inches. If subjected to uniform stressing, the part would be subjected to a uniform strain which is as follows:

$$\text{strain} = \frac{\text{total deformation}}{\text{original length}}$$

$$\epsilon = \frac{\Delta L}{L} \quad (12.23)$$

$$\epsilon = \frac{0.1 \text{ in}}{100 \text{ in}}$$

$$\epsilon = .001 \text{ inches per in}$$

To produce a total deformation of 0.1 inches in 100 inches of length, the strain must be .001 in/in or 0.1%.

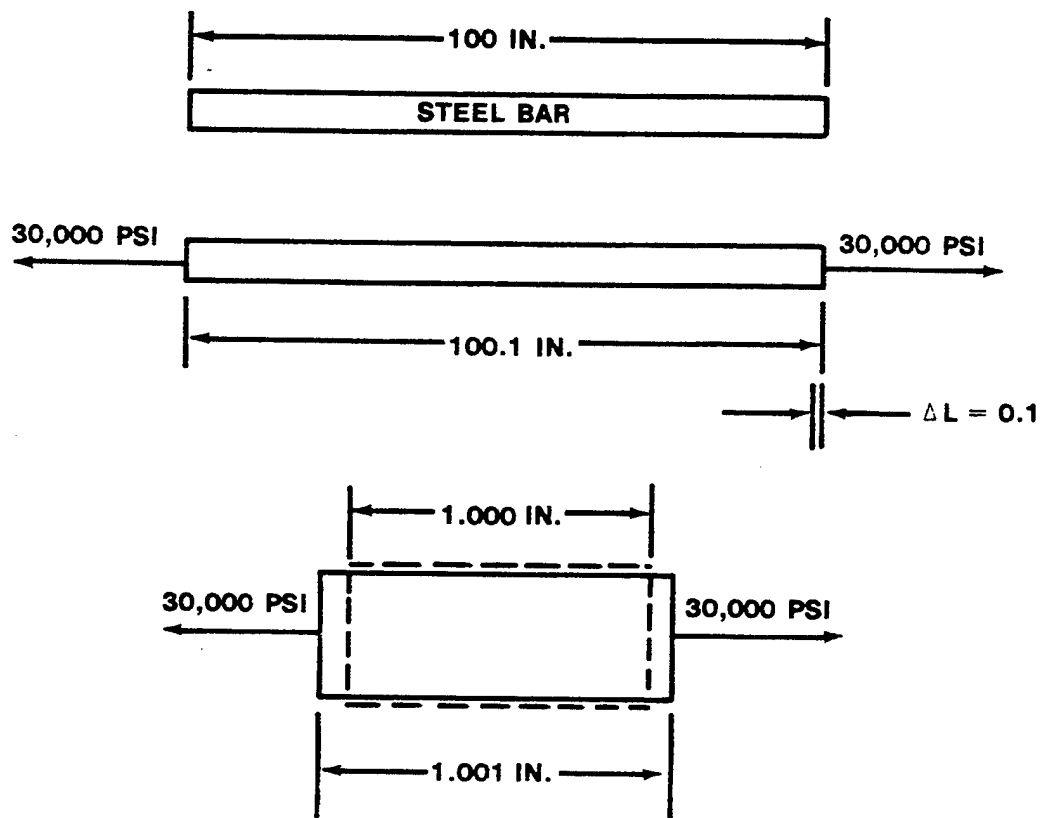


FIGURE 12.36. AXIAL STRAIN

In addition to the longitudinal strain of the part shown in Figure 12.36, there will be a lateral contraction of the metal. For most metals there is a definite relationship between this transverse strain and the longitudinal strain and it is important when considering combined stresses that are dependent upon deflections. The proportion between the lateral strain and the longitudinal strain has been given the name "Poisson's ratio, μ ($\mu\mu$)" and for most homogenous metals this ratio has the approximate magnitude of 0.3 ($\mu = 0.3$). In the case of the previous example the longitudinal extension strain of .001 would be accompanied by a lateral contraction strain of .0003.

Thus, it is important to remember that any metal subjected to stress must strain. The amount of strain, while not necessarily visible, must be present

and is very important. Just as large stresses may produce numerically small strain, any small strain forced on a structure may produce large stresses.

Shear stress also produces shear strains. Shear strain, while not necessarily denoting a change in length, does describe a change in relative position of the part. Figure 12.37 should illustrate this fact.

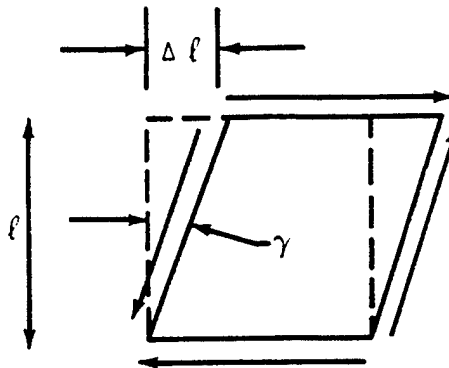


FIGURE 12.37. SHEAR STRAIN

Shear strain is most properly described by the angle of strain, γ (gamma) in radians. When a shear stress is applied to an element, the shear strain, γ , can be computed as the proportion of the change in position of one side, Δl , to the original length, l .

$$\gamma = \frac{\Delta l}{l} \quad (12.24)$$

One of the most important properties of an aircraft material is its stiffness. If a part were subjected to a particular level of stress, small strains would indicate a stiff or rigid material; large strains would indicate a flexible material. The accepted method of measuring the stiffness or rigidity of a material is to compute a proportion between the applied axial stress and the resulting axial strain. This proportion is known as the "Modulus of Elasticity" or "Young's Modulus" and is denoted by the letter, E .

$$E = \frac{\sigma}{\epsilon} \quad (12.25)$$

where E = modulus of elasticity, psi

σ = stress, psi

ϵ = strain, in/in

Typical values for this Modulus of Elasticity are

Steel E = 30,000,000 psi

Aluminum Alloy E = 10,000,000 psi

Magnesium Alloy E = 7,000,000 psi

By a comparison of these values it is seen that an aluminum alloy part subjected to a given stress would strain three times as greatly as a steel part subjected to the same stress level.

There is no true modulus of elasticity in shear. However, for computing shear deflections there exists an equivalent quantity known as the "modulus of rigidity" or "shear modulus" and is denoted by the letter G.

$$G = \frac{\sigma_s}{\gamma} \quad (12.26)$$

where G = modulus of rigidity, psi

σ_s = shear stress, psi

γ = shear strain, in/in

For most metals the shear modulus is approximately 40% of the elastic modulus - e.g.

Steel G = 12,000,000 psi

Aluminum Alloy G = 4,000,000 psi

For homogenous materials the Modulus of Rigidity may be determined by the following equation:

$$G = \frac{E}{2(1+\mu)} \quad (12.27)$$

where G = Modulus of Rigidity

E = Modulus of Elasticity

μ = Poisson's ratio

Bending stresses will cause bending deflections. In this case, no general strain relationship can be defined that is similar to simple axial strain. Since bending stresses do vary throughout the cross-section there will be a variation of axial strains proportional to the axial stress.

For the initially straight beam that is shown in Figure 12.38, an applied pure bending moment will produce a deflection of pure curvature.

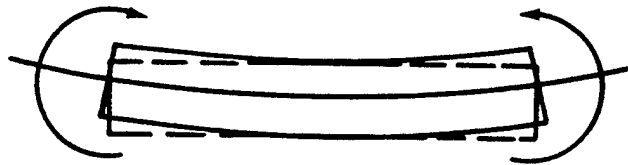


FIGURE 12.38. PURE CURVATURE

Pure bending imposed will cause compression strains on the lower surface, and zero strain at the neutral axis. The result of these strains is a bending of the beam to the arc of a circle with no change in length of the neutral axis. Of course, if one end of the beam is held stationary the other end deflects upward - but only because of the curvature of bending (Figure 12.39).

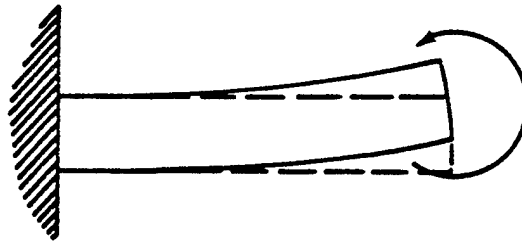


FIGURE 12.39. BENDING DEFLECTION OF CANTILEVER BEAM

A somewhat similar condition exists for a length of shaft subjected to a pure torsion loading. The shear stress distributed on the cross-section will produce shear strains, which are angular displacements. The net effect is to produce a uniform twist throughout the length of the shaft. If a straight line were to be drawn on the shaft, as in Figure 12.40, this line would be displaced upon load application and would finally occupy the position indicated by the dotted line. The helix angle of displacement would depend upon the shear strains developed at the surface of the shaft.

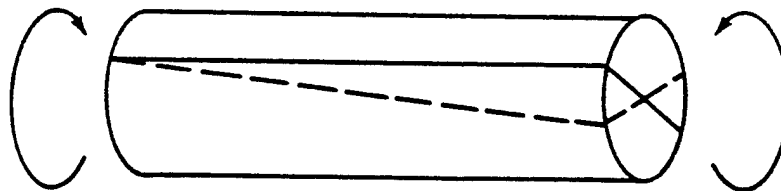


FIGURE 12.40. ANGULAR DISPLACEMENT DUE TO TORSION

Actually, only two factors determine the strain for a particular material subjected to stress. One, of course, is the magnitude of stress; the second is the type of material and characteristic stiffness. The actual amount of

deflection of a loaded structure will depend on the physical arrangement of the structure and the cumulative effect of the local strains existing in various components of the structure.

12.4.11 Stress-Strain Diagrams and Material Properties

In order to evaluate the properties of a material and the possible structural application, it is necessary to determine strains corresponding to various levels of applied stress. Laboratory tests are then conducted which subject a specimen of material to various magnitudes of stress while strains are recorded at each stress. If the stresses and corresponding strains are then plotted on a graph, many useful and important properties of the material may be observed.

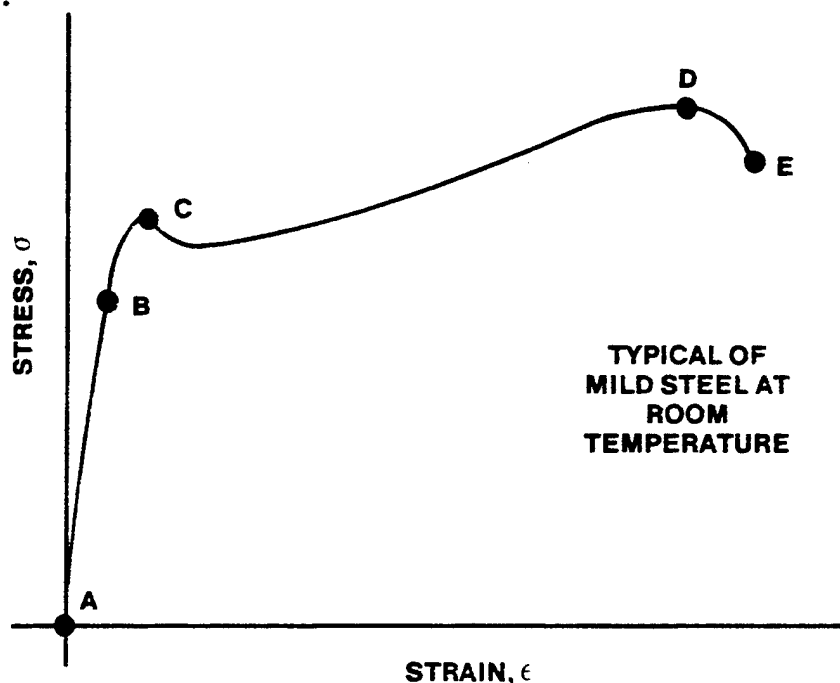


FIGURE 12.41. STRESS-STRAIN DIAGRAM OF TYPICAL MILD STEEL

Figure 12.41 shows a typical "stress-strain" diagram for a mild steel at room temperature. As the stress is first applied and increased, the strain begins and increases in direct proportion to the stress - i.e., the stress-strain diagram is a straight line from A to B; therefore, this material would snap back to zero strain upon the release of stress. Because of the elastic nature of the material in this range of stress, the stress range from A to B is referred to as the "elastic or proportional range" of the

material. This definition then implies that stresses up to Point B will not cause permanent deformation of the material.

If the applied stress is gradually increased above the value at Point B, the plot of stress vs. strain will deviate slightly from a straight line. There will then be some small - but measurable - permanent strains thus incurred. Hence, Point B is the end of the elastic or proportional range of the material and the value of stress at Point B is termed the "elastic or proportional limit; σ_p ."

Should the stress be gradually increased up to Point C, a noticeable yielding of the material will be apparent; at Point C the strain suddenly increases without further increase in stress. In fact, with most ductile steels, there may be a decrease in stress resisted by the material as large plastic strain takes place. It is obvious that any stress above the value at Point C will produce very large and objectionable permanent strains. To verify this condition, assume that a stress is applied up to Point X on the diagram in Figure 12.42. The strain at this point is quite large. If the stress were to be released, the material would "relax" along the dotted line shown which is parallel to the original straight line from B to A. At Point Y the stress is again zero but a large permanent deformation has taken place. The value of stress at Point C is logically termed the "yield point" or "Yield stress, σ_y ", of the material and is the stress beyond which large and objectionable permanent strains take place.

The stress-strain diagram of Figure 12.42 does show that the material is capable of withstanding stresses greater than the yield stress - but not without large permanent strains. If the stresses above Point C are gradually applied, the material will continue to withstand higher and higher stresses until the very ultimate strength capability is reached at Point D. If any attempt is made to subject the specimen to a stress greater than the value at Point D, failure will begin and will be complete at Point E. Since the value of stress at Point D is the very highest stress the material can withstand without failure, it is termed the "ultimate strength" or "ultimate stress, σ_U ", of the material.

The two most important strength properties which are derived from the stress-strain diagram are the "yield strength" and the "ultimate strength." There is a direct analogy between these two properties and the operating

strength limitations of an airframe structure. If the material shown on the stress-strain diagram is never subjected to a stress above the yield point, no significant or objectionable permanent strains will take place; if an airframe structure is never subjected to a load condition greater than the "limit" load, no significant or objectionable permanent deformations will be incurred. If the material shown in the stress-strain diagram were subjected to a stress above the yield point, large and undesirable permanent strains will take place; if an airframe is subjected to a load condition greater than the "limit" load, undesirable permanent deformation of the structure may be anticipated, e.g., permanently distorted fuselage, bent wings, deformed tanks, etc. If an attempt is made to subject a material to a stress greater than the ultimate, failure will then occur; if any flight condition is attempted which produces loads greater than "ultimate" load, actual failure of the airframe is imminent.

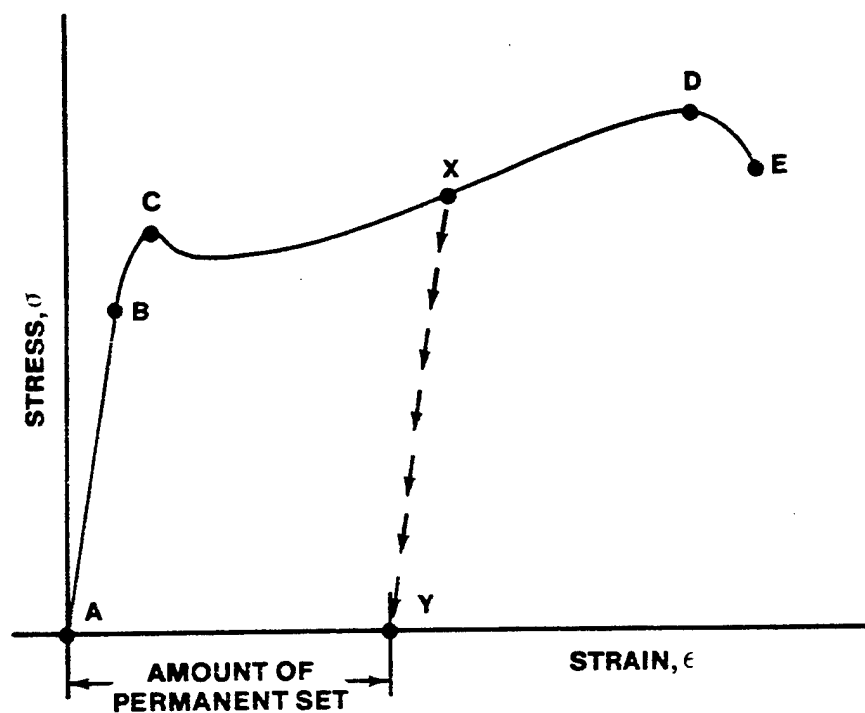


FIGURE 12.42. PERMANENT SET

The basic stress-strain diagram of Figure 12.43 readily defines five of the most important static strength properties of a material:

1. The elastic or proportional limit is the end of the elastic region of the material. A part subjected to stresses at or below the proportional limit will experience no permanent deformation. Upon the release of stress the part will snap back to the original unstressed shape.

2. The yield strength is the highest practical value of stress to which a material should be subjected. Stresses between the proportional limit and the yield point will cause only slight and hardly measurable permanent deformation. Any stress above the yield point will result in large and objectionable permanent deformation.
3. The ultimate strength is the very maximum of stress which a material can withstand without failure. Extremely large and undesirable permanent deformations will ordinarily result when this point is approached.
4. The fracture point, or the effective stress at time of failure, is determined primarily to evaluate the manner of fracture and the ductile quality of the material.
5. The total strain or total elongation of the material at the point of fracture is an indication of the ductility of the material. Any metal which would have less than five per cent elongation in a two inch test length is considered to be brittle - ordinarily too brittle to be applicable to an ordinary aircraft or missile structure.

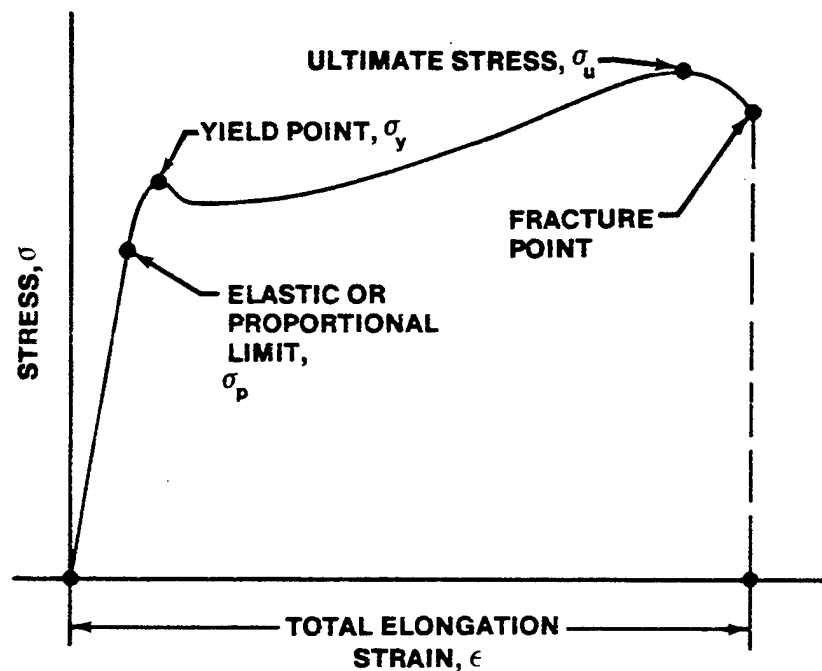


FIGURE 12.43. DEFINITION OF STATIC MATERIAL PROPERTIES

At this point, it is appropriate to present some of the variations in the stress-strain diagrams due to manner of loading or material type. One point to consider is that stress-strain diagrams are not usually used in connection with shear properties of a material. The proportional limit, ultimate strength, etc., in shear are not true properties because of "section or form" considerations. Cross-section dimensions and area distribution will cause significant variations in the shear strength capabilities.

Many materials used in aircraft construction (aluminum alloys, magnesium alloys, and some steels) do not exhibit a definite yield point or a distinct proportional limit. Figure 12.44 illustrates this fact. In such an instance it is necessary to define the yield point and proportional limit as a given departure from the original straight line of 0.0001 in/in. The yield stress is determined as the stress which produces a departure from the original straight line of 0.002 in/in (Figure 12.45). In this case an applied stress equal to the yield stress would result in a permanent set of 0.2%. This amount is considered admissible for ordinary purposes.

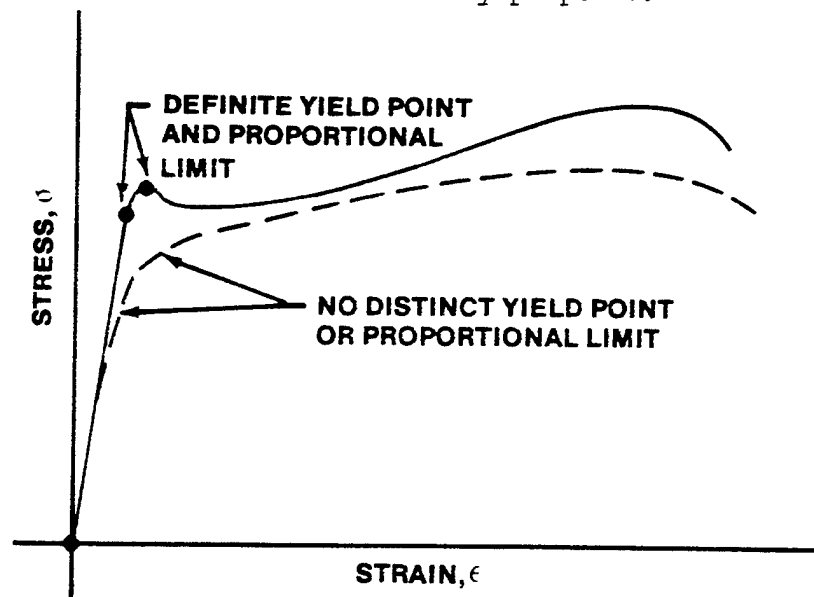


FIGURE 12.44. VARIATIONS IN STRESS-STRAIN RELATIONSHIPS

Compression stress-strain diagrams are similar to tension stress-strain diagrams except that the departure from proportionality generally occurs sooner and more gradually. Compression stress-strain diagrams are more difficult to obtain correctly because of buckling of the specimen. As

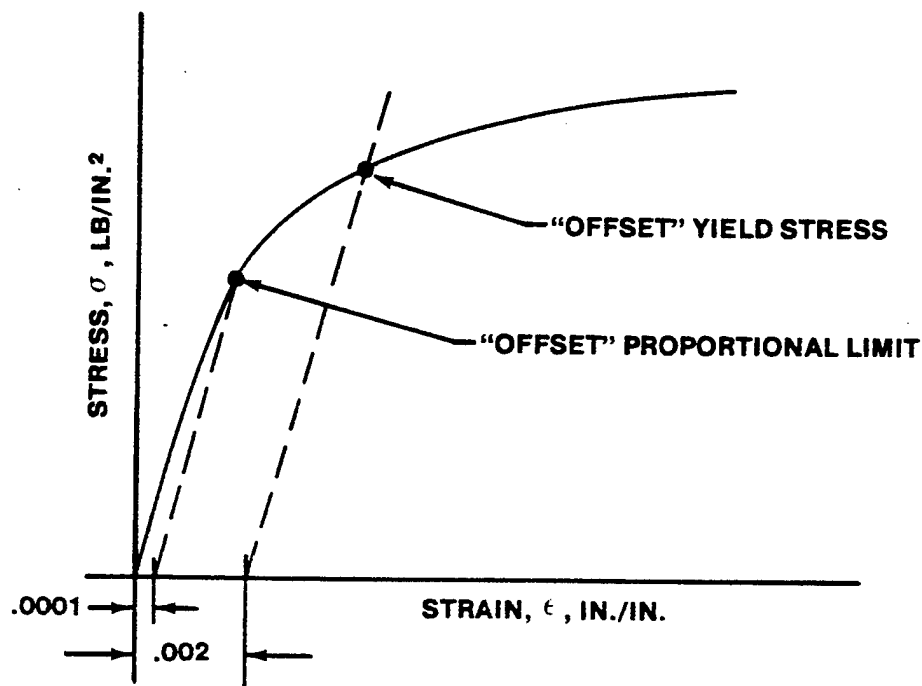


FIGURE 12.45. DEFINITION FOR VARIANT STRESS-STRAIN RELATIONSHIP

compression buckling of a specimen constitutes a failure, it is obvious that compression ultimate strength is not true property and could not be determined as a specific quality of a metal. The stiffness of a metal and the physical arrangement of the structure combine to decide the stability of the structure when subjected to compression loads (Figure 12.46).

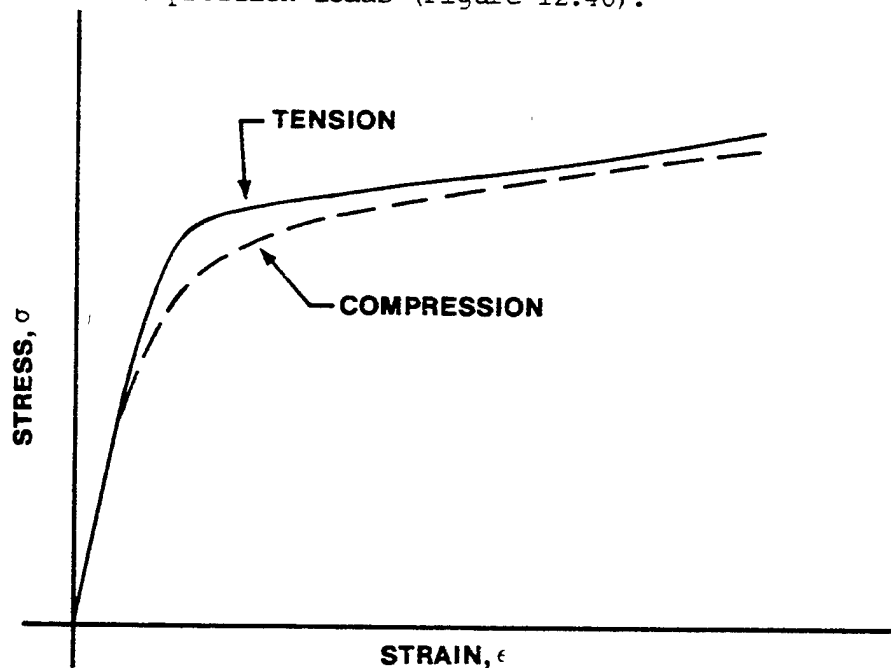


FIGURE 12.46. COMPRESSION STRESS-STRAIN COMPARISON

In order to determine other material properties expressed by the stress-strain diagrams a closer examination must be made of certain areas of the stress-strain diagram.

By an inspection of the straight line portion of the stress-strain diagram, an evaluation may be made of the inherent stiffness of the material. In the elastic range of a material the proportion between stress and strain is the Modulus of Elasticity (sometimes called "Young's Modulus") and the magnitude of this proportion is a direct measure of the inherent stiffness. A high value for the Modulus of Elasticity will indicate a very stiff or rigid material while a low value indicates low stiffness or greater flexibility (Figure 12.47).

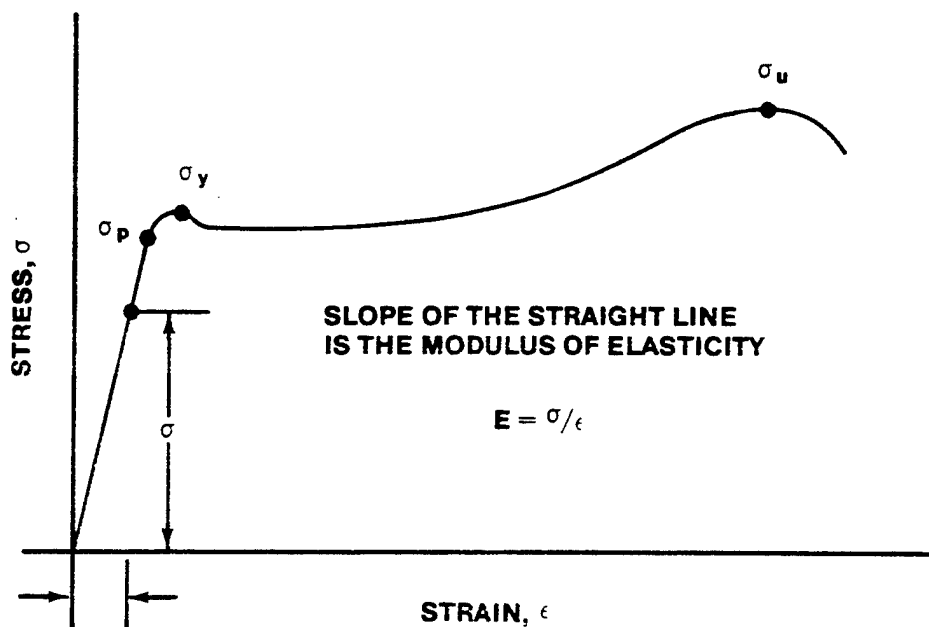


FIGURE 12.47. DEFINITION OF MODULUS OF ELASTICITY

When the stress-strain diagrams for three different materials are compared, the difference in the slopes and the proportions of inherent stiffness are readily apparent as shown in Figure 12.48.

Only two solutions exist: (1) lower the value of the operating stress or (2) change to a material type which has a higher elastic stiffness (higher E).

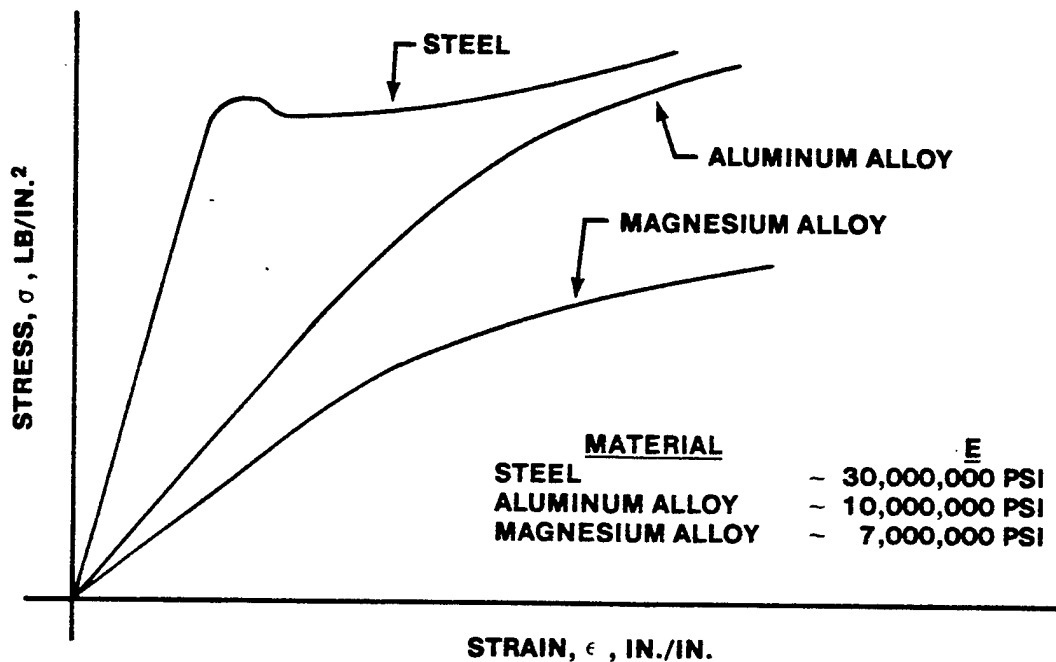


FIGURE 12.48. MODULES OF ELASTICITY COMPARISON

One important point to consider is that the Modulus of Elasticity, E , cannot be altered by heat treatment or changed any significant amount by use of a different alloy. Thus, the Modulus of Elasticity is an intrinsic property of the type of metal. Figure 12.49 shows the typical stress strain diagrams for steel in various conditions of heat treatment. Notice that the origin of each has the same slope. While the strength and ductility are changed by heat treatment, the stiffness of the elastic material remains unaltered. Increasing hardness by heat treatment will simply increase the stress at which plastic flow begins. Thus, if elastic deflections of a part which are excessive already exist, the problem will not be solved by heat treatment of changing alloy.

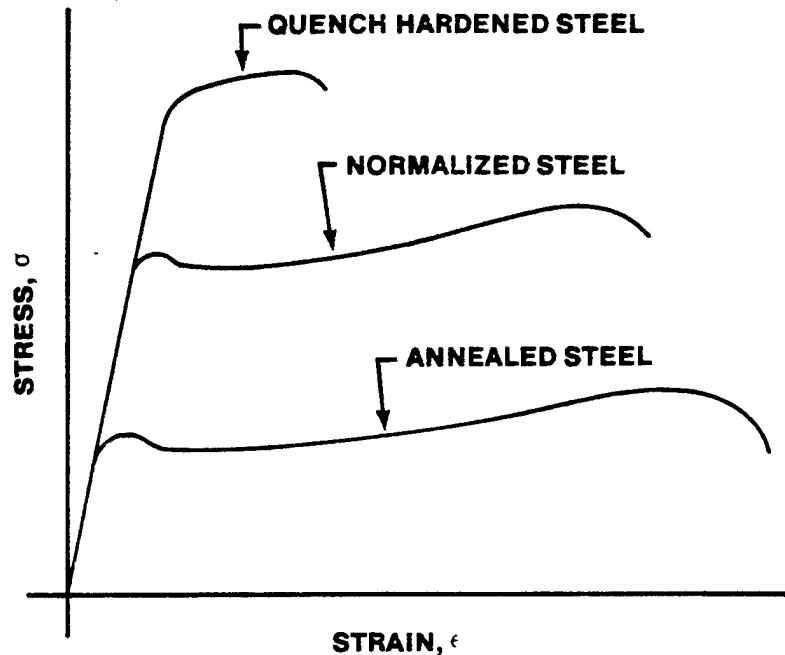


FIGURE 12.49. EFFECTS OF HEAT TREATMENT

Actually, the elastic modulus of a given metal will vary only with temperature, elevated temperature producing a lower Modulus of Elasticity. For example, a high strength aluminum alloy at 600° F will exhibit a Modulus of Elasticity which is only one-half the value shown at room temperature.

The elastic range of a material is the area of most general interest for ordinary structural investigation. However, when investigating the phenomenon of buckling of short columns and the behavior of structures at loads near ultimate, the stiffness of a metal in the plastic range is of particular interest. As was previously noted, the proportion between stress and strain is defined as the Modulus of Elasticity. At any stress below the proportional limit, this proportion is one fixed and constant value. Above the proportional limit, this proportion is one fixed and constant value. Above the proportional limit, this definition results in a proportion which is known as the "secant Modulus". Once beyond the proportional limit, the proportion between stress and strain will noticeably decrease. Hence, the Secant Modulus will have a value lower than the Modulus of Elasticity. Another method of measuring the stiffness in the plastic range is the slope of a line drawn tangent to the stress-strain diagram at some stress above the proportional limit. The slope of this tangent line defines a value known as the "Tangent

Modulus". The Tangent Modulus then measures an "instantaneous" stiffness while the Secant Modulus measures a "gross" or "cumulative" stiffness. Figure 12.50 gives the procedure of calculation of these properties and Figure 12.51 illustrates the typical variations of the Secant and Tangent Modulus for an aluminum alloy.

The loss of stiffness in the plastic range is appreciated when it is realized that small changes in stress will produce larger changes in strain than in the elastic region.

The energy storing and energy absorbing characteristics are of particular importance in defining the properties of a material. Any stress produced in a material requires the application of a force through a distance and, as a consequence, a certain amount of work is done. Consider a cubic inch element of steel with a gradually applied stress of 30,000 psi (as in Figure 12.52). As the stress is gradually increased from zero to 30,000 psi, the strain gradually increases from zero to

$$G = \frac{\sigma}{E} = \frac{30,000}{30,000,000} = .001 \text{ in/in}$$

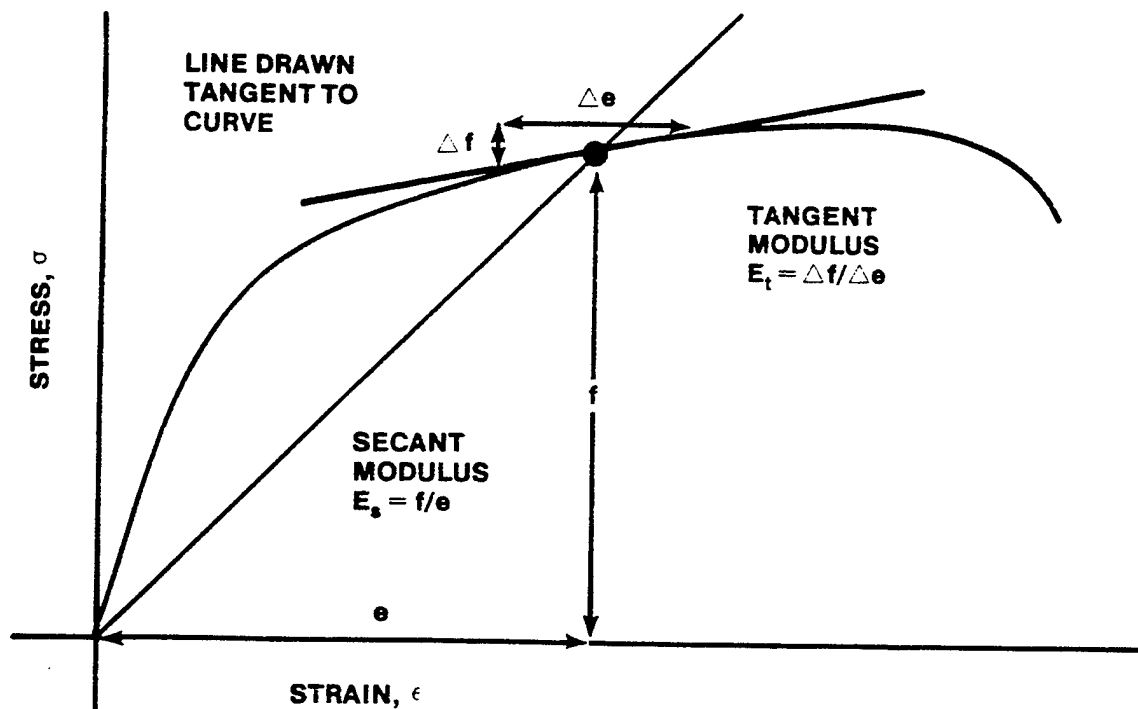


FIGURE 12.50. DEFINITION OF SECANT AND TANGENT MODULI

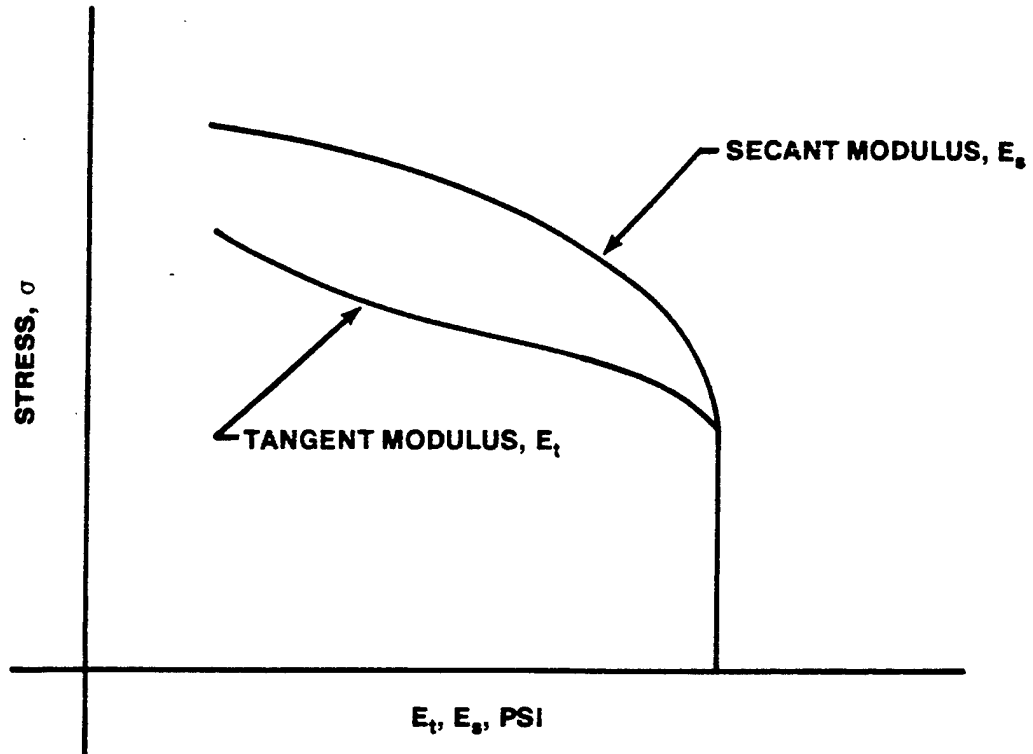


FIGURE 12.51. VARIATION OF SECANT AND TANGENT MODULI

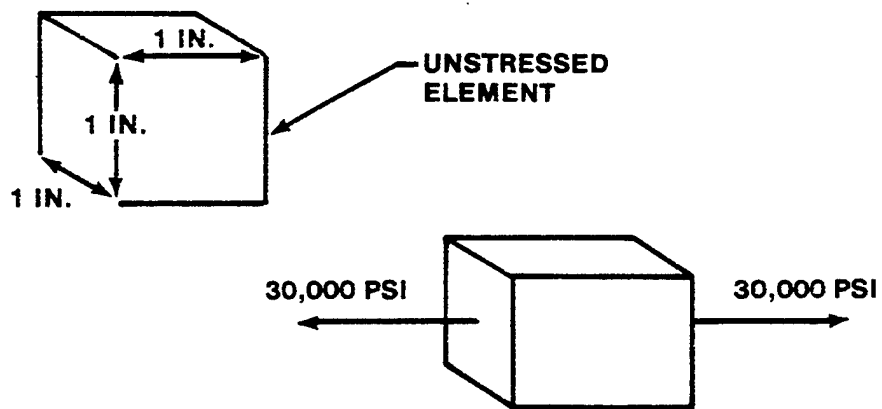


FIGURE 12.52. APPLICATION OF STRESS

The work done during this gradual stressing is the product of the average force and the distance.

$$\begin{aligned}\text{Work done} &= \left[\frac{30,000}{2} \frac{\text{lb}}{\text{in}^2} \right] \times \left[.001 \frac{\text{in}}{\text{in}} \right] \\ &= 15 \frac{\text{in-lb}}{\text{in}^3}\end{aligned}$$

Thus, 15 inch-pounds of work would be required to produce the final stress of 30,000 psi in the cubic inch element. This amount of work is actually represented by the area enclosed on the stress-strain diagram at this particular stress level (Figure 12.53). This area principle is then used with the stress-strain diagram to describe the energy properties of a material.

If a material is stressed to the proportional limit, all work done in producing this stress is stored elastically in the material. Therefore, the area under the straight line portion of the stress-strain diagram is a direct measure of the energy storing capability and is referred to as the "Modulus of Resilience". Of course, the manner of loading-tension, compression, shear, etc., must be specified since the work done will be different depending on the manner of loading.

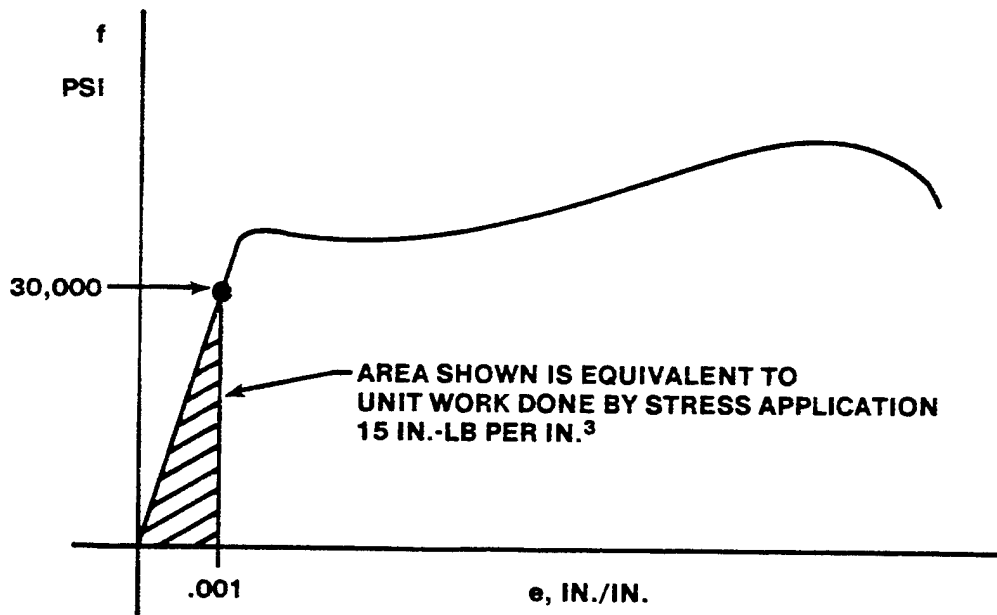


FIGURE 12.53. WORK DONE BY STRESS APPLICATION

If a material were stressed all the way to failure, the entire area under the stress-strain diagram is a measure of the work required to fail the material. The toughness or energy absorbing quality of the material is evaluated in this manner.

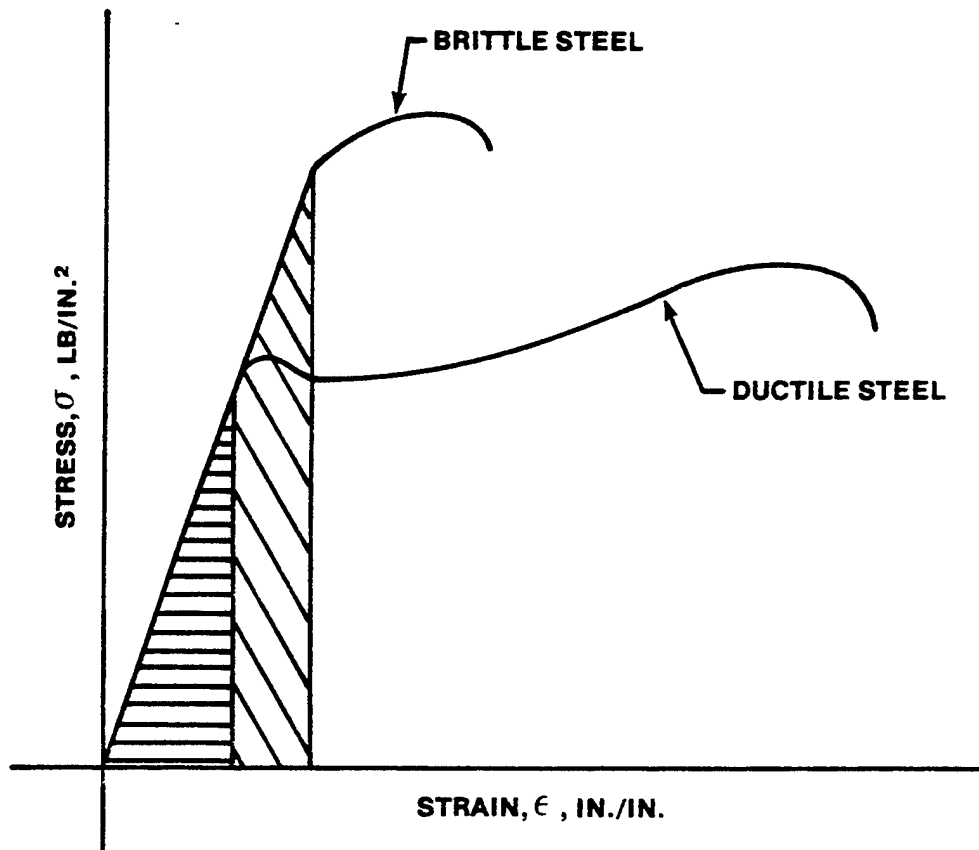


FIGURE 12.54. ENERGY STORING CAPABILITIES (RESILIENCE) OF DUCTILE AND BRITTLE STEELS

A comparison of the stress-strain diagrams for a ductile and brittle steel should define the properties of "resilience" and "toughness". The shaded areas shown in Figure 12.54 denote the energy storing capabilities for the ductile and brittle steels. The brittle material has the higher elastic limit and consequently a higher "Modulus of Resilience". The shaded areas of Figure 12.55 denote the energy absorbing capabilities of the same materials. The ductile material, while having lower strengths, develops much greater strains. As a result, the ductile material will require a greater amount of work to produce failure and is then the tougher material. The additional work

required to break the softer, more ductile, material goes into forcing the metal particles to slip relative to each other. When a specimen of ductile material is fractured during a laboratory test, this effect may be appreciated by handling the broken specimen of ductile material immediately after failure. A ductile specimen will be warm to the touch as the work absorbed by the material is converted into heat.

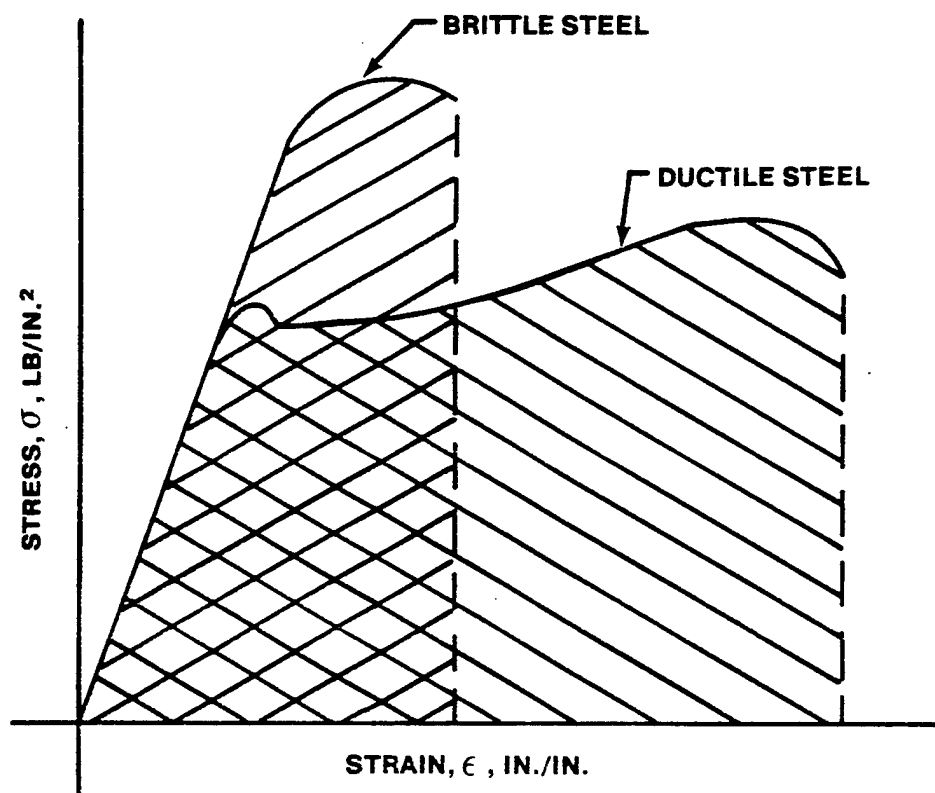


FIGURE 12.55. ENERGY ABSORBING CAPABILITIES (TOUGHNESS) OF DUCTILE AND BRITTLE STEELS

It may seem strange that it is possible to fail the more ductile metal at a lower stress but still require that more work be done. If so, remember that work is the product of average force and distance.

It would be desirable for a structural material to have a high yield point, high resilience, high ultimate strength, and also high toughness. However, materials which have very high strength usually have low ductility and low toughness. The balance between the strength requirements and

toughness (or energy absorbing) requirements will depend on the particular application in a structure. As examples of the two extremes consider: (1) a reciprocating engine valve spring and (2) protective crash helmet or protective headgear. In the fabrication of a valve spring, a material must be selected which has very high strength and great resilience. Such a material would necessarily have low toughness but in such an application toughness is unimportant and resilience is given primary consideration. In the construction of a true protective crash helmet or hard hat, sharp impact blows first must be distributed then the energy of impact absorbed as far as is possible. This requires a thickness of a crushable material for the inner lining which has high toughness per unit weight. Actual strength is not necessarily a factor since energy absorption requirements predominate.

The stress-strain diagram of a material will then furnish all necessary information to determine the static strength properties. Actually there are 10 important points of information that may be gained from an inspection of the stress-strain diagram. As shown in Figure 12.56 these points are as follows:

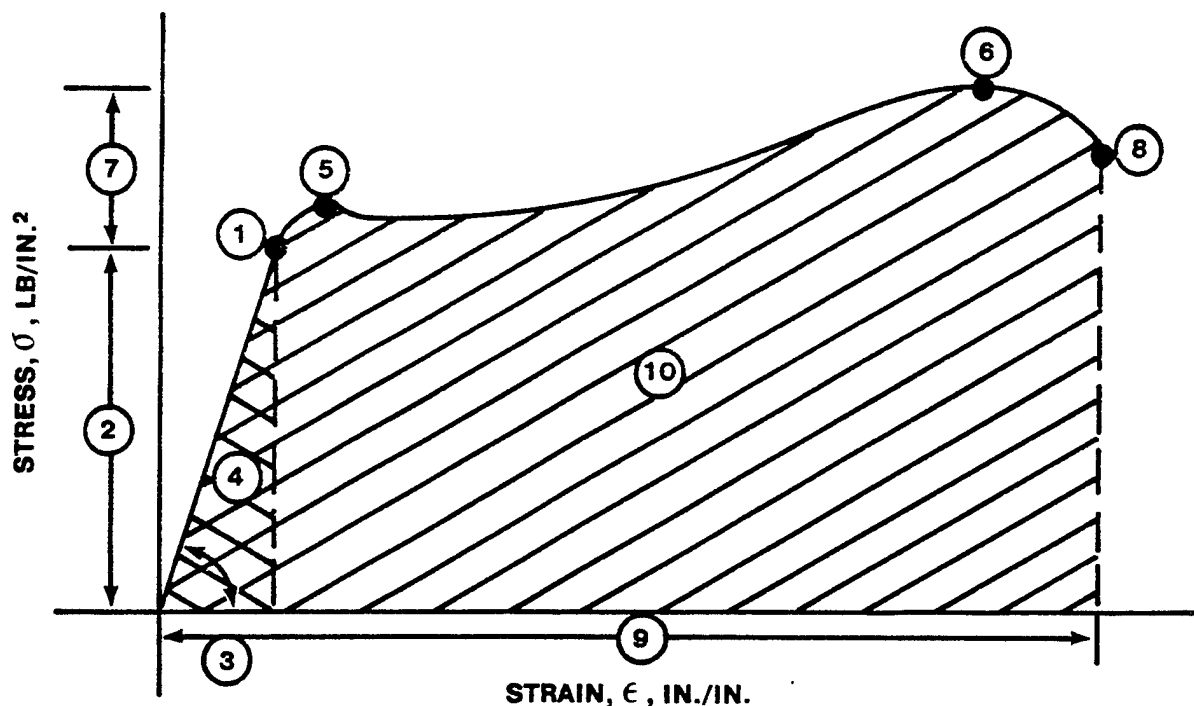


FIGURE 12.56. STATIC STRENGTH PROPERTIES

- (1) The proportional limit is the stress which denotes the end of proportionality between stress and strain. If not clearly defined, 0.0001 in/in offset is used.
- (2) The elastic range of stress is the range of stress and strain up to the proportional limit.
- (3) The Modulus of Elasticity is the slope of the straight line portion of the stress-strain diagram. This slope measures inherent stiffness. Beyond the proportional limit, the Secant or Tangent Modulus will be appropriate.
- (4) The resilience is measured by the area under the straight line portion of the stress-strain diagram. This indicates ability to store energy elastically.
- (5) The yield stress is the value of stress above which objectionable amounts of permanent strain are incurred. If not clearly defined, 0.002 in/in offset is used.
- (6) The ultimate strength is the very highest stress that the material can withstand without failure. This represents the maximum load-carrying capability for static loads.
- (7) The plastic range of stress is between the proportional limit and the ultimate stress. Permanent strains occur in this area. Below the yield stress these permanent strains are relatively small and insignificant; above the yield stress these permanent strains are large and objectionable.
- (8) The fracture point is the effective stress at time of failure. It is noted primarily to evaluate the manner of failure and the ductile quality of the material.
- (9) The total elongation is a measure of ductility. If less than five percent in a two inch specimen length, the material is considered brittle.
- (10) The toughness of a material is represented by the total area under the stress-strain diagram. This indicates the amount of work required to fail the material and denotes energy absorption capability.

An interesting phenomenon in connection with the stress-strain diagram is "work hardening" or "strain hardening". Suppose that a material is subjected to a stress beyond the yield point and then released. If stress is subsequently reapplied, the new stress-strain diagram will be a straight line up to the point where stress was released and then it continues along the original curve. Figure 12.57 illustrates this process. The material which

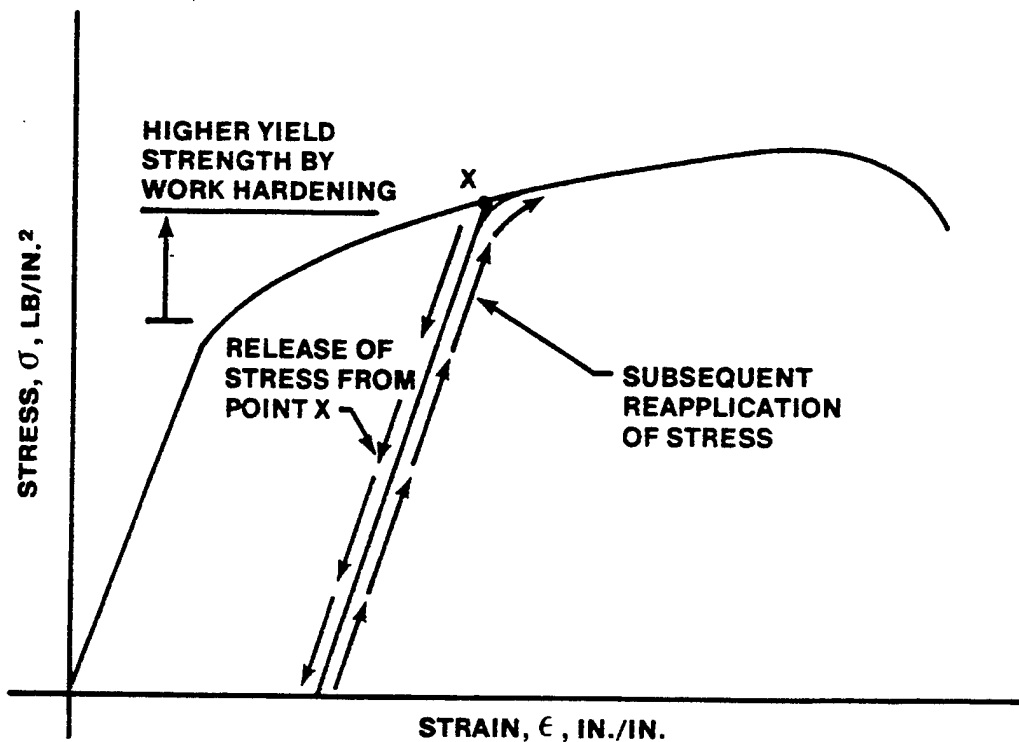


FIGURE 12.57. WORK HARDENING

has been permanently stretched will then have higher proportional and yield strengths. Many of the typical aircraft materials - aluminum alloys, stainless steels, etc. - are work hardened to produce these beneficial gains in strength properties. Of course, the work hardening must be limited to prevent loss of ductility and the formation of flaws and fissures.

The effects of ductility and the plastic range of stress are quite significant in predicting the failing load of a structure. The ultimate stress has been defined previously at the maximum stress a material will withstand without failing. This stress is designated as the "tension ultimate" (σ_{t_u}) or "shear ultimate" (σ_{s_u}) depending on the manner of loading and is determined by tests of small specimens. If these values of strength are used to predict the ultimate strength capability of large sections in bending and torsion, noticeable errors may result. An elastic stress distribution in bending may be predicted by the following relationships:

$$\sigma_b = \frac{My}{I}$$

where σ_b = bending stress, lb/in²

M = applied bending moment, in-lb

y = element distance from neutral axis, in

I = moment of inertia of the cross-section, in⁴

Such stress distribution is linear - varying directly with the element distance from the neutral axis, y . A typical elastic stress distribution is shown in Figure 12.58. Whenever stresses are produced which are beyond the proportional limit of the material, the bending stress distribution tends to remain linear but due to the loss of proportionality between stress and strain in the plastic range, the stress distribution is non-linear. Figure 12.59 shows a typical stress distribution resulting from bending loads which create stresses in excess of the proportional limit.

Notice that for a given maximum stress at the outer fiber, the inelastic bending stress distribution requires a greater applied bending moment than the elastic stress distribution. The reason for this is that the outer fibers begin to yield allowing the underlying fibers to develop a stress higher than predicted by elastic theory. Thus, the use of the equation

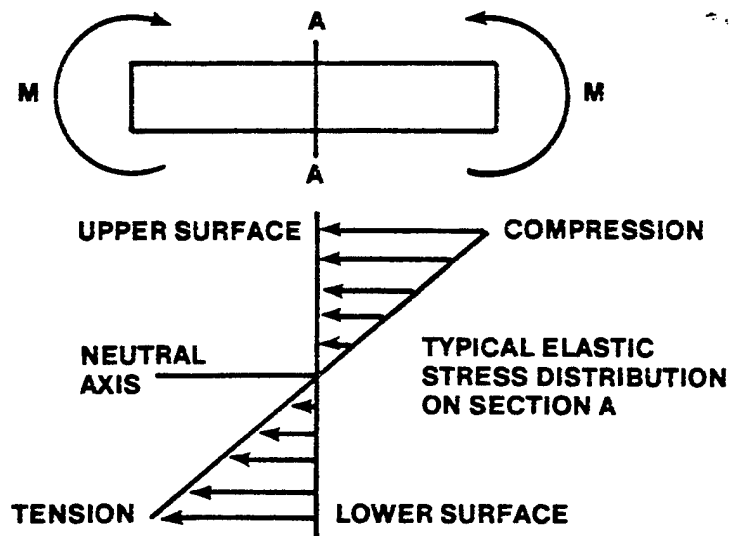


FIGURE 12.58. ELASTIC STRESS DISTRIBUTION

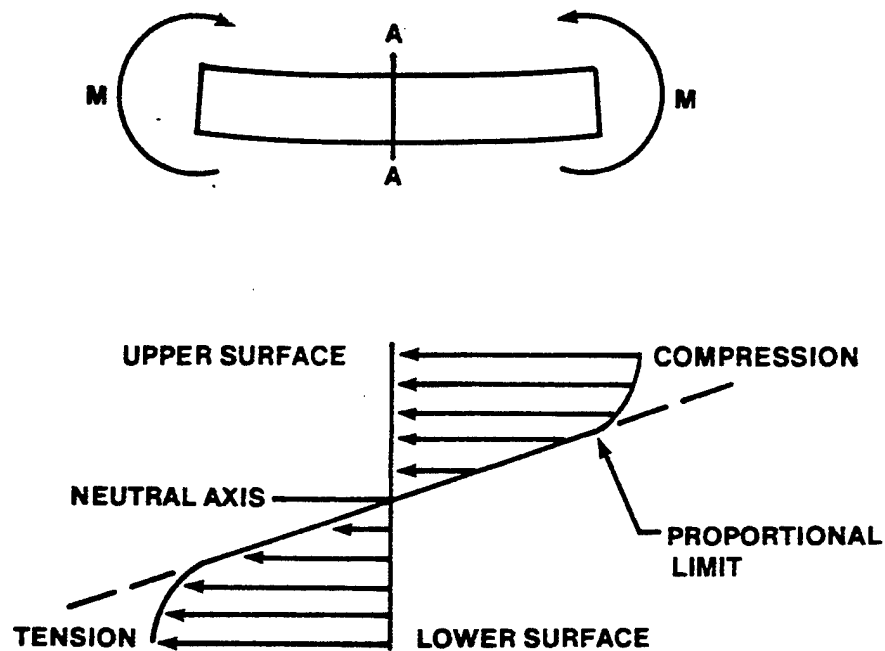


FIGURE 12.59. PLASTIC (NON-LINEAR) STRESS DISTRIBUTION

$$\sigma_b = \frac{Mc}{I}$$

to compute the maximum bending stress is valid only for maximum stresses which do not exceed the proportional limit. In order to predict the failing load of a structure in bending, the same form of equation may be used with a fictitious ultimate stress referred to as the "bending modulus of rupture", σ_b . This bending modulus of rupture is defined by the following equation:

$$\sigma_b = \frac{M_b c}{I}$$

where σ_b = bending modulus of rupture, lb/in²

M_b = bending moment to cause failure, in-lb

c = distance to critical outermost element, in.

I = section moment of inertia, in⁴

If the material is ductile and no buckling of the section occurs, the bending modulus of rupture will be some value greater than the tensile ultimate strength. In a perfectly ductile, stable cross-section the bending modulus of rupture could be 1.5 times the tensile ultimate; in a very brittle, stable cross-section the bending modulus of rupture would be equal to the tensile ultimate. If the cross-section is composed of thin walled unstable elements which are apt to buckle, the bending modulus of rupture may be much less than the tensile ultimate strength. The bending modulus of rupture is obviously dependent upon the type of material (especially ductility) and the shape or form of the cross-section.

An analogous situation exists for sections subjected to torsion loading and is due to the form of the cross-section and the character of the material. In order to predict the failing torsion load of a structure, another fictitious stress is used which is referred to as the "torsion modulus of rupture", σ_{s_t} . This torsion modulus of rupture is defined by the following equation:

$$\sigma_{s_t} = \frac{M_t b c}{J}$$

where σ_{s_t} = torsion modulus of rupture, psi

M_{t_b} = torque or moment to cause failure, in-lb

c = distance to critical outermost element, in

J = polar moment of inertia of cross-section in⁴

If a metal is subjected to a stress in the plastic range, the strain will continue to change in the direction of stress although the stress is held constant. This is a condition which is most common to metals at high stresses and high temperatures and the phenomenon is known as "creep". Figure 12.60 is a typical creep curve for a metal at a constant stress and temperature.

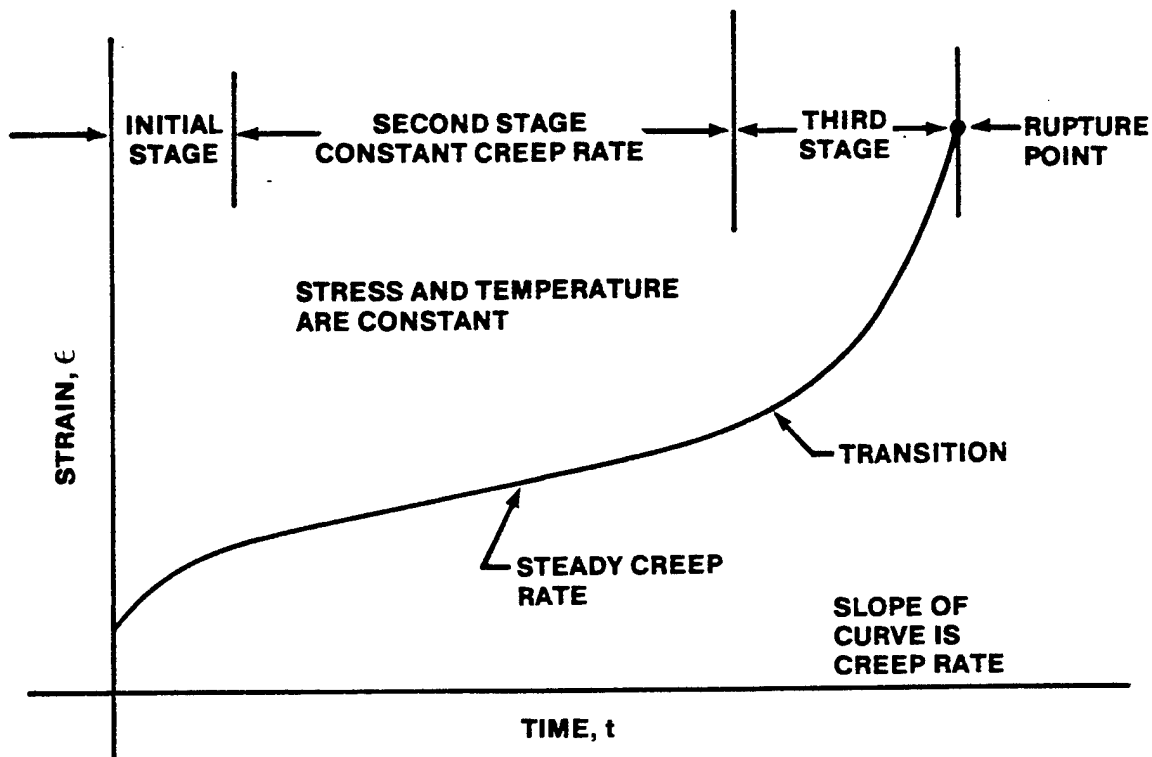


FIGURE 12.60. CREEP CURVE FOR A METAL AT CONSTANT STRESS AND TEMPERATURE

Upon the application of stress, a high initial creep rate will develop, then decrease to the minimum value of steady creep. During the second stage the creep rate is essentially constant. After a period of time the third and final stage of creep will take place with an increase in creep rate and final rupture. Since the stress to cause rupture varies inversely with time and temperature, creep problems are of the greatest importance in light weight, high temperature structures.

In the design of high temperature structures the amount of deformation allowable may be a more severe criteria than actual rupture strength. This would be the case for components which - if excessively strained - would not function properly or would fail at loads lower than normally anticipated.

Stress-strain diagrams for a material may be greatly altered when the rate of stressing is very high. When stress is applied very suddenly (almost instantaneously) the result is "impact" stresses. The amount of energy absorbed under impact conditions may be significantly different from the

energy absorbed when the load is applied steadily and gradually. The actual speed or rate at which a material is stressed will determine what changes in energy absorption take place. In the case of an ordinary structural material, an increase in the rate of stressing (above that of very gradual load application) will initially produce a slight increase in the energy absorbed. With continued increase in rate of stressing, a "critical speed" will be reached and the energy absorbed will be at maximum. Above this speed the toughness will be greatly reduced. If the stress-strain diagrams for impact stressing were recorded and compared with the stress-strain diagram obtained from gradual load application, the result would be similar to Figure 12.61.

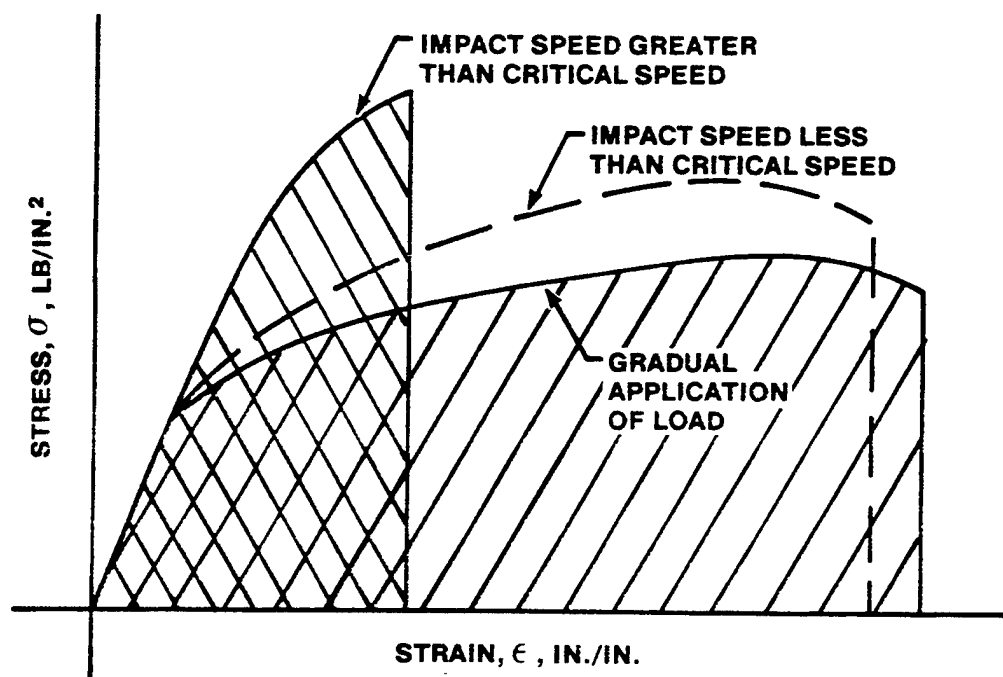


FIGURE 12.61. EFFECTS OF APPLICATION RATE ON STRESS

When stress is applied above the critical speed, the failing stress would be higher but the elongation would be greatly reduced. In fact, the effect of impact stresses beyond the critical speed is to produce brittle type failures in tough or ductile materials. On the other hand, a brittle material will not show any great effect of high stress rates since there is very little ductility or energy absorbing capability for gradually applied loads.

While impact stresses near the critical speed are not ordinarily encountered in airframe structures, due consideration must be given to the case of dynamic machinery and mechanisms. The effect of impact stresses is most important when there are severe discontinuities in the shape of a part or when a part is operated at low temperatures.

Figures 12.62-12.69 are illustrations of failure of different types of materials under tension, torsion or shear.

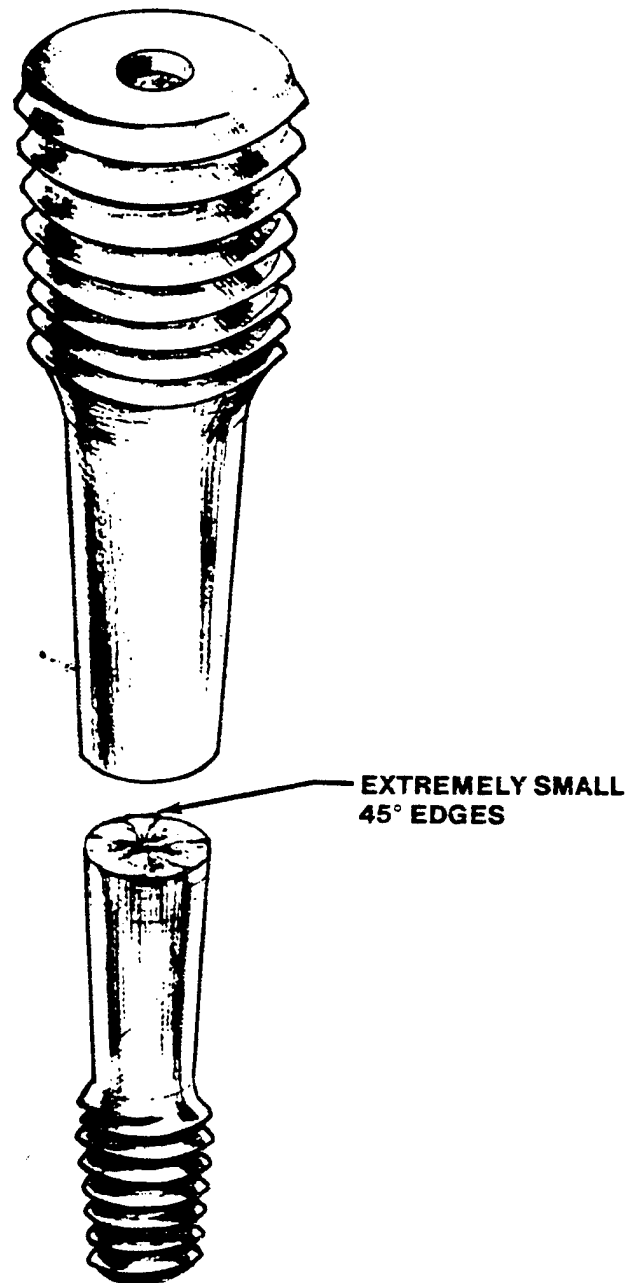


FIGURE 12.62. BRITTLE TENSION FAILURE

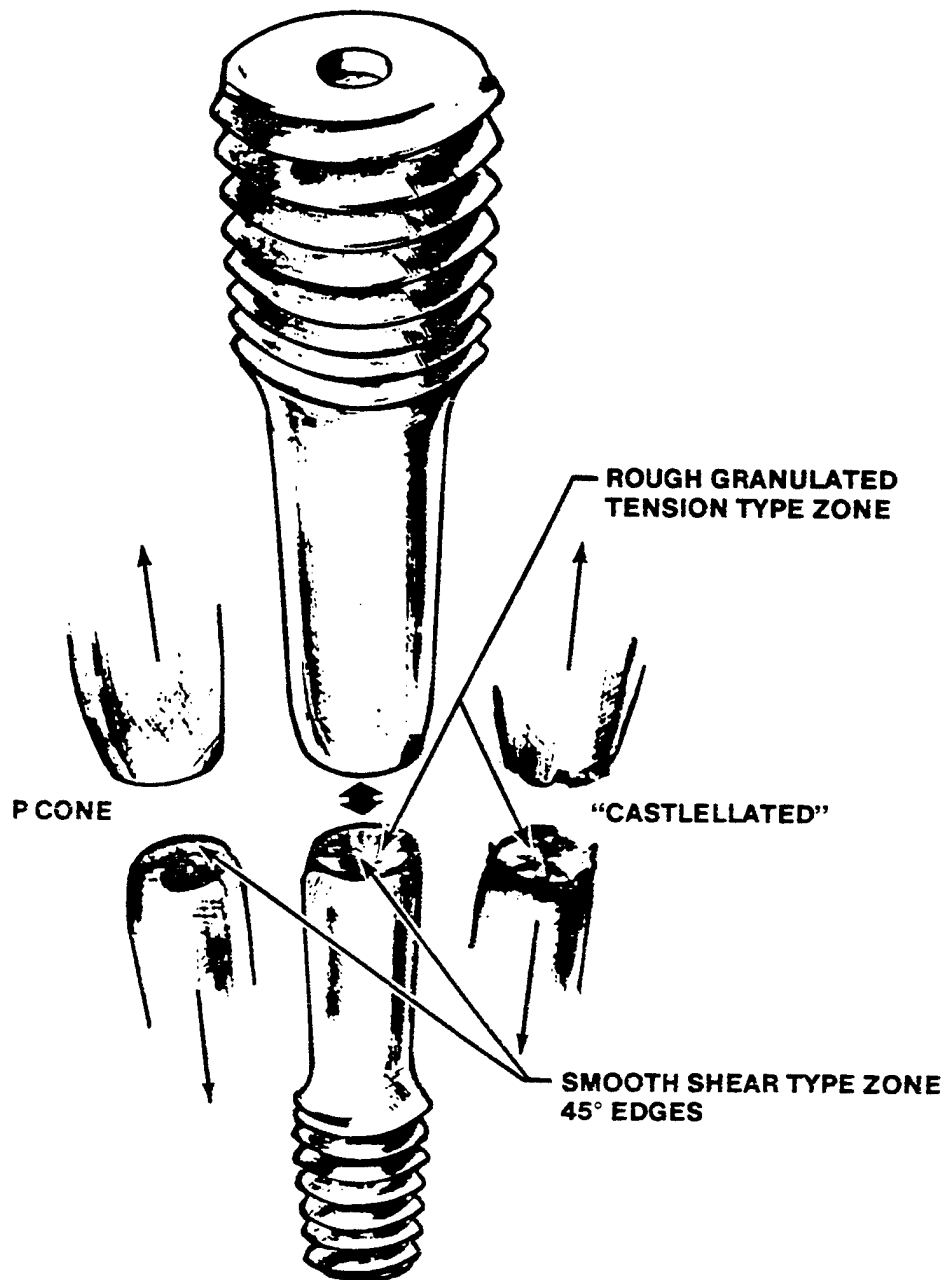


FIGURE 12.63. MEDIUM DUCTILITY TENSION FAILURE

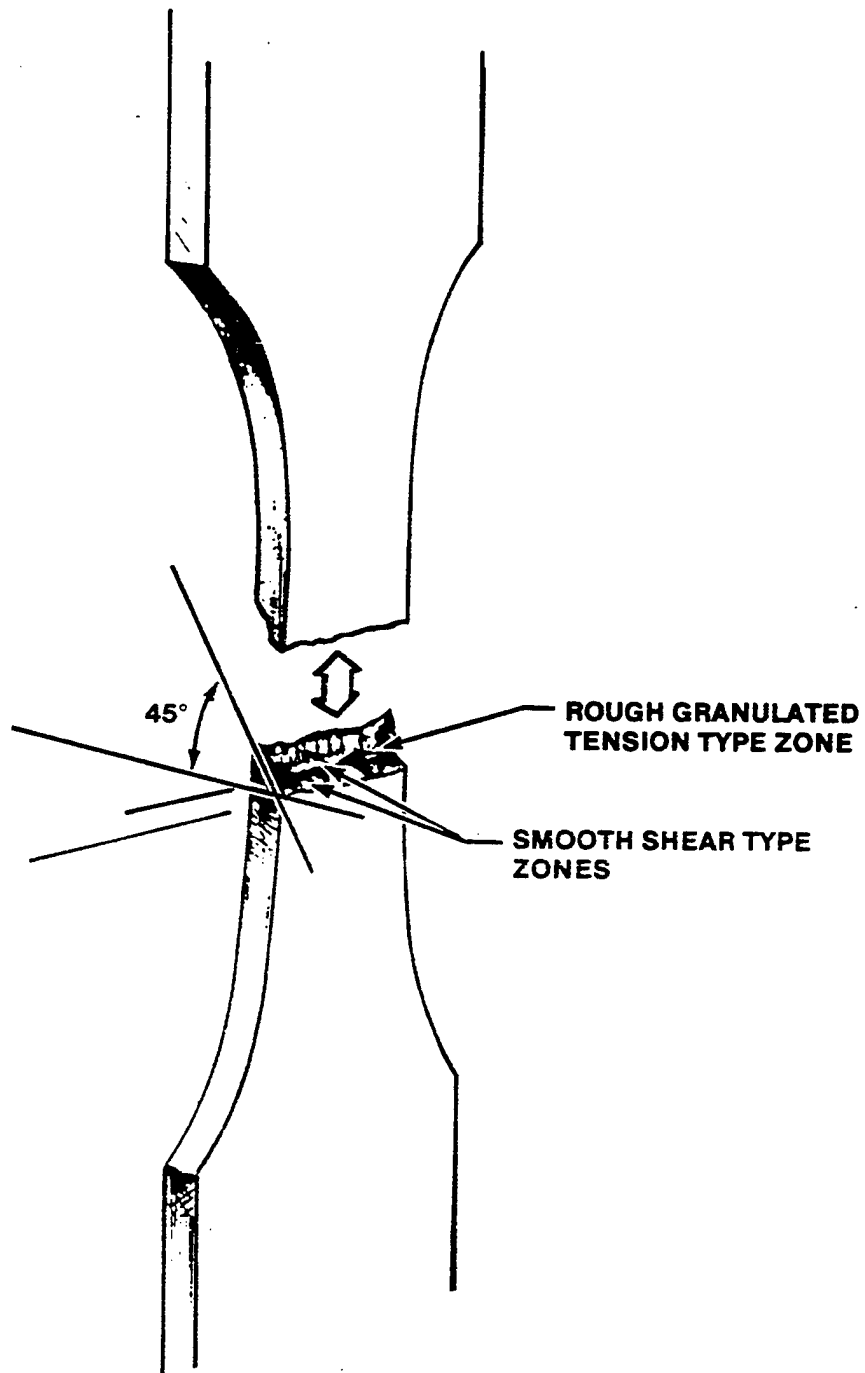


FIGURE 12.64. HIGHLY DUCTILE TENSION FAILURE SHEET OR THIN BAR STOCK

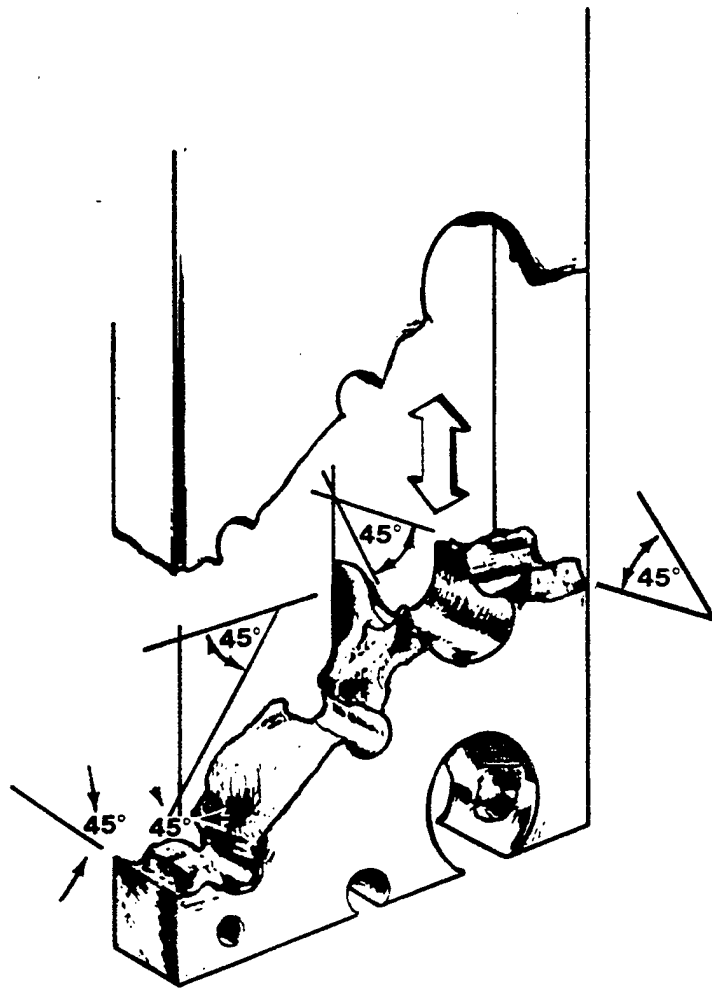


FIGURE 12.65. TYPICAL TENSION FAILURE DUCTILE AIRCRAFT MATERIAL

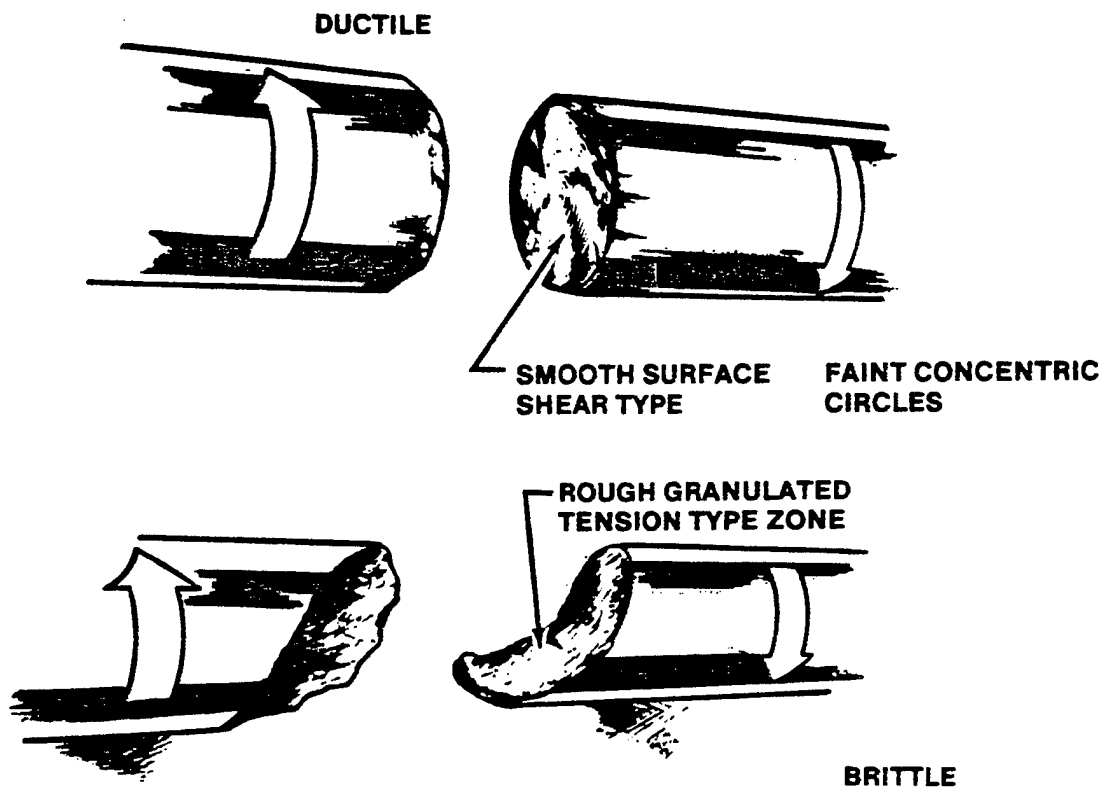


FIGURE 12.66. TORSION FAILURE

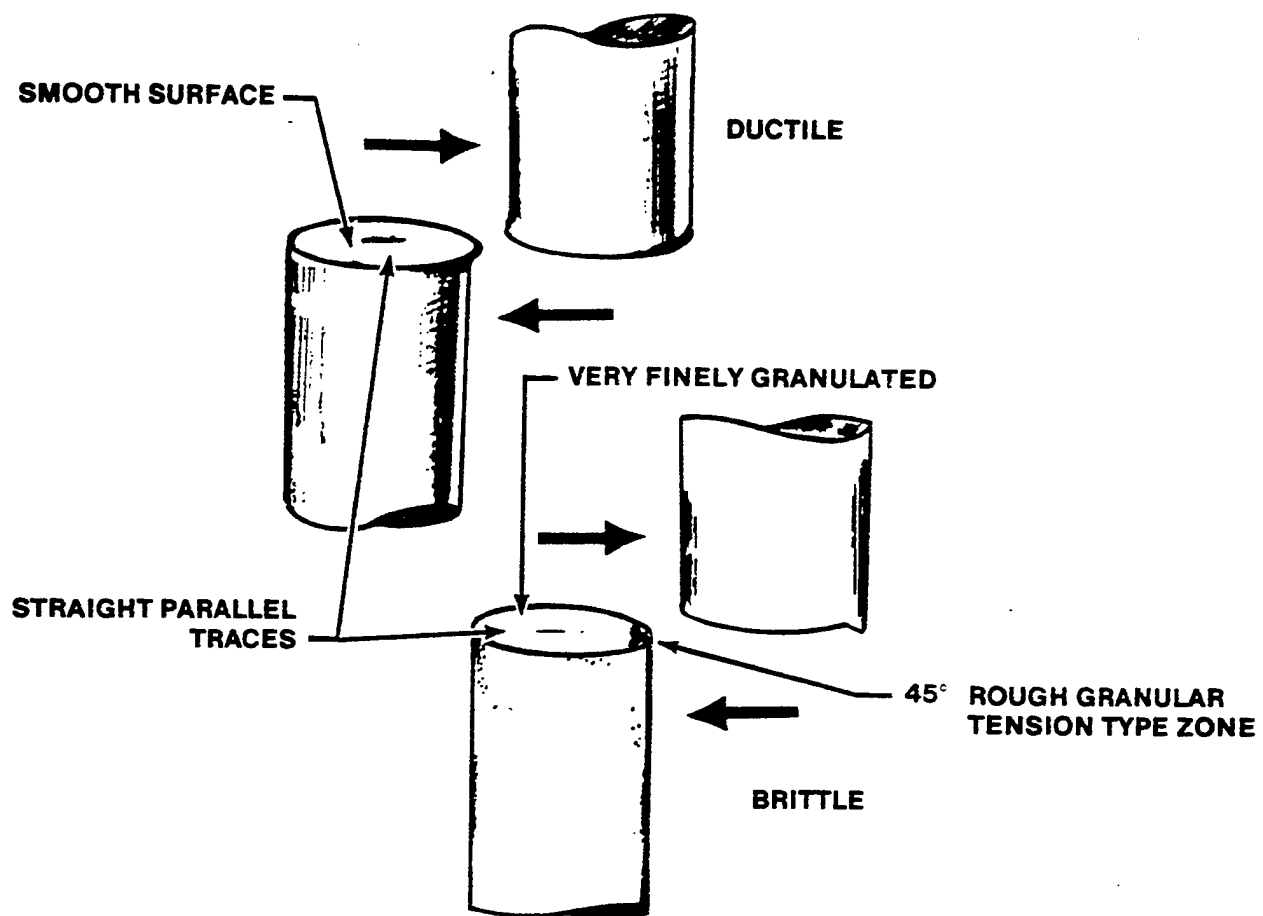


FIGURE 12.67. SHEAR FAILURE

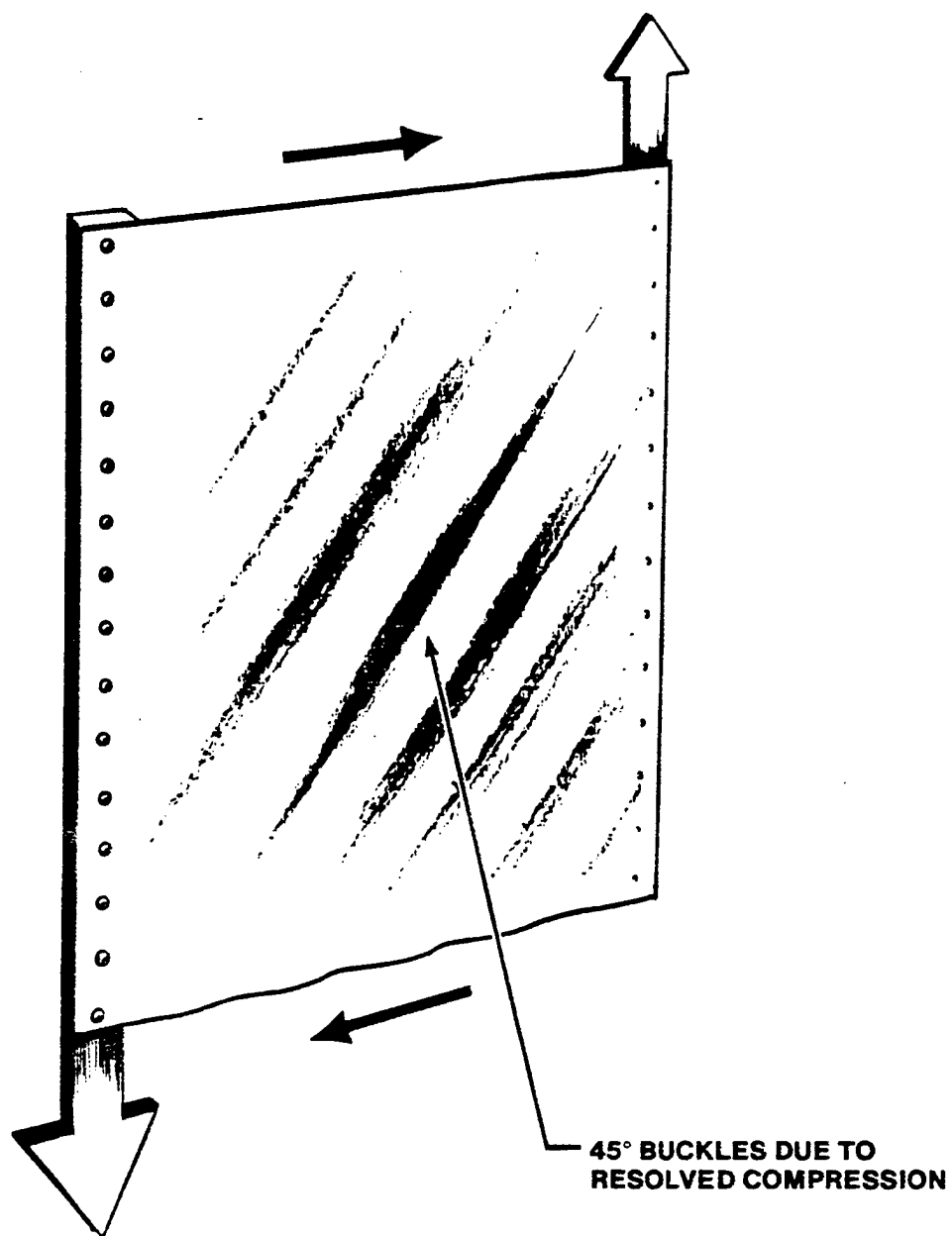


FIGURE 12.68. SHEAR IN PANELS COMPRESSION TYPE FAILURE

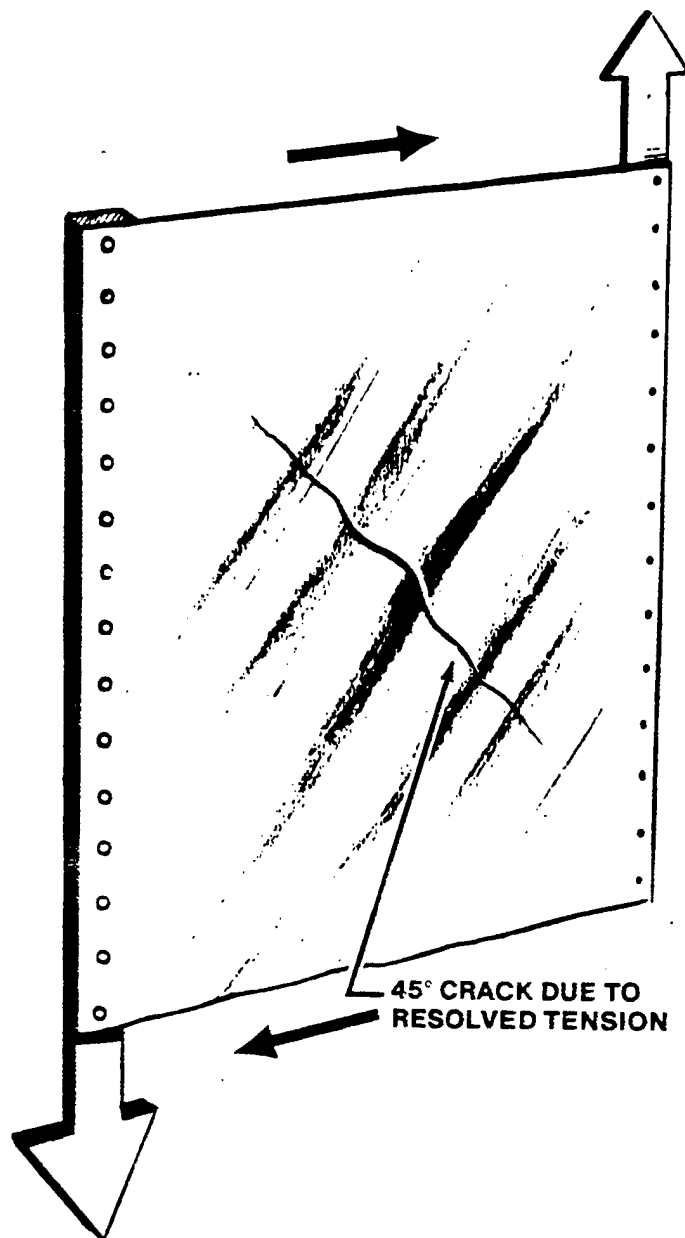


FIGURE 12.69. SHEAR IN PANELS TENSION TYPE FAILURE

12.5 AEROELASTICITY

12.5.1 INTRODUCTION AND DEFINITIONS

Except for a few isolated examples in the TPS curriculum, the aircraft has been treated as a rigid body. That is, no bending, twisting, or deformations were assumed to occur on the structure in the definition and derivation of the performance and stability characteristics. For example, lateral bending of the fuselage was ignored in determining the steady straight sideslip equations. Or the effects of wing bending and subsequent load redistribution were not taken into account in the lift, drag, and moment equations.

In reality, though, airplanes deform under aerodynamic loads. These effects can be significant, especially in high speed lightweight aircraft at high maneuvering accelerations, or in the large category aircraft such as the C-5A, Boeing 747 or Lockheed L-1011 during normal flight conditions. The degree to which the analytical computations are affected is dependent upon flight conditions. However, aeroelastic effects must be included in any precision analysis. We therefore must treat the stability derivatives as functions of dynamic pressure (q), as well as Mach (M) and angle of attack (α). Designing and building a totally rigid airplane is not practical because of the weight penalty (the development of lightweight composites has lessened the problem somewhat but high cost becomes a major factor in that area). The designer is thus faced with the dilemma of conflicting requirements for lightweight (for improved aircraft performance) versus structural rigidity (to preclude aeroelastic effects).

The study of aeroelasticity is important, therefore, simply because the aeroelastic problem is a reality. A decision has to be made as to how much rigidity can be sacrificed before the bending, twisting and inertial effects of the structure restrict the performance and handling qualities. Is there assurance that catastrophic structural failure will not occur somewhere in the aircraft's flight regime?

Aeroelasticity is often defined as the science which studies the mutual interaction between aerodynamic, elastic and inertial forces of an airplane in flight. Again, the phenomenon would be nonexistent if aircraft structures were perfectly rigid but the weight/cost penalties for that privilege would be too severe. By itself, structural bending or flexibility is not

objectionable. The problems arise when the deformations in turn cause changes in the aerodynamic forces. If the deformations and aerodynamic forces vary rapidly, inertial forces become important.

In 1946, A.R. Collar presented a paper to the Royal Aeronautical Society that ingeniously classified problems in aeroelasticity by means of a triangle of forces. Referring to Figure 12.70, the three types of forces (aerodynamic, elastic, and inertial) are placed at the vertices of a triangle. Each aeroelastic phenomena can be located on the diagram according to its relation to the three vertices. For example, dynamic aeroelastic phenomena such as flutter, F, lie within the triangle, since they involve all three types of forces and must be bonded to all three vertices. Static aeroelastic phenomena such as wing divergence, D, lie outside the triangle on the upper left side, since they involve only aerodynamic and elastic forces. Although it is difficult to define precise limits in aeroelasticity, the classes of problems connected by solid lines to the vertices are usually accepted as principal ones. Of course, other borderline fields can also be placed on the diagram. For example, mechanical vibrations, V, and rigid body aerodynamic stability, DS, are connected by dotted lines. It is very likely that in certain cases the dynamic stability problem is influenced by aircraft flexibility and it would therefore be moved within the triangle to correspond with DAS, where it would be regarded as a dynamic aeroelastic problem.

Collar's Aeroelastic Triangle (or more completely "Aero inertia-Elastic" Triangle) was revised to a tetrahedron some 15 years later by I.E. Garrik to include Aerothermoelasticity, Figure 12.71. Aerodynamic thermal effects associated with high-speed flight vehicles introduce deformations, stresses, and changes in material properties that can greatly extend the field of aeroelasticity. This chapter will not formally address Aerothermoelasticity, except to introduce it as an influencing factor of aeroelasticity in high-speed flight.

Static Aeroelastic Phenomena:

These phenomena are the ones which are concerned with steady state (i.e. non-oscillatory) aerodynamic loads, and the associated steady state distortion. Static implies the absence of inertial forces, thus it requires only coupling between the aerodynamic and elastic forces of the aircraft. It includes the following classical cases:

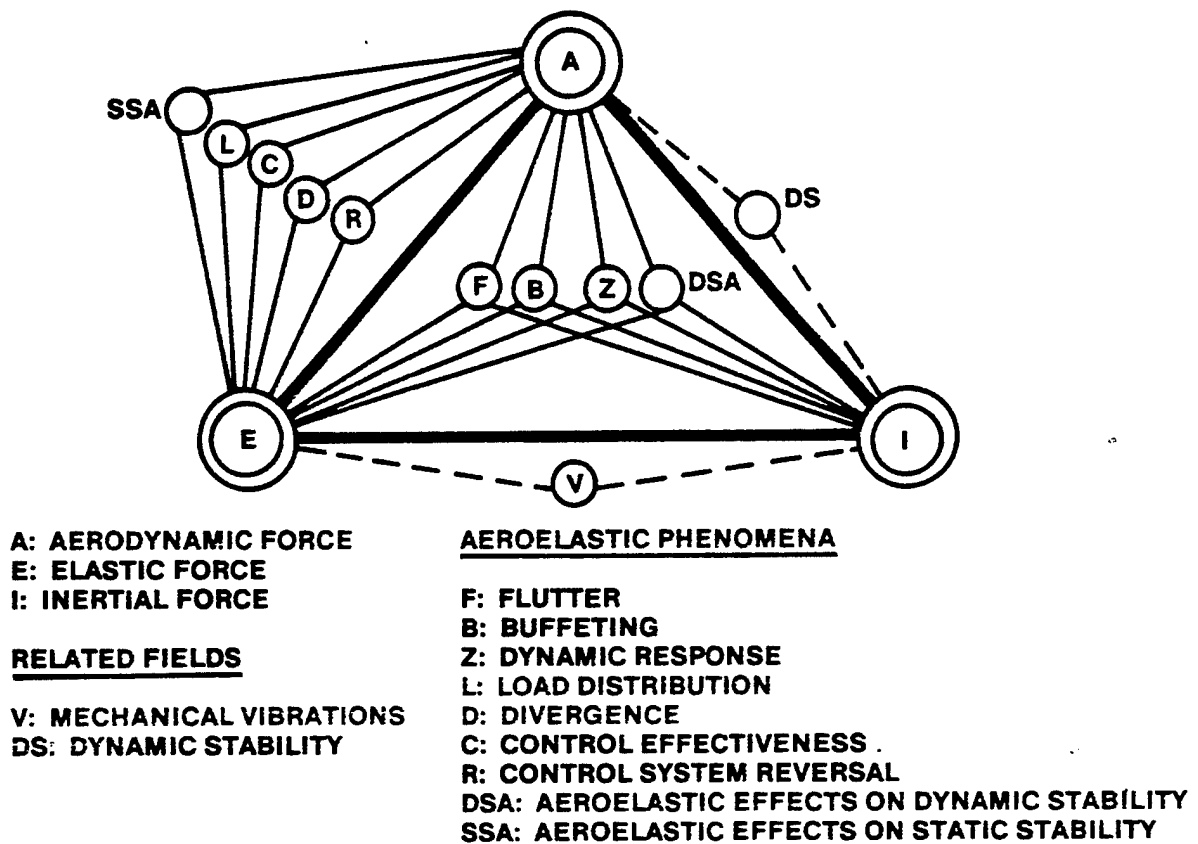
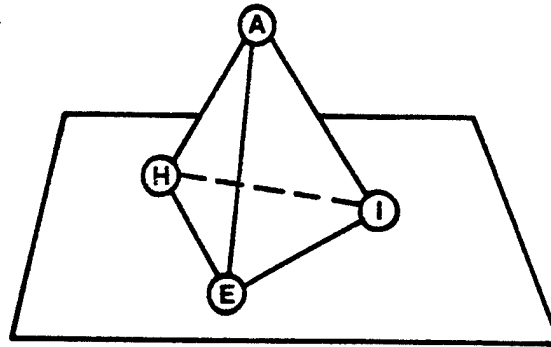


FIGURE 12.70. COLLAR'S AEROELASTIC TRIANGLE OF FORCES



A: AERODYNAMIC FORCE
E: ELASTICITY FORCE
I: INERTIA FORCE
H: HEATING

FIGURE 12.71. TETRAHEDRON OF AEROTHERMOELASTICITY

Aeroelastic Effects on Static Stability, SSA. As the aerodynamic and elastic forces combine, the deformations of the structure can be of sufficient magnitude to influence the static stability derivatives.

Load Distribution, L. Influence of elastic deformation of the structure on the distribution of aerodynamic pressures over the structure.

Control Effectiveness, C. This phenomena attempts to evaluate the influence of the elastic deformations on the controllability of the aircraft.

Torsional Divergence, D. A static instability of a lifting surface at a speed U_D called the divergence speed where the elasticity of the lifting surface plays an essential role in the instability. At a speed slightly above the wing divergence speed, the elastic restoring moment about a spanwise with elastic axis can no longer balance the aerodynamic moment created by the airloads.

Control Reversal, R. A condition occurring in flight at a speed called the control reversal speed, where the intended effects of displacing a control surface are nullified by the elastic deformations of the structure. For example, a right roll aileron deflection may result in a roll to the left because of a wing twist caused by the deflected ailerons. The B-47 for example exhibited an aileron control reversal phenomena at .80 Mach.

Dynamic Aeroelastic Phenomena:

In dynamic aeroelastic problems, we are concerned with the oscillatory motion of various parts of aircraft, and particularly interested in the conditions under which these oscillatory modes tend to diverge (increase in amplitude), because this may result eventually in the structural failure. As mentioned previously, dynamic aeroelastic phenomena are the interaction

between aerodynamic, inertial, and elastic forces. Some examples of this problem are:

Flutter, F. A self-excited dynamic instability of the structural components of an aircraft, usually involving the coupling of separate vibration modes, where the forcing function for oscillation is drawn from the airstream. The coupling of the bending and twisting modes of a wing results in a bending-torsional wing flutter. Other examples of flutter modes are: wing-aileron, tail-fuselage, and bending-torsion-aileron. Simply stated, flutter is the dynamic instability of an elastic body in an airstream. Flutter speed U_F and corresponding frequency are defined as the lowest airspeed and frequency where a flying structure will exhibit sustained, simple harmonic oscillations.

Buffeting, B. Transient vibrations of aircraft structural components due to aerodynamic impulses produced by the wake behind wings, nacelles, fuselage pods, or other components of the airplane. The problem can be serious in fighter aircraft during maneuvering to $C_{L_{max}}$ at high speed, often resulting in rugged transient vibrations on the tail due to aerodynamic impulses from the wing wake. Since these impulses are quite random there is no analytic theory to adequately describe the phenomenon. Cures are usually made as necessary by proper positioning of the tail assembly.

Aeroelastic Effects on Dynamic Stability, DSA. Changes in an aircraft dynamic stability can result due to elastic bonding, twisting, or deformation of its structure (e.g., the changes in the short period frequency and damping due to fuselage bending).

Mechanical Vibration, V. A mechanical vibration of the airplane structure mainly due to the coincidence of a powerful engine harmonic with an airframe frequency. Aerodynamic interaction may not be necessary.

It should be noted from the above discussion that flutter and divergence corresponded to conditions of aeroelastic instability, and that speeds beyond the critical flutter and divergence speeds will result in an eventual structural failure. However, control reversal is not a condition of instability, and speeds beyond control reversal speed will result only in a reversal of the action of the control system and not necessarily in a failure of the structure. Control effectiveness influences maneuverability, and it is important that the control system designer has a thorough understanding of this phenomena.

Thus, the three critical airspeeds involving aeroelasticity are flutter (U_F), divergence (U_D), and aileron reversal (U_R) speeds. In the early design

stages of an aircraft, the comparative values of these speeds must be completely analyzed. Figure 12.72 shows the relation between the critical speeds for a typical wing with varying amounts of forward and backward sweep.

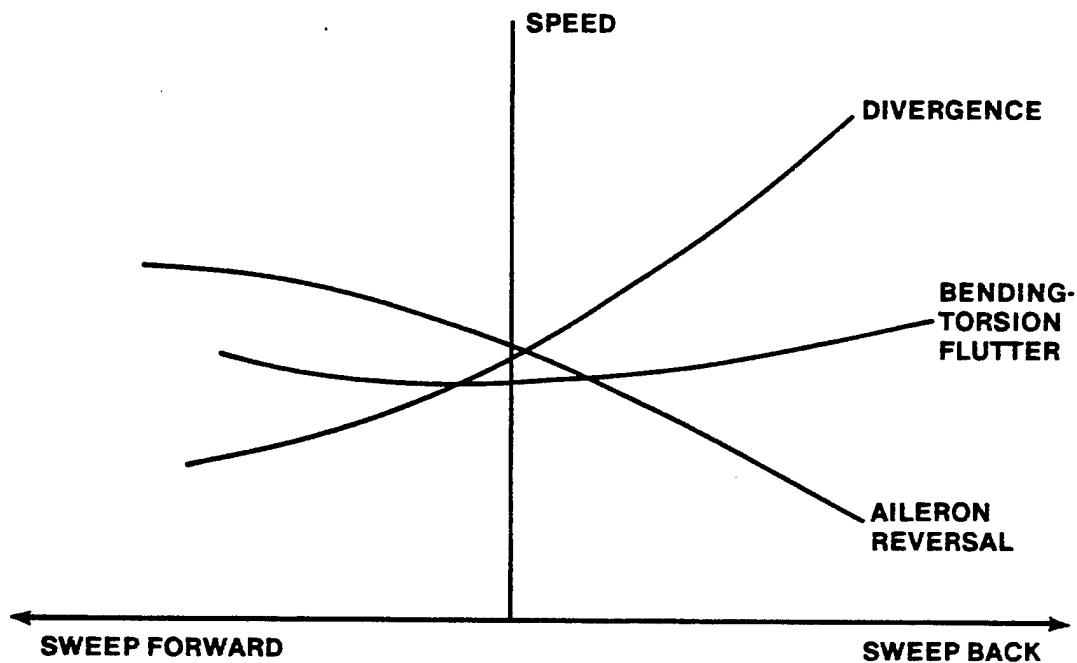


FIGURE 12.72. EFFECT OF WING SWEEP ON CRITICAL SPEEDS

12.5.2 Historical Background

Aeroelastic problems were relatively unknown until World War II. Prior to that time, aircraft speeds were relatively low and the load requirements and lack of design refinements produced an aircraft structure rigid enough to preclude most aeroelastic phenomena. Except for the time spans of the two World Wars, aircraft top speeds had increased approximately 19 knots per year from 1910 to 1955. As the speed of aircraft began to increase with no increase in load or stiffness requirements, the designers and pilots began to encounter problems associated with aeroelasticity.

When airplanes were first built there were no logical stiffness criteria for design. Hence, increasing speeds led to the wide variety of aeroelastic problems. Control surface flutter first occurred at about 110 knots; wing

flutter started at around twice that speed. The strength questions posed by the speed increase were solved partly by material developments and partly by constructional techniques, but not before many in-flight failures had occurred.

Samuel P. Langley was probably the first airplane designer affected. His misfortune occurred just prior to the Wrights' first flight. During the launch of Langley's monoplane off the Potomac River houseboat, catastrophic wing divergence occurred. His failure with the monowing and the Wrights' success with the biplane, combined with the lack of a torsional stiffness criterion for the monowing, resulted in the favoring of the dual wing design during the early period. The partiality was understandable since no designer wanted to over-stiffen the wing at the expense of added weight.

Although a few externally braced monoplanes were built prior to World War I, military monoplane design virtually stopped between 1917 and the mid-thirties. During the biplane era, the most common aeroelastic problem was tail flutter. One of the first documented cases occurred on the tail of the British twin-engined Handley Page 0/400 bomber at the start of the first war. The noted aerodynamicists Lanchester and Bairstow investigated the reasons for the flutter incidents and the following is a quote from Lanchester's report:

"The difficulty experienced is that at certain critical speeds of flight a tail wobble is set up, involving heavy torsional stresses on the fuselage, the type of vibration being an angular oscillation approximately about the axis of the fuselage; I am informed that the angular magnitude of this oscillation amounts at times to something approaching 15° , and is undoubtedly extremely dangerous to the structure of the machine. I gather that the experience of the pilots when this vibration is at its worst is terrifying."

The problem was being caused by the coupling between the fuselage torsion mode and the anti-symmetrical elevator excitation mode. In the latter, the left and right elevators oscillated about their hinge lines in opposite phase. There was no interconnecting torque tube to prevent the occurrence. The other mode was merely the low frequency torsional oscillation of the aircraft fuselage. Since the vibrating frequencies of these two separate oscillatory modes were almost the same, a resonant coupling occurred, with the resulting tail wobble phenomenon. A same type of tail flutter problem was experienced by the DH-9 in 1917, resulting in several fatalities. The fix used then was

the same one used for the Handley Page bomber. It has been a design feature ever since for reversible flight control systems - the left and right elevators were connected with a stiff torque tube.

Wing problems appeared with the return of the monowing. Insufficient torsional rigidity led to divergence, loss of aileron effectiveness, and flutter. An early problem occurred on the Fokker D-8. The aircraft was built for WWI and due to superior performance was immediately placed in combat. Within a few days several wing failures occurred during high speed dives. The wing torsional stiffness criterion used in the initial design was the same as that previously used for biplanes.

The Army ran static strength tests and discovered that the wings were more than capable of withstanding the 6g design limit. Why then, the failures? Confronted with the dilemma, Fokker decided to conduct his own static tests. He found that although the wing did indeed have the design strength, under increasing loads the angle of incidence at the wing tips increased, relative to the roots: the necessary condition for divergence. In the high speed dives the air loads increased faster at the tips and the resulting torsion caused the wings to fail.

After the war, the U.S. Army encountered a violent but nondestructive case of wing-bending/aileron-rotation flutter on the same Fokker D-8. The cure for the problem, as with virtually any control surface type flutter, was mass balancing of the control surface.

The period of monoplane development, because of the accompanying resurgence of aeroelastic problems, initiated the first serious research in the field of aeroelasticity. Early day techniques were mainly cut-and-try. Many analytic theories were presented on wing load distribution, wing divergence, loss of lateral control and aileron reversal. Potential flow flutter analysis was sufficiently understood by 1935 to be incorporated into aircraft design but the majority of airplane designers were reluctant to trust the mathematicians to formulate criteria for the strength and rigidity of aircraft structural components.

From 1934 to 1937, the perennial arms race resulted in the development of many new types of aircraft. Numerous cases of flutter appeared, mainly of the wing or tail type. The accidents served to underscore the critical nature of mass distribution and control surface mass balancing. In 1938, a panel of

scientists boarded a four-engined Junker aircraft for an in-flight observation of a planned flutter test. All perished when a catastrophic condition occurred. The accident served due warning to the community of the difficulties and hazards of flight flutter testing.

With the development of improved excitation and measuring equipment, and a better theoretical understanding of the nature of the flutter problem, flutter testing came of age during the late forties. Analytic predictions are still imprecise, but with improved model and wind tunnel technology, and with the tremendous surge in the development of the high speed computers, investigation of aeroelastic phenomena is becoming more and more a controlled science.

12.5.3 Mathematical Analysis

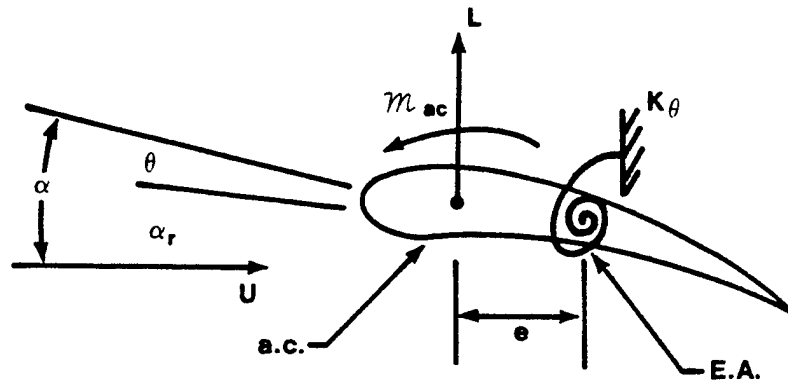
The mathematical treatment of aeroelastic phenomena is somewhat complex and tedious. It requires a knowledge of the structural properties of the vehicle and of the nature of the aerodynamic forces acting on the surface of the airplane. Many textbooks and other publications exist which treat the subject in thorough detail (References 12.1, 12.2, 12.10, and 12.11). This chapter will attempt to only touch upon the essential and basic ideas behind the mathematical formulation.

Specifically, we will look at wing torsional divergence, aileron reversal, and flutter. The first two are static phenomena and are not significant present-day problems. We treat them because they are easy to analyze and visualize. Flutter is always a primary design consideration and will therefore be treated in detail.

12.5.4 Wing Torsional Divergence

If a wing in steady flight is slightly perturbed, an aerodynamic moment will be induced which tends to twist the wing further. Since the structure's stiffness is independent of speed of flight, and the aerodynamic moment is proportional to the flight velocity squared, there may exist a critical speed at which the elastic stiffness of the wing is barely able to sustain the wing in its deformed state. This speed is called the divergence speed and the wing is said to be torsionally divergent.

More simply stated, wing divergence is the condition where the aerodynamic moment exceeds the elastic restoring moment in torsion. Figure 12.73 illustrates a typical cambered wing section moving with a flight speed U .



$$\alpha = \alpha_r + \theta$$

α_r = INITIAL ANGLE OF ATTACK (RIGID)

θ = ANGLE OF TWIST

FIGURE 12.73. CAMBERED WING SECTION

Acting at the aerodynamic center is the lift (L) and the moment about the a.c. (m_{ac}). The elastic restoring moment on the wing opposing the total aerodynamic moment is depicted by a linear coiled spring with spring constant K_θ attached at the elastic axis (E.A.) located a distance e behind the a.c. The elastic axis is defined as the axis about which the wing section would twist, subjected to pure moment. A vertical force applied at the E.A. would effect only a vertical deflection (bending). No twisting would result. For the sake of definition, the bending and twisting of a wing are illustrated separately in Figure 12.74.

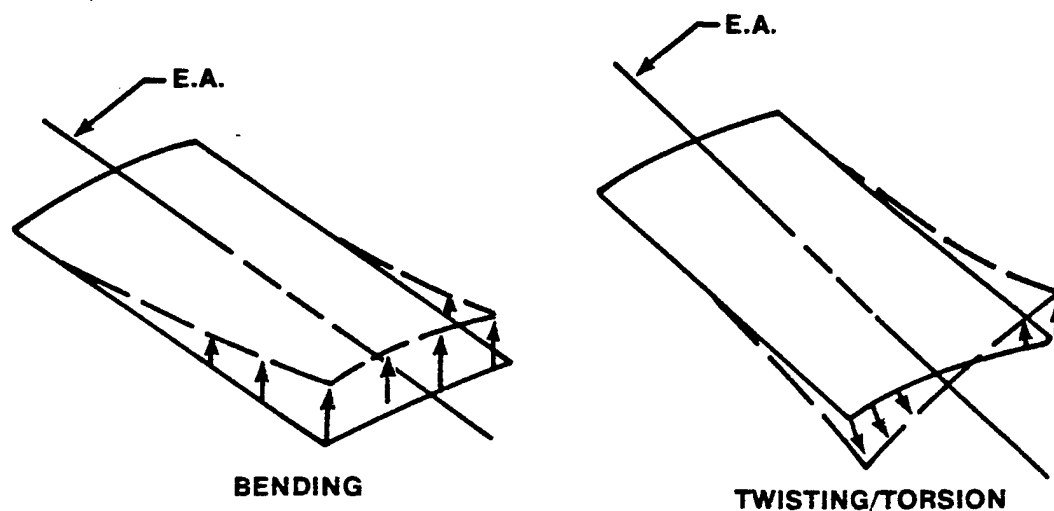


FIGURE 12.74. WING BENDING AND TWISTING

For the wing section in Figure 12.73, the angle of attack on the airfoil is composed of two parts: α_r , the angle of attack that a rigid wing would see, and θ , the angle resulting from elastic twist. At equilibrium, the aerodynamic moment about the elastic axis must equal the elastic restoring moment $K_\theta \theta$.

Aerodynamic moment about the elastic axis

$$M_{\text{AERO}} = I_e M_{\text{ac}} = K_\theta \theta$$

From subsonic aerodynamics, we know that

$$L = q S C_{L_\alpha} = q S C_{L_\alpha} (\alpha_r + \theta) \text{ and}$$

$$M_{\text{ac}} = q S c C_{\text{Mac}}$$

Equating the moments,

$$K_{\theta} \theta = \mathcal{M}_{AERO} = l e - \mathcal{M}_{ac}$$

$$= q S \left[e C_{L_{\alpha}} (\alpha_r + \theta) - c [C_{Mac}] \right]$$

Solving for the twist angle θ ,

$$\theta = \frac{q S (e C_{L_{\alpha}} \alpha_r - c C_{Mac})}{K_{\theta} - q S e C_{L_{\alpha}}} \quad (12.30)$$

At the divergence condition the twist angle grows without bound (i.e., $\theta \rightarrow \infty$). This condition occurs mathematically when the denominator of Equation 12.30 equals zero.

$$K_{\theta} - q S e C_{L_{\alpha}} = 0$$

where $q = q_D$ (Dynamic Pressure at Divergence)

$$q_{D_2} = \frac{\rho}{2} U_D^2 = \frac{K_{\theta}}{S e C_{L_{\alpha}}}$$

or, solving for the divergence speed U_D ,

$$U_D = \sqrt{\frac{K_{\theta}}{\frac{\rho}{2} S e C_{L_{\alpha}}}} \quad (12.31)$$

The design parameters affecting the divergence of straight wings are primarily the wing torsional stiffness (K_{θ}) and the offset distance e . Increasing K_{θ} is a costly process at the expense of considerable weight. An approach more frequently employed is to proportion the wing structurally so as to move the elastic axis forward. Aft wing sweep lessens the divergence problem since swept wing tip angles of attack are effectively reduced by wing bending.

If a real, three dimensional, wing were considered, the actual divergence speed must be obtained by integration across the span of the wing since local spanwise properties will vary.

12.5.5 Aileron Reversal

The aeroelastic problem of aileron reversal is closely related to wing torsional divergence in that both depend strongly upon the torsional stiffness of the wing. The history of this subject closely parallels that of wing torsional divergence; however, it was during World War II that the problem came into importance. The increasing speeds and the requirements for rolling performance precipitated the problem greatly. Following WW II, and with the advent of thin-wings, moderately high aspect ratio, and sweepback, the aileron reversal speed became of prime importance.

Aircraft with conventional planforms may suffer serious loss of aileron, elevator, and rudder control effectiveness due to elastic deformations of the structure. The aileron controls the rolling motion of an aircraft, and when placed downward, the lift over the wing is increased and a rolling moment is produced. The down aileron also produces a twisting moment on the wing which tends to twist the wing nose down and reduce the angle of attack and hence this reduces the rolling moment. A similar situation exists for the up aileron wing. The up aileron produces a torque which increases the angle of attack and decreases the effective rolling moment. Since the wing stiffness is independent of the flight velocity and the aerodynamic force ineffective in producing a rolling moment and the resulting wing segment twist and aileron deflection produce no effective change in lift. Beyond this critical speed, the effect of ailerons is actually reversed. This analysis also applies to the other control surface and is sometimes known as "Control Surface Effectiveness." Figure 12.75 shows how aileron effectiveness as measured by the ratio of rolling velocity to aileron angle is affected by forward speed for a WW II fighter-type aircraft at sea level.

Avoidance of aileron reversal in a straight wing with conventional ailerons is a matter of providing sufficient wing torsional stiffness. If the wing is swept back aileron reversal is a serious problem and wing bending stiffness must also be increased. This sometimes becomes prohibitively large in a weight analysis, hence, the other means are employed. Spoilers, fully moving wing tips, and even moving the aileron inboard all produce suitable means to combat this occurrence. Figure 12.76 shows that the aileron reversal speed can be increased by changing the configuration of the aileron controls. Additionally, this figure shows that control effectiveness can be increased

with decreasing sweepback. Inboard ailerons are used in the F-4, while the T-38 has ailerons at the semi-span position. Often aircraft are fitted with two sets of aileron surfaces, the outboard being locked out at high speeds and only the inboard ailerons being used for roll control. The cases of elevator and rudder control effectiveness and reversal are usually less critical than those of aileron, they are, however, more complicated due to the large deformations of the fuselage and attachments.

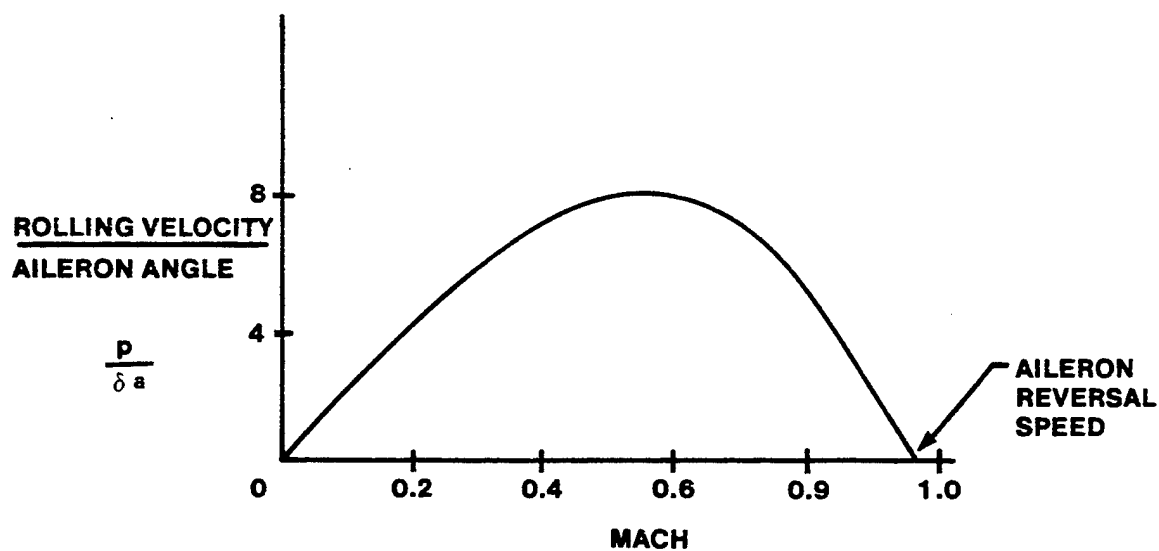


FIGURE 12.75. AILERON EFFECTIVENESS

It should be noted that flutter and divergence correspond to conditions of aeroelastic instability, and that speeds beyond critical flutter and divergence speeds will result in an eventual structural failure. Control reversal is not a condition of instability, and speeds beyond the control reversal speed will result only in a reversal of the action of the control system and not necessarily a failure of the structure. The prime concern here is the loss of maneuverability. With the advent of fully boosted systems, additional complications result because of the deformations resulting in the controlling mechanism and the enormous mechanical advantage available.

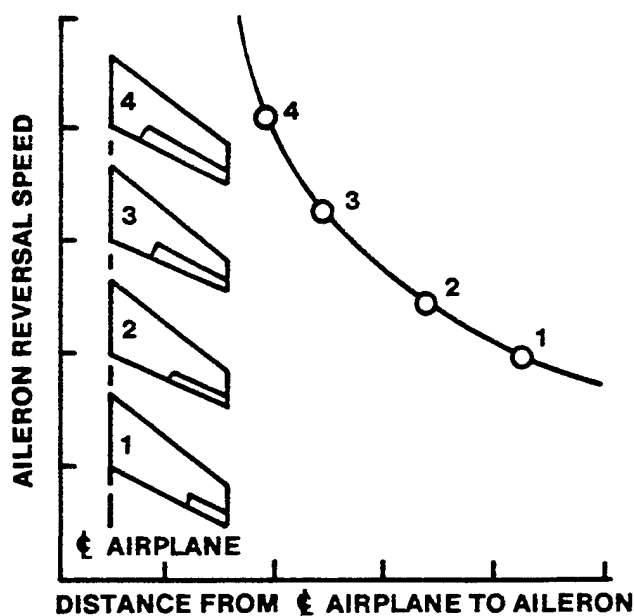


FIGURE 12.76. AILERON REVERSAL SPEED VS AILERON POSITION

Figure 12.77 illustrates a typical cambered wing section with ailerons. σ_a represents a downward deflection of the aileron. If the wing were rigid, the aileron displacement would be accompanied by an increase in lift. However, for an elastic wing the deflected aileron would also cause a nose-down twist of the wing, reducing the effective angle of attack. The nose down twisting moments increase with the square of airspeed whereas the elastic restoring moment stays constant. At some critical airspeed U_R , called the aileron reversal speed, the increase in lift caused by the deflected aileron is completely negated by the loss in lift due to the reduction of the effective angle of attack caused by the twist. The mathematics follow. Again, the elastic restoring moment is $K_\theta \theta$.

Aero dynamic moment about the elastic axis

$$\mathcal{M}_{AERO} = I_e - \mathcal{M}_{ac} - \mathcal{M}_{ac\delta_a}$$

where $\mathcal{M}_{ac\delta_a}$ is the contribution to the moment about the a.c. due to aileron deflection.

$$L = q S C_{L_\alpha} (\alpha_r - \theta) + q S C_{L_{\delta_a}} \delta_a$$

or

$$L = q S \left[C_{L_\alpha} (\alpha_r - \theta) + C_{L_{\delta_a}} \delta_a \right]$$

Substitution into the moment equation yields

$$\begin{aligned} \mathcal{M}_{AERO} &= q S e \left[C_{L_\alpha} (\alpha_r - \theta) + C_{L_{\delta_a}} \delta_a \right] \\ &\quad - q S c \left[C_{Mac} + C_{M_{\delta_a}} \delta_a \right] \end{aligned}$$

Again, equating elastic and aerodynamic moments,

$$\begin{aligned} K_\theta \theta &= \mathcal{M}_{AERO} = I_e - \mathcal{M}_{ac} - \mathcal{M}_{ac\delta_a} \\ &= q S e C_{L_\alpha} (\alpha_r - \theta) - q S c C_{Mac} \\ &\quad + q S e C_{L_{\delta_a}} \delta_a - q S c C_{M_{\delta_a}} \delta_a \end{aligned}$$

Solving for the twist angle θ ,

$$\theta = \frac{q S \left(e C_{L_{\delta_a}} - c C_{M_{\delta_a}} \right) \delta_a}{K_\theta + q S e C_{L_\alpha}} + \frac{q S \left(e C_{L_\alpha} \alpha_r - c C_{M_{ac}} \right)}{K_\theta + q S e C_{L_\alpha}} \quad (12.32)$$

Ultimately, we will be interested in only the change in twist angle due to a change in aileron deflection i.e., $\partial\theta/\partial\delta_a$. Consequently, the second term in the θ equation drops out since it remains invariant with a change in aileron deflection. As a result,

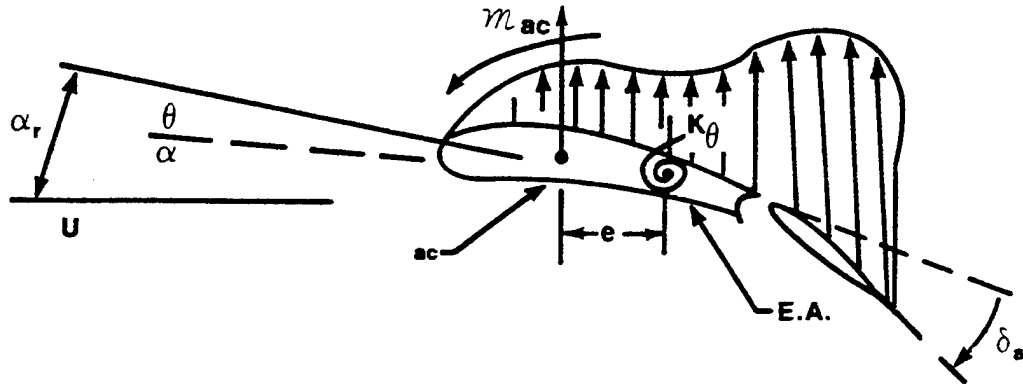


FIGURE 12.77. CAMBERED WING SECTION WITH AILERON

$$\frac{\partial\theta}{\partial\delta_a} = \frac{q S \left(e C_{L_{\delta_a}} - c C_{M_{\delta_a}} \right)}{K_\theta + q S e C_{L_\alpha}} \quad (12.33)$$

At U_R , the change in lift due to a change in aileron deflection, ΔL_{δ_a} , becomes zero.

$$\Delta L_{\delta_a} = 0$$

The change in lift ΔL_{δ_a} is represented by

$$\Delta L_{\delta_a} = L_{\delta_a} + L_{\Delta\theta}, \text{ where}$$

$$L_{\delta_a} = \text{lift increase due to the increase in camber} = q S C_{L_{\delta_a}} \delta_a$$

$$L_{\Delta\theta} = \text{lift decrease due to the leading edge twist} = - q S C_{L_\alpha} \frac{\partial \theta}{\partial \delta_a}$$

Therefore,

$$\Delta L_{\delta_a} = q S C_{L_{\delta_a}} \delta_a - q S C_{L_\alpha} \frac{\partial \theta}{\partial \delta_a}$$

Substituting Equation 12.33 for $\partial \theta / \partial \delta_a$ yields

$$\Delta L_{\delta_a} = q S \left[C_{L_{\delta_a}} \delta_a - C_{L_\alpha} \frac{q S (e C_{L_{\delta_a}} - c C_{M_{\delta_a}} \delta_a)}{K_\theta + q S e C_{L_\alpha}} \right]$$

Rearranging and cancelling, we obtain

$$\Delta L_{\delta_a} = \frac{q S (K_\theta C_{L_{\delta_a}} + q S c C_{L_\alpha} C_{M_{\delta_a}}) \delta_a}{K_\theta + q S e C_{L_\alpha}} \quad (12.34)$$

At the reversal speed $\Delta L_{\delta_a} = 0$. Since q , S , and δ_a in the numerator of Equation 12.34 are all non-zero, the terms within the parentheses must vanish to satisfy the equation

$$K_\theta C_{L_{\delta_a}} + q_R S c C_{L_\alpha} C_{M_{\delta_a}} = 0$$

where $q = q_R$ (Dynamic Pressure at Control Reversal)

$$q_R = - \frac{K_\theta C_{L_{\delta_a}}}{S c C_{L_\alpha} C_{M_{\delta_a}}}, \quad \text{or}$$

$$U^R = \sqrt{-\frac{K_\theta C_{L_{\delta a}}}{\frac{\rho}{2} S c C_{L_\alpha} C_{M_{\delta a}}}}$$

(12.35)

All the terms are positive except for $C_{M_{\delta a}}$ so U_R is, of course, real. A noteworthy observation is the fact that the reversal speed is independent of twist axis location (e). The aerodynamic moment at the reversal condition is a pure couple and therefore independent of axis position. Also notice the U_R decreases with a decrease in altitude.

Preventing aileron reversal in a straight wing is a matter of increasing torsional stiffness (K_θ), increasing the aileron effectiveness ($C_{L_{\delta a}}$), or of decreasing the magnitude of $C_{M_{\delta a}}$. In the case of swept wings, where aileron reversal has been a serious problem, bending stiffness must also be increased. Since weight increases accompany stiffness increases other methods should be employed. Alternative methods such as spoilers and all moving wing tips have proved beneficial. Also, the effective K_θ is increased as the aileron locations are moved inboard.

12.5.6 Flutter

First we assume a cantilever straight wing without ailerons mounted in a wind tunnel and with no airflow. When the model is disturbed, oscillations are induced which gradually damp out since the elastic structure provides a damping ratio of its own, known as structural damping, usually from 2% to 8%. As the speed of the wind flow is increased, the rate of damping of the oscillations increases due to aerodynamic damping. With further increases of speed, a point is reached where the damping starts to decrease rapidly. At the next point, the Critical Flutter Speed, the oscillation can just maintain itself with steady amplitude. Speeds above the critical flutter speed trigger a violent oscillation and subsequent destruction of the section when subjected to a small disturbance. This airfoil is said to have oscillatory instability and is said to flutter. Moreover, once the oscillation starts, it is self sustained and no further external forces or forcing functions are required.

Additional types of flutter can involve aileron motion where there may be one or more ranges of speeds for which flutter occurs. The aileron flutter induces the wing to flutter. Usually these regimes are bounded at both ends by critical speeds where one has an oscillation of constant amplitude.

The oscillatory motion of a fluttering cantilever wing has both bending and torsional components. If the airfoil is rigid in torsion and is constrained to have only a flexural degree of freedom, it will not flutter. With only torsional degrees of freedom it can flutter only if the angle of attack is near the stall angle. Thus, coupling of several degrees of freedom is a necessary portion of flutter. Furthermore, bending movements at all points across the span are approximately in phase with one another. The torsional movements are all approximately in phase; however, the bending mode is usually considerably out of phase with the torsional movement. This phase difference is responsible for flutter.

An airplane wing is an elastic body and has infinitely many degrees of freedom in vibration. The basic construction allows any elastic deformation in the chordwise section to be described by (1) deflection of a reference point, (2) and angle of rotation about that point. With control surfaces, the freedom to turn about the hinge line is so much more important than elastic deformation that this deflection is best described by an angle of rotation about its hinge line.

One must consider three variables in wing flutter (this does not include a time variable):

- (1) Bending
- (2) Torsion
- (3) Control surface rotation

A flutter mode which contains all three is termed ternary flutter. A flutter mode which contains only two (usually the first two) is called binary flutter. Occasionally, a single degree of freedom oscillation may exist. This usually occurs with control surfaces and is referred to as "buzz."

In general the design criteria requires that an aircraft must be able to fly near U_f without the appearance of undesirable marginal stability in its structural vibrations. Yet, bending and torsional flutter can emerge suddenly

and violently, and at about five knots above U_f the wing will possibly destroy itself after two or three cycles of oscillations.

The classical type of flutter nearly always involves the coupling of two or more degrees of freedom. The analysis can be very complex, depending upon the desired detail. We shall attempt only an elementary treatment here, with emphasis on formulation and physical interpretation. The basic second order system will be studied in depth because it conveniently demonstrates the stability problem, the basis of all flutter phenomena. We will be mainly concerned with the changes in system response resulting from changes in damping and/or excitation frequency.

Figure 12.78 shows a typical wing section with two degrees of freedom: x , a vertical displacement downward (bending), and α , the angular deflection about the elastic axis. For simplification, the E.A. and the c.g. are coincident.

Unlike the static divergence and control reversal problems, the flutter analysis will require knowledge of the mass and inertial properties of the wing since an oscillatory motion will be involved, resulting in a "generation" of inertial forces. By use of Newton's second law, the equations of motion for the wing in the two degrees of freedom can be derived.

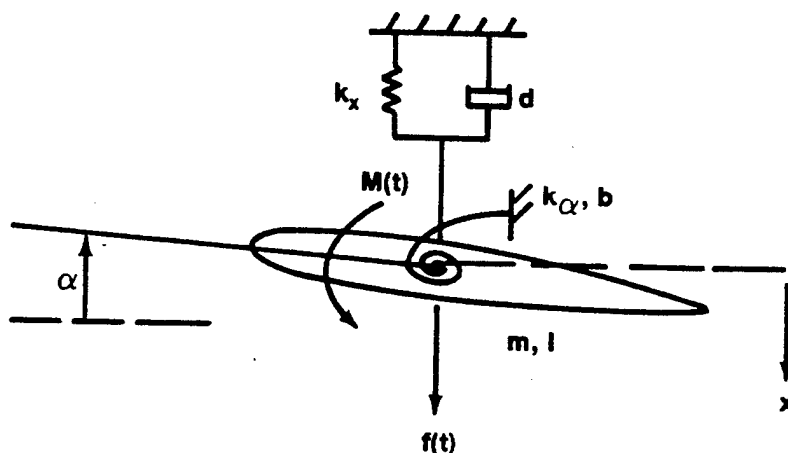


FIGURE 12.78. TWO DEGREE OF FREEDOM WING SECTION

NOTE:

$f(t)$ = time varying force acting at c.g.

$M(t)$ = time varying moment acting on wing section

m = mass of section

I = moment of inertia about c.g.

k_x, k_a = spring constants of displacement (bending) and torsion, respectively

\bar{d}, b = bending and torsion damping coefficients

$$m \ddot{x} + \bar{d} \dot{x} + k_x x = f(t)$$

$$I \ddot{a} + b \dot{a} + k_a a = M(t)$$

As the equations stand, for small displacements there is neither inertial nor elastic coupling between the two degrees of freedom. That is, in the absence of the external driving forces $f(t)$ and $M(t)$, the free body motion is independent in both x and a . The motions do not interfere. This is obvious from inspection (no α in the x equation, and vice versa) and is the result of our collocating the c.g., the axis of twist, and the displacement axis. The only way coupling can be introduced is through the driving forces $f(t)$ and $M(t)$.

Before showing how the equations can be coupled aerodynamically, let's first look at the solutions to the equations. As they are presented, the equations are linear and can be solved separately. The solution for x , for example, is the sum of a transient (homogeneous) and a steady-state solution.

$$x(t) = x_t(t) + x_s(t)$$

Placing the x equation in standard form

$$\ddot{x} + 2\zeta\omega_n\dot{x} + \omega_n^2 x = f'(t)$$

where

$$\omega_n^2 = \frac{K_x}{m}$$

$$\zeta = \frac{d}{2\sqrt{mk_x}}$$

$$f'(t) = \frac{f(t)}{m}$$

The undamped natural frequency ω_n^* , is the frequency the system would oscillate in the absence of damping. The damping ratio ζ is simply a convenient way of representing the degree of damping (due to the dash-pot coefficient, d) relative to the size of the mass and spring constants. The method for finding the transient solution can be found in numerous texts on differential equations.

$$x_t = e^{-\zeta\omega_n t} (C_1 \cos \omega_d t + C_2 \sin \omega_d t) \quad (12.38)$$

$$\omega_d = \omega_n \sqrt{1 - \zeta^2}, \quad 0 \leq \zeta < 1$$

where the constant ω_d is the damped frequency, and for obvious reasons is less than the undamped frequency ω_n . We see that the transient response has the form of a sinusoidal oscillation whose envelope decreases exponentially with time.

To solve for the steady-state solution x_s , knowledge of the driving force $f(t)$ is required. Flutter has been observed to be sinusoidal, therefore we can assume that the nature of the driving force is also sinusoidal.

NOTE: *In this example, ω_n is the undamped translational structural frequency.

$$f(t) = F \cos \omega t$$

We can then assume a steady-state solution of the form

$$x_s = A \cos (\omega_t + \phi)$$

Substitution into the differential equation yields values for the constants. Chapter 3 of Reference 11 gives the details to the solution.

$$A = \frac{F/k_x}{\sqrt{\left(1 - \frac{\omega^2}{\omega_n^2}\right)^2 + \left(2 \zeta \frac{\omega}{\omega_n}\right)^2}}$$

and

$$\phi = \tan^{-1} \left(\frac{-2 \zeta \frac{\omega}{\omega_n}}{1 - \frac{\omega^2}{\omega_n^2}} \right)$$

The steady-state response with amplitude A and phase angle ϕ is of the same form as the driving force. The amplification factor $A/(F/k_x)$ is the ratio of the amplitude A of the steady-state solution to the static deflection F/k_x due to a constant force of magnitude F . Figure 12.79 shows a plot of the amplification factor versus frequency for different values of ζ .

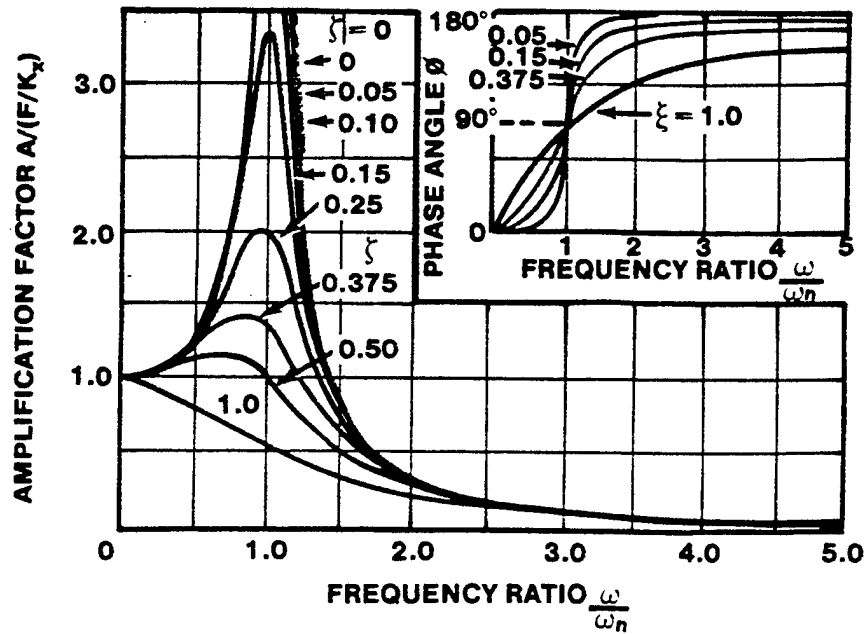


FIGURE 12.79. AMPLIFICATION FACTOR AND PHASE ANGLE VERSUS FREQUENCY RATIO

The amplification factor is unity when the input frequency is zero, regardless of the damping ratio ζ . It is important to note that when the forcing frequency (ω) equals the undamped natural frequency (ω_n), the amplification factor is $1/(2\zeta)$. Consequently, any amount of damping is very critical in holding down the response. Lack of damping results in an unbounded output.

Note also that at the critical frequency ($\omega = \omega_n$) the phase angle ϕ is 90° , regardless of ζ . It can be shown that during this condition, the response (bending) velocity \dot{x}_g is exactly in phase with the driving force $f(t)$, which is the condition for maximum power input into the oscillating wing system from the external force.

How do we relate the above analysis to a meaningful wing flutter problem? Looking back at Figure 12.78 we can take the x degree of freedom as the basic wing bending mode with natural frequency of oscillation $\omega_n = \sqrt{k_x/m}$, a value obviously dependent upon the mass and elastic properties of the wing. The external force $f(t)$ can be inferred to be the aerodynamic lift acting on the given wing section.

$$f(t) = -L(t) = -q S C_{L_\alpha} \alpha(t)$$

If $\alpha(t)$ were to vary sinusoidally at frequency ω , we'd have

$$f(t) = -q S C_{L_\alpha} \alpha_0 \cos \omega t \quad (\alpha_0 \text{ is the magnitude of the angle of attack variations with time})$$

or,

$$f(t) = F \cos \omega t$$

This is exactly the same type of external driving force described in the example above. Such a variation in α can also result from the rotational equation of motion.

$$I\ddot{\alpha} + b\dot{\alpha} + k_\alpha \alpha = M(t)$$

Solving for the free body response [$M(t) = 0$], the solution is similar to the displacement transient solution (Equation 12.38)

$$\alpha(t) = e^{-\zeta_T \omega_\alpha t} \left[C_1 \cos \left(\omega_\alpha \sqrt{1 - \zeta_T^2} t \right) + C_2 \sin \left(\omega_\alpha \sqrt{1 - \zeta_T^2} t \right) \right]$$

In most wing structures, bending damping is much greater than torsional damping. Therefore, without loss of generality we can assume torsional structural damping (ζ_T) to be small. The solution then has the approximate form

$$\alpha(t) = C_1 \cos \omega_\alpha t + C_2 \sin \omega_\alpha t,$$

where $\omega_\alpha = \sqrt{k_\alpha/I}$ represents the natural undamped torsional frequency of the wing. If the initial conditions are picked appropriately, $\alpha(t)$ can be represented by

$$\alpha(t) = \alpha_0 \cos \omega_\alpha t \quad (12.39)$$

The critical condition now occurs when $\omega = \omega_\alpha = \omega_n$ i.e., when the natural frequencies of wing bending and wing torsion are the same. Substituting $\omega = \omega_\alpha$ in Equation 12.39 yields

$$\alpha(t) = \alpha_0 \cos \omega t$$

or,

$$\cos \omega t = \frac{\alpha(t)}{\alpha_0}$$

Substituting this into the forcing function for displacement $f(t)$ gives

$$f(t) = \frac{F}{\alpha_0} \alpha(t)$$

If F/α_0 is set equal to some constant A , then

$$f(t) = A\alpha(t)$$

Equation 12.36 then becomes

$$m \ddot{x} + d \dot{x} + k_x x = A \alpha(t)$$

In this example the result is aerodynamic coupling between the two degrees of freedom, bending and torsion. Under certain conditions of damping, the end product from the coupling will be classical bending-torsional flutter.

A side view of the flight path of the wing in bending-torsional flutter is shown in Figure 12.80.

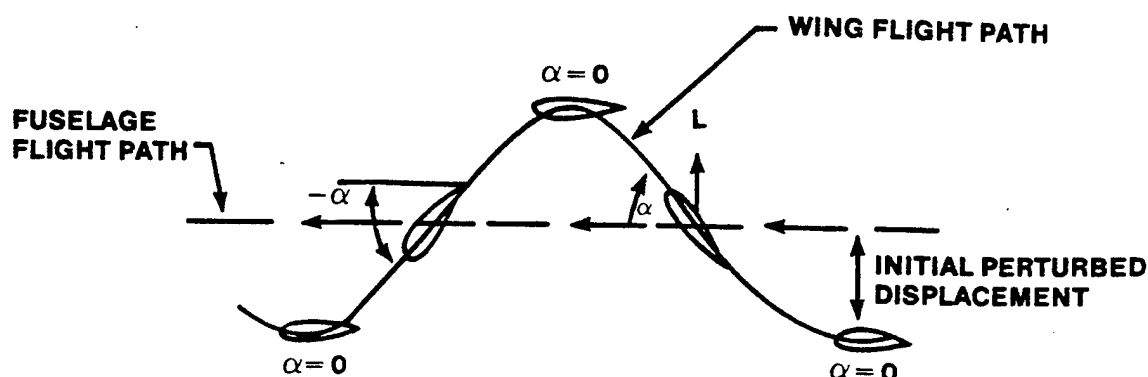


FIGURE 12.80. BENDING-TORSIONAL FLUTTER ($\omega = \omega_{\alpha} = \omega_n$)

This is a very simplified explanation of wing bending-torsion flutter. The bending mode is coupled aerodynamically with the torsion mode to effect the dynamic instability. The physical interpretation is rather straightforward but precise predictions on actual wing flutter speeds and frequencies are extremely difficult to obtain analytically. In our example, several specific assumptions and simplifications were made: (1) the elastic axis was placed at the c.g., (2) the wing section was treated as a rigid one, and (3) the aerodynamic damping and air mass accelerations were ignored. However, these assumptions did not detract from the general ideas basic to the dynamic instability.

Other types of flutter which may occur usually involve the rotation of some control surface about its hinge line. Wing bending/aileron rotation flutter, or fuselage torsion/rudder rotation flutter are examples. It is also possible, in fact more common for more than two modes to be present, such as in wing bending/wing torsion/aileron rotation flutter. Theodore Theodorsen presented a NACA paper in 1935 which treats the three-degree-of-freedom wing-aileron airfoil in somewhat complete and tedious detail.

12.5.7 Structural Modeling

To expand the analysis to treat the total aircraft structure and to cover all interactions between structural components is considerably more difficult.

The problem is basically twofold in the derivation of the equations of motion. First, the free body mass and structural relationships have to be determined. Second, the aerodynamic forces acting on the entire surface have to be derived. These forces will in turn depend upon the deflections, velocities, and accelerations of the structure.

General equations can be formulated by treating the aircraft as composed of a large number of discrete masses. Rewriting Equation 12.36 in matrix form yields the general equation

$$[m] \{\ddot{x}\} + [d] \{\dot{x}\} + [k] x = f(t)$$

The brackets $[]$ signify a square matrix and the braces indicate a column matrix. Represented are n simultaneous equations in degrees of freedom x_i^* ($i = 1, 2, \dots, n$). The equations are difficult to formulate and difficult to solve. The main problem lies in determining the stiffness coefficients K_{ij} .

To obtain the harmonic solution to the above equations a continuous forcing function, F_i , is applied equal to the structural damping d_{ij} . As a result, the forcing function and structural damping cancel and the equations are simplified to

$$[m] \{\ddot{x}\} + [k] \{x\} = 0$$

Next, a matrix of flexibility influence coefficients C_{ij} is defined as the inverse of the stiffness matrix

$$[c] = [k]^{-1}$$

The equations now become

$$[c] [m] \{\ddot{x}\} + \{x\} = 0$$

The influence coefficients are preferred to the stiffness coefficient because they are more conveniently determined by actual measurements on the structure or a scaled model. Using the simple spring relationship shown in Figure 12.81, the force F required to deflect a spring (or wing section equivalent) a distance x in static equilibrium is governed by

$$F = kx$$

Or, taking a different view, the displacement x resulting from the application of a force F is given by

$$x = 1/k F = C F.$$

*The coordinate x_i can represent either a displacement or an angular deflection.

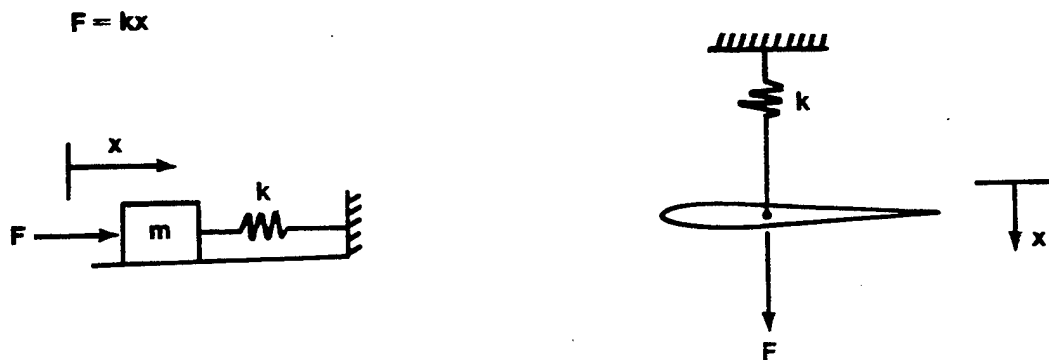


FIGURE 12.81. SIMPLE SPRING RELATIONSHIP

If we assume, for example, that a wing in Figure 12.82 is approximated by five separate sections, the displacement at section 3 due to forces F_2 and F_4 applied at stations two and four, respectively, is given by

$$X_3 = C_{32} F_2 + C_{34} F_4$$

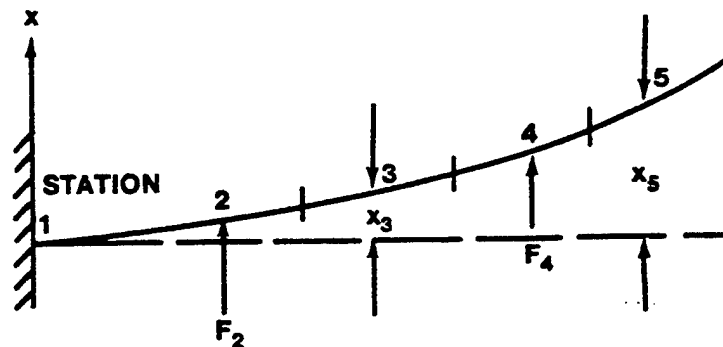


FIGURE 12.82. CANTILEVER WING

In general, a displacement at Station (or mass point) i due to the existence of forces at Station j is given by the following relationship:

$$x_i = C_{i1} F_1 + C_{i2} F_2 + \dots + C_{in} F_n$$

$$x_i = \sum_{j=1}^n C_{ij} F_j$$

Conversely, a force at Station i will cause deflections at Stations j , governed by

$$F_i = k_{i1} x_1 + k_{i2} x_2 + \dots + k_{in} x_n$$

$$F_i = \sum_{j=1}^n k_{ij} x_j$$

The C_{ij} can be determined by

$$C_{ij} = \left[\frac{x_i}{F_j} \right]_{F_k = 0, k \neq j}$$

Therefore C_{ij} will not become undefined.

For example, if a unit force were applied at station 27, (i.e., $F_{27} = 1$) and all other forces were zero, all the $C_{i,27}$ can be determined from

$$C_{i,27} = x_i$$

On the other hand, the $k_{27,j}$ are not as conveniently determined since it is difficult to isolate a force when a unit displacement is applied at any station. Consequently, it is much easier and more accurate to measure a displacement than to measure a force and the influence coefficient is more often used.

For the equations

$$[c] [m] \{\ddot{x}\} + \{x\} = 0$$

we can assume sinusoidal solutions of the form

$$x_i = A_i \sin \omega t, \text{ or}$$

$$\{x\} = \{A\} \sin \omega t$$

Substitution into Equation 12.40 leads to

$$-\omega^2 [c] [m] \{A\} \sin \omega t + \{A\} \sin \omega t = 0$$

or, since $\sin \omega t \neq 0$

$$\frac{1}{\omega^2} \{A\} = [c] [m] \{A\}$$

This is a standard eigenvalue problem which can be solved using iterative techniques. Values of the model vectors or mode shapes A can be found, corresponding to a specific frequency ω . There are as many eigenvalue solutions ω and corresponding eigenvectors A as there are degrees of freedom in the system. That is, an n degree of freedom system has n mode shapes and frequencies. The concept of mode shapes is so basic to flutter analysis that further discussion is justified at this time.

12.5.8 Structural Vibrations - Mode Shape Determination

The basic discussion of mode shapes and frequencies will use the uniform cantilever beam of length L shown in Figure 12.83 as an example.

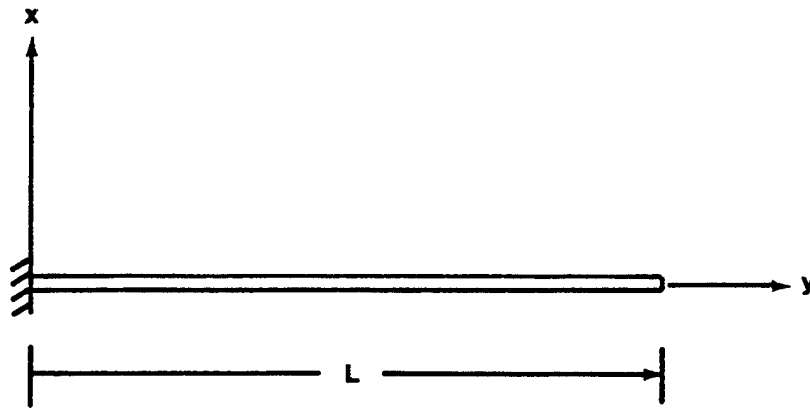


FIGURE 12.83. UNIFORM CANTILEVER BEAM

What do the natural mode shapes represent and how do we compute them? The real question to address is: If the beam were to vibrate freely at some resonant condition* what vibrating shape would it assume and what would the frequency of vibration be?

Since the beam is continuous it has an infinite number of mass points and, consequently, an infinite number of degrees of freedom. We state, without proof, that there are also an infinite number of distinct vibration shapes, each of which has a unique vibration frequency.

The Equation of Motion for this system leads one to a complex or double eigenvalue problem, where the eigenvector determines the modal shape of the beam, $X(y)$, and corresponding eigenvalue, ω_z^2 , represents the square of the vibration frequency. These eigenvalues are derived given the mass and stiffness distributions, and the specific boundary conditions. For the beam

*Definition: Resonant Condition - Vibrating at a maximum amplitude in phase with an oscillating input at the systems undamped natural frequency, ω_n .

in Figure 12.83 the boundary conditions are: zero displacement and slope at the fixed end ($y = 0$), and zero shear and moment at the free end ($y = L$). The eigenvectors are solutions to homogeneous equations so that if $X_k(y)$ is a mode shape, $C X_k(y)$ is one also. As a result, each mode shape function represents relative displacements along the beam. The absolute values are determined from the initial conditions.

The differential equation for the cantilever beam as given in Reference 1 is

$$EI \frac{d^4 x}{dy^4} + m \frac{d^2 x}{dt^2} = 0 \quad (12.41)$$

where

E = modulus of elasticity
 I = area moment of inertia
 m = mass distribution.

Equation 12.41 is a separate partial differential equation with a solution $x(y, t)$ a product of a function of y only, $X(y)$, times a function of time only, $T(t)$.

$$x(y, t) = X(y) T(t)$$

Substituting $x(y, t)$ into Equation 12.41 yields

$$EI \frac{d^4 X}{dy^4} T + m \frac{d^2 T}{dt^2} X = 0$$

or

$$-\frac{1}{T} \frac{d^2 T}{dt^2} = \frac{EI}{m} \frac{d^4 X}{dy^4} \frac{1}{X}$$

Since y and t are independent, they can be equated to a separation constant. In this example the separation constant will be the square of the mode shape frequency, ω^2 . The result will be two linear differential equations.

$$\frac{d^2 T}{dt^2} + \omega^2 T = 0$$

$$\frac{EI}{m} \frac{d^4 X}{dy^4} - \omega^2 X = 0$$

or,

$$\frac{d^4 X}{dy^4} - \frac{\omega^2}{a^2} X = 0$$

where

$$a = \sqrt{\frac{EI}{m}}$$

The solutions to Equations 12.42 and 12.43 are

$$T = A \sin \omega t + B \cos \omega t$$

$$X = C \sinh \sqrt{\frac{\omega}{a}} y + D \cosh \sqrt{\frac{\omega}{a}} y \\ + E \sin \sqrt{\frac{\omega}{a}} y + F \cos \sqrt{\frac{\omega}{a}} y,$$

where, A, B, C, D, E, and F are constants. Applying the boundary conditions for a uniform cantilever beam: $X(0) = 0$, $X'(0) = 0$, $X''(L) = 0$, and $X'''(L) = 0$, yields the following transcendental equation. The solution of which gives the mode shape frequency ω_i .

$$\cos \sqrt{\frac{\omega}{a}} L + \frac{1}{\cosh \sqrt{\frac{\omega}{a}} L} = 0, \quad (12.44)$$

where

$$a = \sqrt{\frac{EI}{m}}$$

The solution to Equation 12.44 can be found by iterative techniques or through graphic depiction. What follows is the graphical solution that satisfies Equation 12.44.

The abscissas of the points of intersection of the curves yield values for $\sqrt{\frac{\omega}{a}} L$.

$$\sqrt{\frac{\omega}{a}} L = 0.597 \pi, 1.49 \pi, \frac{5}{2} \pi, \frac{7}{2} \pi, \frac{9}{2} \pi, \dots$$

or

$$\omega_1 = (0.597)^2 \left(\frac{\pi^2}{L} \right) a$$

$$\omega_2 = (1.49)^2 \left(\frac{\pi^2}{L} \right) a$$

⋮

$$\omega_i = \left(i - \frac{1}{2} \right)^2 \left(\frac{\pi^2}{L} \right) a, \text{ (i sufficiently large).}$$

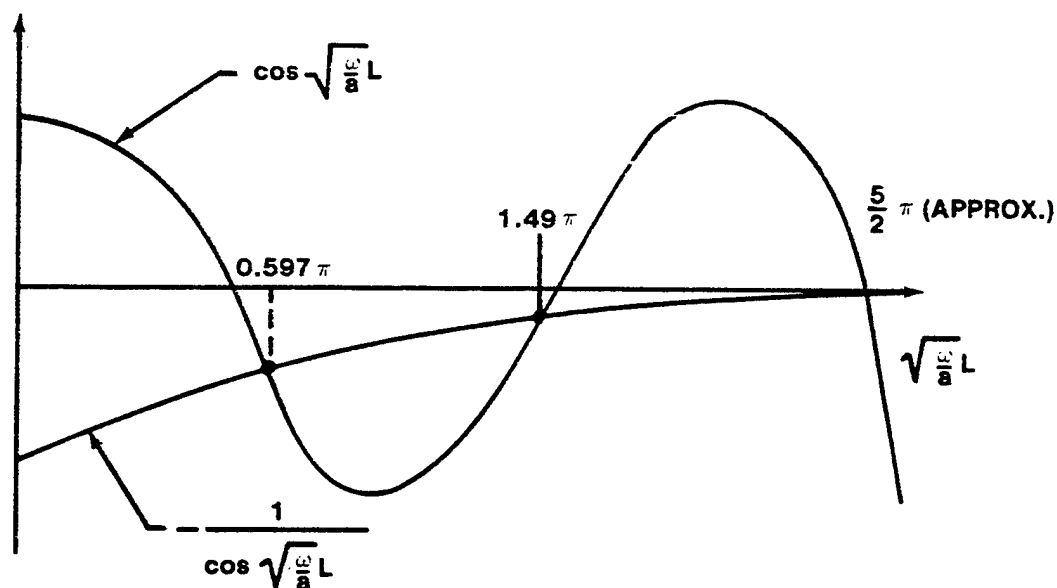


FIGURE 12.84. GRAPHICAL SOLUTION TO THE TRANSCENDENTAL EQUATION OF A UNIFORM CANTILEVER BEAM

Having determined the model frequencies, ω_1 , the specific mode shapes, $X_1(y)$, can be derived by substituting the frequency values ω_1 into the general mode shape equation for the cantilever.

$$X_i(y) = \left[\left(\frac{\sin \sqrt{\frac{\omega_i}{a}} L - \sinh \sqrt{\frac{\omega_i}{a}} L}{\cosh \sqrt{\frac{\omega_i}{a}} L + \cos \sqrt{\frac{\omega_i}{a}} y} \right) \left(\sinh \sqrt{\frac{\omega_i}{a}} y - \sin \sqrt{\frac{\omega_i}{a}} y \right) + \left(\cosh \sqrt{\frac{\omega_i}{a}} y - \cos \sqrt{\frac{\omega_i}{a}} y \right) \right]$$

Where D is a constant determined by the boundary conditions. Do not be concerned at how these equations were derived. They are simply the solutions of the fourth order differential equation for the vibrating cantilever beam. The important thing to note is that there are an infinite number of solutions ω_i , and that for each ω_i there corresponds an $X_i(y)$. Figure 12.85 shows four of the lowest frequency mode shapes.

The significance of the application of mode shapes and frequencies is that any vibration of any elastic body will be a summation of individual mode shape vibrations. The characteristics of mode shapes are such that (1) for each natural vibration frequency there exists one and only one natural mode shape, (2) in the vibration of any single mode, the displacements of the structure reach their zeros and their extreme simultaneously [as is evident from the solution $x(y,t) = X(y) T(t)$], (3) the natural mode shapes are linearly independent (i.e., no shape can be formed by any linear combination of the others), and (4) in any free vibration of a beam, wing, aircraft structure, bridge, and so forth, any combination of natural modes can exist simultaneously without mutual interference. In the case of aircraft flutter, the mode shapes become coupled due to the action of the external aerodynamic driving forces, which are in turn functions of the critical mode shapes. Using the general discrete mass free body problem discussed earlier, we can relate to a specific aircraft example.

$$[c] [m] \ddot{x} + x = 0$$

with solution

$$\frac{1}{\omega^2} \{A\} = [c] [m] \{A\}$$

The "wing" in Figure 12.82 has five separate stations, each with mass m_i and each having two degrees of freedom, x_i , a vertical displacement, and α_i an angular rotation about the elastic axis as shown in Figure 12.86.

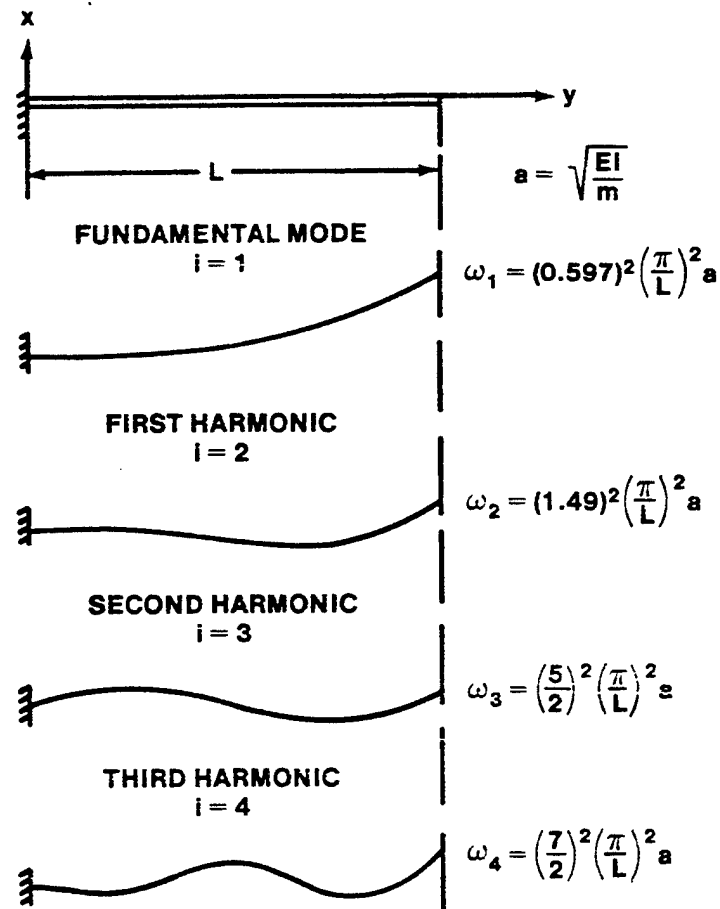


FIGURE 12.85. FREQUENCY MODE SHAPE FOR A VIBRATING BEAM

The model vector $\{A\}$ is comprised of ten-degrees of freedom; five vertical displacements and five angular deflections.

$$\{A\} =$$

$$\begin{bmatrix} x_1 \\ \cdot \\ \cdot \\ x_5 \\ \alpha_1 \\ \cdot \\ \cdot \\ \alpha_5 \end{bmatrix}$$

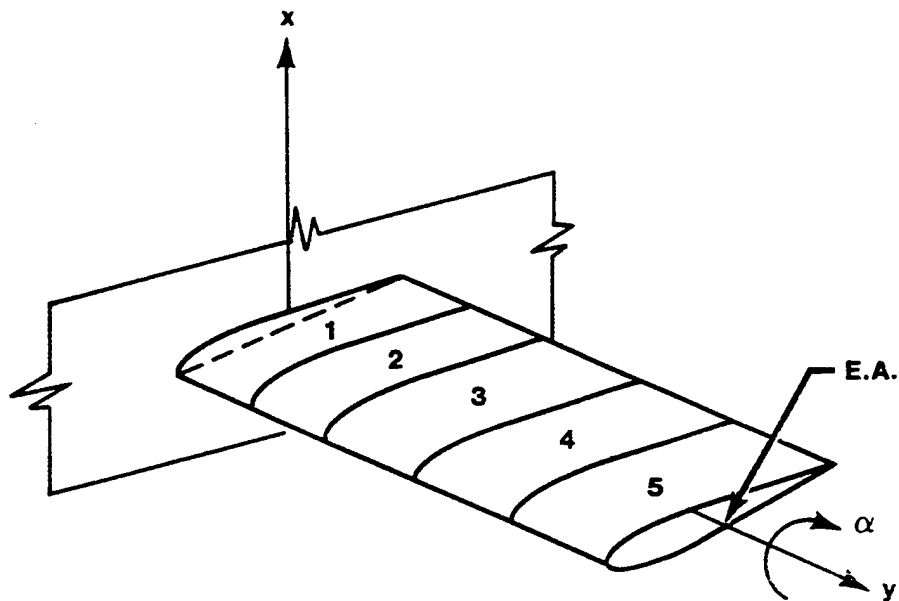


FIGURE 12.86. CANTILEVER WING

From experimental measurements we can determine the mass and moment of inertia of each section, along with the influence coefficients (D_{ij}) for the total wing with respect to the ten degrees of freedom. Recall that C_{28} represents the vertical deflection x_2 at wing Station 2 due to a unit moment applied at wing Station 3 (α_3 being the eighth degree of freedom by definition).

The matrix equation

$$\frac{1}{\omega^2} \{A\} = [c] [m] \{A\}$$

thus, represents 10 simultaneous equations in the 11 unknowns $\omega, X_1, \dots, \alpha_5$. Again, the mode shapes are relative displacements in the A matrix. A typical solution might be

$$\omega = 3.5, \quad A$$

$$\begin{bmatrix} 1.00 \\ 1.21 \\ 1.63 \\ 2.23 \\ 3.05 \\ 0.74 \\ 1.13 \\ 1.74 \\ 2.57 \\ 3.49 \end{bmatrix}$$

At any given time, therefore, the wing station deflections for the given 3.5 rad/sec mode might be represented by

$$\{x\} = K \{A\} \sin(3.5t + \phi_1)$$

where the values K and ϕ_1 would depend on the initial conditions. Other modes at different frequencies will, of course, exist simultaneously. Flutter is the result of the aerodynamic coupling of these modes.

Even for simple structures the mode shapes and frequencies may be difficult to determine analytically. As a result, many simplifying assumptions are normally made. For the wing just described, the assumption that it can be represented by five rigid sections seems a bit gross, but for the low frequency mode shapes the simulation is quite reasonable. In actual aircraft problems the critical modes are usually the lower frequency ones for very fundamental reasons. The large bending and structural deformations are the ones which more efficiently extract energy from the airstream. These are usually the lower frequency modes.

A useful technique for the flutter analyst is to assume that a structure will take on certain predetermined mode shapes based on previous observations of similar type structures. The assumed mode shape can then be used in the energy equations to arrive at the particular mode shape frequency. This technique aids in the solution of complex structures but there is obviously an accompanying reduction in accuracy. The subject of mode shapes will be brought up again in the discussion of ground vibration tests.

12.5.9 Wind Tunnel Modeling

The use of aircraft models has produced solutions to practical problems in the areas where existing theory is not yet dependable. Particularly in dealing with flutter, the testing of wind tunnel models with properly scaled mass and stiffness properties has often yielded better results than equivalent analytical efforts.

12.5.10 Buckingham π Theorem

Model theory must be based on a clear understanding of the principles of dimensional analysis. The writing of equations in dimensionless form with a reduction in the number of variables was generalized by Buckingham in his " π Theorem" which states that if a physical situation can be represented by the equation

$$\psi (S_1, S_2, S_3, \dots, S_n) = 0$$

where the n arguments S_i include all the primary quantities (mass, length, time, etc.), the secondary quantities, and dimensional constants which must be considered in the problem, the equation can be rewritten in the form

$$\phi (\pi_1, \pi_2, \pi_3, \dots, \pi_{n-m}) = 0$$

in which $\pi_1, \pi_2, \dots, \pi_{n-m}$ are the $(n-m)$ independent products of the arguments S_1, \dots, S_n , which are dimensionless in primary quantities. The form of these dimensionless π 's can be found by a formal procedure but they can usually be constructed by inspection. Typical π 's in general use are aspect ratio AR , reduced frequency $k = \omega b/V$, Mach M , and Reynolds number Re . There are two main advantages in using dimensionless variables. First, since the dimensionless equation of motion is completely unaffected by scale effects the values of the dimensionless variables should be the same for both the original problem and its model.

As a sample problem we can use the wing twist relationship derived earlier to determine the wing divergence speed.

$$\theta = \frac{q S (e C_{L\alpha} \alpha_r + c C_{Mac})}{K_{\theta\alpha} - q S e C_L}$$

θ , α_r , C_{L_α} and $C_{M_{\bar{e}c}}$ are already dimensionless. The other quantities have the dimensions as indicated ($n + 5$).

$$q = \frac{F}{L^2}$$

$$S = L^2$$

$$K_\theta = FL$$

$$e = L$$

$$c = L$$

Force (F) and length (L) were chosen as the primary quantities ($m = 2$).

By inspection we can form independent dimensionless ratios e/c and qSc/K_θ so that the equation may be rearranged to read

$$\theta = \frac{\left(\frac{qSc}{K_\theta}\right) \left[\left(\frac{e}{c}\right) C_{L_\alpha} \alpha_r + C_{M_{\bar{e}c}} \right]}{1 - \left(\frac{qSc}{K_\theta}\right) \left(\frac{e}{c}\right) C_{L_\alpha}}$$

The number of arguments has been reduced by two, as predicted by the Theorem (since there are the two primary quantities F and L in the equation). The equation really implies that any model of the semi rigid wing having the same shape ($C_{M_{\bar{e}c}}$ and C_{L_α}) must have the same dimensionless location of the elastic axis (e/c), the same rigid angle of attack (α_r), and the same ratio of aerodynamic to elastic forces (qSc/K_θ). It is also desirable to have similar Mach and Reynolds numbers if the effects are significant.

12.5.11 Aeroelastic Model

All aeroelastic models are designed along three fundamental airplane properties: (1) structural stiffness distribution, (2) mass distribution, and (3) the external shape. The model designer has to decide beforehand which of the properties will require a more exact simulation, depending on the nature of the planned tests. Property (1) is important for accurate loading measurements and property (3) is important for aerodynamic force evaluations. A flutter model obviously requires an accurate reproduction of all three properties and is therefore difficult to design.

The usual first approach is to attempt a scaled replica. However, for low speed models the required skin thickness (using the same material) may be prohibitively small. For a more workable thickness a softer material must be used but this in turn tends to reduce the accuracy of the stiffness reproduction. It also limits the amount of structural detail which can be obtained. The designer most often finds that the best plan is to lay out a simplified structure, making sure that it does not use up too much of the available mass. A shell is then formed to enclose the structure with the proper external shape. Finally, the remaining mass is distributed over the sections. The type of construction used for both the structure and the external shell depends upon the size, speed range, and ratio of the air density between aircraft flight altitude and test chamber conditions.

The types of aeroelastic testing fall into three general areas, whether with models or with full scale airplanes. The first area requires no airstream, such as in fatigue, static loading, and ground vibration tests. The second and third test areas involve airflow, in either the tunnel or full scale flight. The second area encompasses the static phenomena divergence, (control effectiveness) and the third area includes the unsteady phenomena such as flutter, gust loading and dynamic stability.

The test programs for nearly all prototypes include "shake testing", to determine the normal modes of vibration. These derived mode shapes and frequencies can be compared with the analytical calculations to verify the mass and stiffness properties of the math model. Sometimes the experimental data serve as the basis for a new set of calculations.

Once an adequate model is built the testing takes place. There are basically two different approaches to the problem. In the first, the testing is designed to evaluate the coefficients in the differential equation governing the problem. In the second approach the model is designed and tested as an analog. The model can simulate parts of airplanes, such as wings or tails, or the whole airplane. Each scheme has peculiar advantages and drawbacks as well as the usual problems of excitation, mounting and measurement. The particular details of tunnel testing and measurement is a total subject in itself.

12.5.12 Wind Tunnel Model Flutter Prediction Methods

Four methods used to measure the subcritical (below the actual flutter speed) response characteristics are co/quad, randomdec, power spectral density (PSD), and peak-hold spectrum methods. These methods are used to measure the frequency and damping (or an inverse response amplitude proportional to the damping in the peak-hold spectrum case) in the predominant or critical vibration modes. By suitably plotting and extrapolating the subcritical damping in the vibration mode or modes of interest, the flutter point can usually be established. With each method, the response can be approximated by that of a single-degree-of-freedom system. All of these methods can be used real-time, that is, used to translate the response time history samples into quantitative information for the test engineer while the test is in progress.

Briefly, the co/quad method measures the in-phase and out-of-phase components of the forces response generated by the sinusoidal frequency sweep technique. The randomdec method, a relatively new method used in the F-16 flight flutter testing, makes use of ensemble averaging of transient response to random excitation. The PSD method is a well-known procedure for the analysis of random response data. It is obtained directly from an ensemble average of the square of the magnitude of the Fourier transform of a number of segments of the time history. In the peak-hold spectrum method, Fourier components of a number of time history segments are determined and the envelope of the peak values of these components is obtained as a function of frequency.

Co/Quad Method. The co/quad method involved measuring the forced response of a model to an input force such as that generated by a trailing-edge control surface as illustrated schematically in Figure 12.87. If a transfer function relating the response to the input force is determined as a function of frequency, then the damping on each mode can be obtained. Cross spectrum between the control surface command signal and the model dynamic response can be determined with a co/quad analyzer. This type analyzer presents two outputs in terms of in-phase (called co for coincident) and out-of-phase (called quad for quadrature) components between signals. Several means of calculating the damping are available directly from a co and quad type of presentation. As indicated in Figure 12.87, the damping of a

mode can be estimated from the out-of-phase component by the frequencies labeled f_A and f_B . These are the frequencies at the half-power points and the structural damping g can be expressed in terms of these frequencies (Figure 12.87).

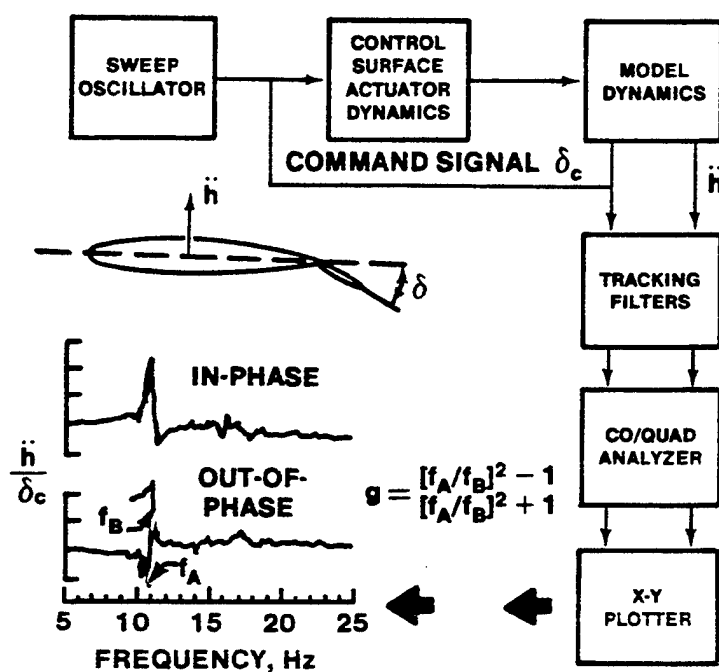


FIGURE 12.87. IMPLEMENTATION OF CO/QUAD METHOD

Randomdec Method. The Random Decrement method is basically an ensemble averaging of the turbulence-induced random vibrations of the test article. As is illustrated in Figure 12.88, triggering each data sample at a constant level, Y_t . Assuming linear superposition, the time history of each sample can be regarded as the combined solution from (1) an initial step displacement, (2) an initial velocity and (3) a random forcing function. Note that the Figure 12.88C sample represents the response to the same initial displacement as Figure 12.88B, a different initial velocity with the opposite sign, and a different random forcing function. It can be reasoned intuitively that when a large number of samples are averaged, only the response to the constant initial displacement will remain because the average of responses due to the

alternating initial velocities and the random forcing functions will tend to zero. Thus, it is seen that the ensemble average converges toward the transient response to an initial step. For a constant trigger level, the ensemble average (Randomdec Signature) will be constant even if the amplitude of the forcing function varies. If the ensemble average is made up of samples with initial positive slopes only, then the resulting trace represents the transient response to a combined step and initial velocity. Under these conditions the Randomdec Signature would vary with the intensity of the forcing function, thus minimizing the use of the signature trace as a failure detector. However, the damping as determined from the decay rate of the signature trace would be valid.

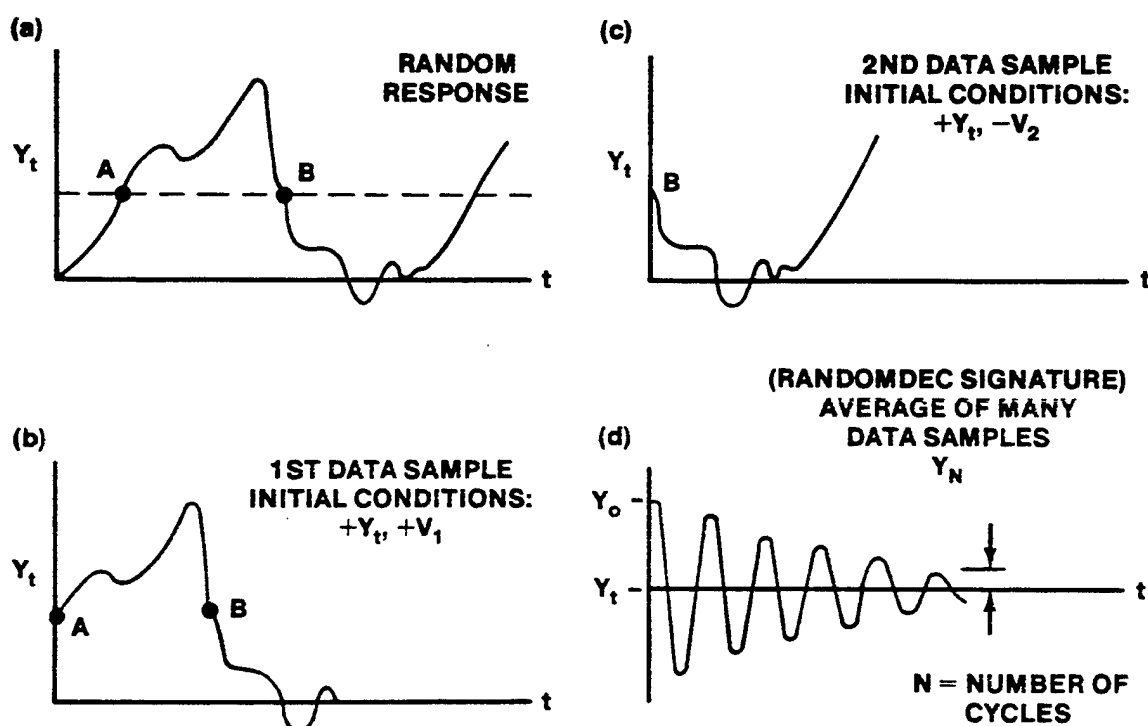


FIGURE 12.88. RANDOM DECREMENT CONCEPT

Structural damping, g , may be determined directly by

$$g = \frac{1}{N\pi} \log_e \left(\frac{Y_0}{Y_N} \right)$$

PSD and Peak-Hold Spectrum Methods. The PSD and the peak-hold spectrum methods are implemented as shown in Figure 12.89. Both methods are implemented using a spectroscope. This analyzer employs time compression techniques to achieve minimum analysis time for the frequency-tuned band-pass filter to convert the input signal from the time domain to the frequency domain. Following compression, the input signal is frequency analyzed. Shown on the left of Figure 12.89 is a typical PSD obtained from the model dynamic response h . The resulting signature has a peak for each structural mode and, for well-separated peaks, the damping ratio may be obtained. As indicated in Figure 12.89, the structural damping is equal to the frequency bandwidth, taken at the half-power point, and divided by the mode frequency.

An additional mode of operation of a spectroscope allows for detection and storage of the peak values of frequency windows. In this mode of operation, an ensemble spectrum composed of frequency windows is obtained.

Upon receipt of each subsequent spectrum, peak filter response at each location is updated in a positive direction. That is, only an increase in value causes an update to the new higher value. On the right of Figure 12.89, a typical peak-hold spectrum is shown. With this method the damping parameter

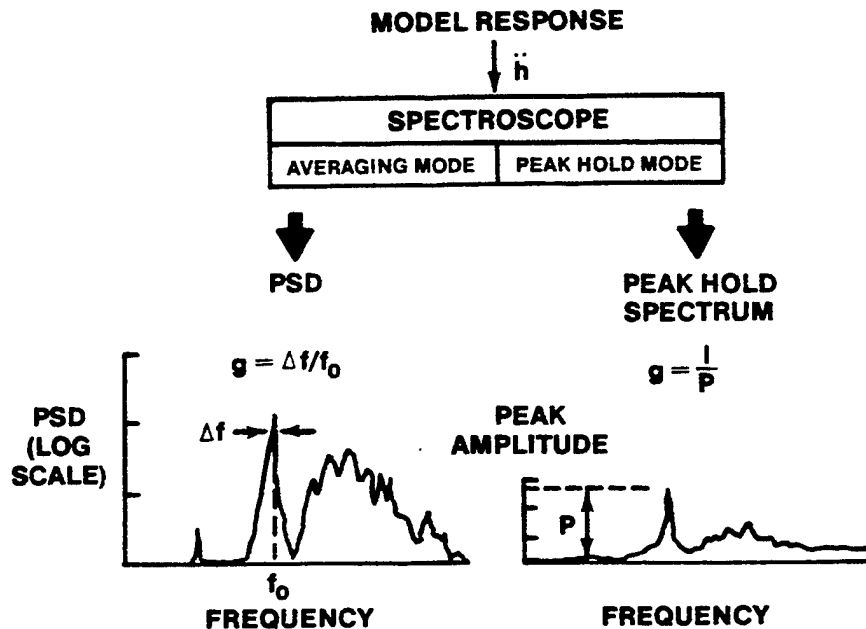
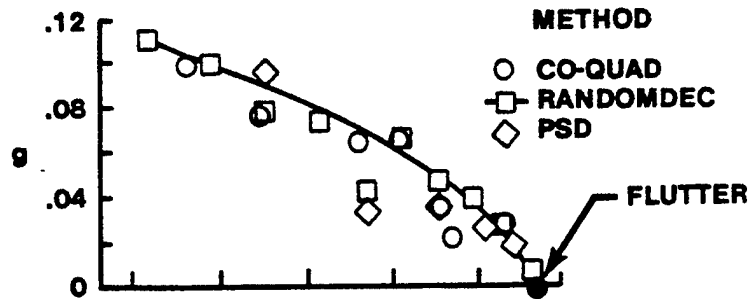


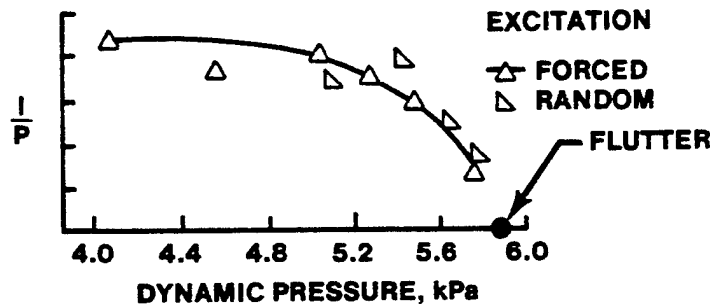
FIGURE 12.89. IMPLEMENTATION OF SPECTRUM METHODS

is not obtained. However, the reciprocal of the peak spectrum amplitude $1/P$ is proportional to the damping ratio and is used as a measure of system stability. The peak-hold method can be applied using two forms of excitation, model response to tunnel turbulence and model response to sinusoidal force.

Typical results obtained from the four subcritical response methods are presented and compared in Figures 12.90 and 12.91. Figure 12.90 presents the variation of structural damping coefficient of a delta wing flutter model with dynamic pressure. The damping results obtained with co/quad, randomdec, and PSD are indicated with open symbols. The model fluttered at a dynamic pressure of 5.89 kPa (1231bf/ft²) as indicated with the closed symbol. A plot of the inverse amplitude of the peak spectrum (used as the stability criteria) is presented in Figure 12.90B as a function of dynamic pressure. Shown are results from forced excitation and random excitation (turbulence).



(a) CO/QUAD, RANDOMDEC, PSD RESULTS



(b) PEAK-HOLD SPECTRUM RESULTS

FIGURE 12.90. COMPARISON OF SUBCRITICAL METHODS, DELTA-WING MODEL ($M = 0.90$)

Further illustration of the type of data generated with the use of the four subcritical methods is presented in Figure 12.91. Shown are the data plots from which the damping levels presented in Figure 12.90 were obtained. The wind-tunnel conditions were the same for each method (Mach $M = 0.90$; dynamic pressure $q = 5.42 \text{ kPa}$ (113 lbf/ft^2)).

12.5.13 Ground Vibration Testing (GVT)

As mentioned earlier, the primary purpose of ground vibration testing (shake testing) is to measure the structural mode shapes and frequencies. Sometimes the data serve to generate a new set of calculation. At other times, the measured mode shapes serve as the model for flutter predictions, especially when the effects of configuration changes on flutter speeds are being investigated.

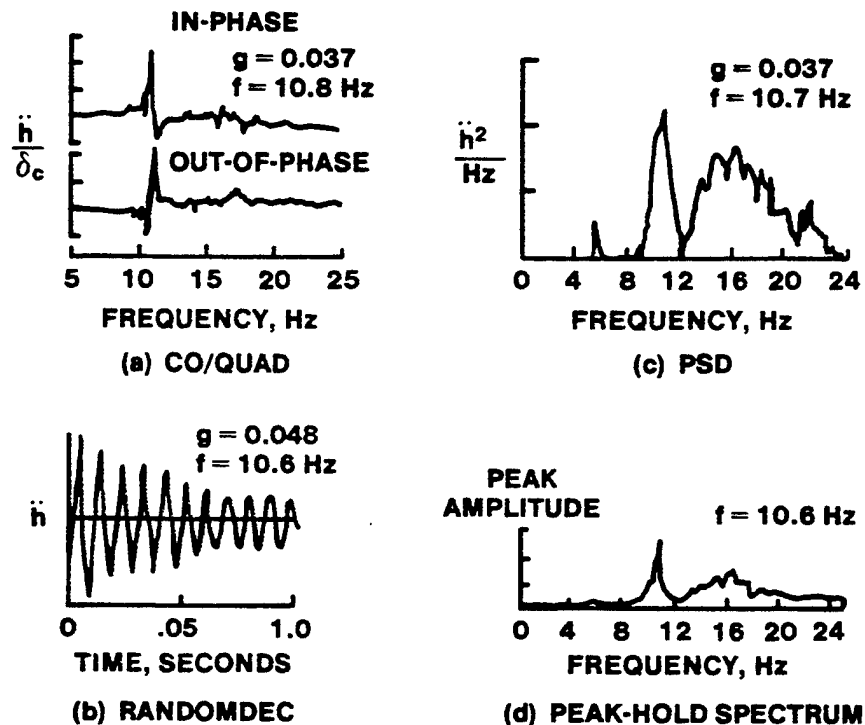


FIGURE 12.91. ILLUSTRATION OF SUBCRITICAL METHODS

$$M = 0.90; q = 5.42 \text{ kPa (113 lbf/ft}^2\text{)}$$

The X-24B "lifting body" is an excellent example of a reconfigured aircraft (from the X-24A). The structural modifications include the addition of right and left strake/aileron combinations and the modification of the two outboard vertical fins. The fin, strake and aileron form a single sub-assembly mated to the airframe. From analyses and previous test experience with the X-24A, the only possible flutter problems would occur with the strake/aileron and fin/rudder components. For further definition of the model characteristics of these components a ground vibration test program was conducted.

The objective in the program (as in all GVT's) was to measure the frequency, mode shape and structural damping for each significant mode of the

new tail section configuration. Especially important was the degree of interaction between the strake/aileron and the fin/rudder in the vibration modes.

For GVT, there is always the requirement to isolate the rigid body modes so that the highest frequency of rigid body motion is well below the lowest frequency of any structural vibration or mode shape. For example, if the natural frequency of rotation of the elevators were 10 Hz, the aircraft as it is supported should not have a pitch frequency close to the 10 Hz value. Otherwise there may be a problem in properly isolating and in determining the existence of that particular elevator rotation mode.

Ideally, the way to isolate the rigid body modes is to suspend the aircraft through the c.g. by a long cable but the methods cannot conveniently be employed. Two practical techniques are (1) to support the vehicle on air cushion stands, or (2) to suspend the aircraft with soft-spring ceiling mounted suspension systems. The approach used on the X-24B was to deflate the tires to half pressure.

The way to excite the structural modes on ground vibration tests is through some variable frequency vibrating device attached to the structure. Typically used are constant force electromagnetic or hydraulic shakers on which there is precise frequency tuning and an automatic frequency sweep feature.

For the X-24B, electromagnetic shakers with current feedback and individual gain and phase controls were used to input the sinusoidal forcing function to the structure. Seven excitation conditions involving six different shaker locations were required to completely investigate the model characteristics. Seven accelerometers were used to obtain data during the test. Acceleration measurements were recorded at predetermined grid points marked on the structure.

The test procedure was to first conduct a frequency sweep from 10 to 200 Hz at each of six different shaker locations. Possible modes were identified by observing Lissajous patterns on an oscilloscope of input force versus reference acceleration, and of other acceleration ratios. Essentially, at resonant condition the force would be in phase with the velocity and this situation would be indicated by the scope patterns. Once a mode was spotted the shaker could be retuned more precisely to the resonant frequency.

Acceleration and phase measurements were then taken along the predetermined grid locations labeled on the structure. Structural damping values were obtained by dumping the armature current to the shakers and measuring the vibration decay traces.

The mode shape and frequency data would be used in a flutter analysis whereby the aerodynamic forces (through a Theodorsen type analysis) would be evaluated in their interaction with the structure. Any conditions of instability could be predicted and the results used to refine the V-g diagrams or equivalent.

12.5.14 Flight Test

Most of the preflight functions have been accounted for. We can now approach the subject at the user's level and discuss the subject of flight test. Is the aircraft free of aeroelastic problems and if so, to what extent?

The criteria for strength and dynamic instabilities are listed in Reference 12.18. V_L , the limit speed for the basic and high drag configurations, is the maximum attainable speed commensurate with the operational use of the airplane, considering shallow and steep dive angles, thrust, operation, and nonoperation of speed brakes, and inadvertent upsets from gusts, or as specified in the contract documents. The airplane or its components should not exhibit flutter, buzz, divergence or other aeroelastic, aerothermoelastic or aeroservoelastic instabilities. The fifteen percent safety margin shall be shown by analytical or experimental data (including flight test up to V_L). In addition, the damping coefficient g for any critical flutter mode or any significant dynamic response mode shall be at least three percent (0.03) for all altitudes and flight speeds up to V_L .

Reference 12.18 also furnishes guidelines on how the math analyses are to be performed, specifying the use of (1) compressible aerodynamics in high subsonic flight, (2) finite span assumptions, and (3) three-dimensional flow effects, if significant. Model and ground vibration tests are also specified when necessary.

For the project manager or project pilot, then, what should the important considerations be in the formulation of the test program. The driving force should be the probability of the flutter condition and its anticipated seriousness. For example, if the airplane were apt to destroy itself well

inside its performance envelope the program would be handled differently from that of a flutter clearance demonstration where the predicted safety margin was 50%.

If the program were solely for flutter, the problem would probably be very specific. In a larger prototype eval program, flutter investigations are usually clearance demonstrations, although there might be occasions when specific problems are anticipated.

At a critical flutter condition the damping ratio of one of the modes becomes zero. The object of flight flutter testing is, then, to obtain a measure of the damping values associated with the flight modes and their trends as the airspeed is progressively increased so that, from the damping trends as sub-critical conditions, the approach of a critical condition may be indicated and its speed determined by extrapolation.

Prototype airplanes represent tremendous investments in time and money. Extensive analytical, model and shake tests are performed in the design and development phase so that for most of the newer aircraft the flutter margins will have been assured. If not, the predictions on speed and damping for the problem areas will be reasonably accurate. On the initial flights the tests will be carried out to increasingly higher speeds and an actual occurrence of flutter can be spectacularly destructive. Even though many preventive measures may have been taken by the designers the possibility of such an occurrence cannot be overlooked.

For most fighter type aircraft the problem areas will not be with the basic airplane but instead with the various wing stores configurations. On large bomber or transport aircraft an aeroelastic instability may exist on the basic airplane. Regardless of whether the aircraft is new or old, large or small, the primary consideration in the program formulation should be the seriousness and probability of the flutter condition.

Other considerations in the program development are time and monetary constraints. Is the problem serious enough that the airplane may face either a grounding or a severe restriction on the envelope until a solution is found? A grounding of the entire T-37 fleet due to a potential rudder flutter problem would place an unacceptable restriction on the USAF UPT program. An airspeed restriction on a front line attack aircraft due to a possible wing flutter

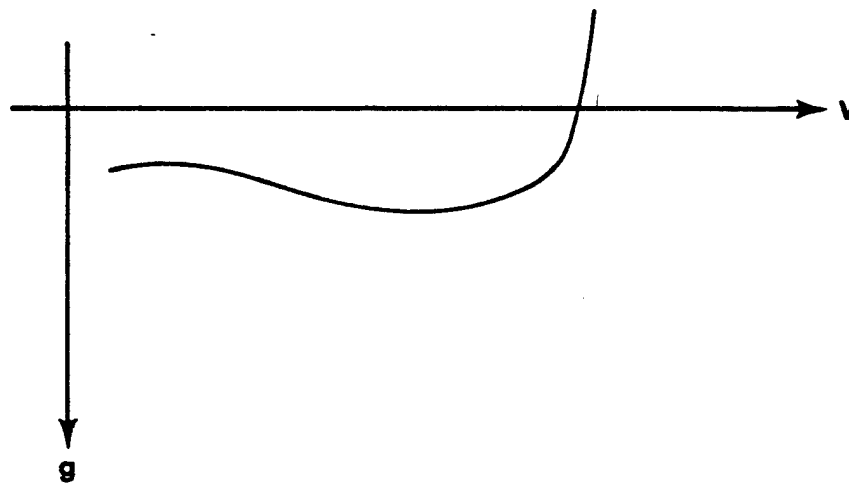


FIGURE 12.92. HYPOTHETICAL V-g DIAGRAM

problem would be intolerable during a crisis situation. In either case there is an immediate need to find a solution - as was the case for the wing divergence problem of the Fokker D-8 during WW I.

Along with the time constraint is the problem of money. Are there enough funds to conduct a thorough, ground vibration test (time permitting)? What about money to contract for an in-depth mathematical analysis? These factors are discussed separately simply for clarity.

In preparing the test plan, of prime importance is attitude and understanding of the details of the testing to be performed. Are all test specifications and the pertinent aircraft characteristics totally familiar? Can critical speeds be achieved in level flight? Will there be time at the test points for adequate frequency sweeps by an on-board excitation system? Do the handling qualities change significantly in the transonic range? Will the on-board method of excitation will be adequate?

During the late 30's the Germans encountered destructive flutter on several flight tests due to their inability to detect its onset. The recording equipment was not satisfactory in obtaining the required data at the

time needed. The excitation equipment was inadequate in properly exciting and controlling the critical modes at subcritical speeds. It is extremely important that the approach to a critical flutter condition be recognized by observing the subcritical airplane response. Damping trends become very important as the airspeeds are increased toward the potential flutter condition, especially if the V-g diagram is of the type shown in Figure 12.92 where the slope steepens quickly at the critical condition.

12.5.15. In-flight Excitation

To assure that the critical mode is adequately excited at subcritical speeds, a special excitation system may have to be manufactured. The following methods for in-flight excitation presently exist:

- (1) Manual Pulses (stick raps) - can excite frequencies up to six or seven HZ or with powered control systems, up to 10 to 12 Hz depending on aircraft size and servo capabilities. The main advantages of this technique are convenience and cost. A quick, solid rap with the open palm to the side of the stick is the method usually employed. It was used on the F-8 supercritical wing flutter investigation. The same technique was used with the TACT-F-111 except that a wooden mallet was used instead of the open hand. The main disadvantages are lack of frequency selection and the inability to excite the higher frequency modes. It is difficult to manually simulate an impulse input. The energy content in the high frequency modes is usually deficient.
- (2) Ballistic Charges "Bonkers" - pulse charges have been used to excite flutter modes. These mini-explosions more closely simulate the ideal impulse with its large frequency content. The disadvantage is that these charges are usually one shot devices, if pyrotechnic.
- (3) Sinusoidal Shakers (inertial Exciters) - these devices consist of either a rotating out-of-balance wheel or a mass wand oscillating at a desired frequency. The obvious advantage is frequency selectivity. The disadvantage of inertia exciters becomes apparent at low frequencies (i.e., below 3 c.p.s.) when an extremely large out-of-balance, or equivalent, is required to produce the desired force and the weight of the exciter may become prohibitive. Also, in the case of the wheel there may be an excess of shaking force at the high frequencies. The F-5, YF-17 and B-1 prototypes used mass shakers for flutter excitation.
- (4) Oscillating Vanes - In this method an auxiliary aerofoil, of symmetrical section, is attached externally to the aircraft structure and is made to oscillate with a sinusoidal change of incidence by a variable-frequency driving mechanism. The method is

best suited to the excitation of low-frequency modes. In order to control the force exerted by the aerofoil it is necessary to provide some type of force-measuring link between the aerofoil and the aircraft structure and also to have independent control of incidence as well as of frequency. Nevertheless, it may be difficult to control the force with accuracy in the transonic region when large changes of lift may occur with small changes in Mach. Care must be taken to ensure that the installation of the aerofoil does not significantly affect the flutter characteristics of the aircraft. Oscillating Vanes were used in the C-141, C-5A, B-52, and A-10 test programs.

- (5) Autopilot/Autostabilizer Excitation - As the state-of-the-art is advanced and more sophisticated control augmentation systems are developed, increasing dependence will be placed on Autopilot/Autostabilizer systems for flutter excitation. This method may be adopted for tests on aircraft having powered flying controls. A sinusoidal voltage signal of variable frequency is fed, as an error signal, into the autopilot and this produces appropriate oscillations of the main control surfaces. Alternatively, the signal may be fed to the autostabilizer unit to produce the same result. Both methods will be effective down to zero frequency but it may be difficult to excite the higher-frequency modes of the aircraft because of attenuation which may be inherent in the transmissibility characteristics of the power control system. The advantages are obvious but the control system response plus freeplay and stiffness must be very accurately known. The F-15 flight test program involved use of the CAS for flutter excitation. The Advanced Aerial Refueling Boom (AARB) flight test program used its fly-by-wire control system to program frequency sweeps and control inputs to excite various structural modes.
- (6) Turbulence - with the growth of statistical analysis applications, much more use will also be made of turbulence and other atmospheric phenomena as sources of excitation for flutter testing. A spectral density analysis of a random input can be analyzed against the output to find the correlation function. The main disadvantages are that there is no control over the amplitude and frequency characteristics of the input, and that turbulence is hard to find. Another disadvantage is that an on-line computer is required to make the responses meaningful, real time. The YF-16 test program incorporated the use of turbulence as a flutter excitation method.

The selection of the excitation method is very important. The critical mode must have sufficient excitation at subcritical speeds so that the damping behavior can be observed. This point cannot be overemphasized.

Experience has shown that it is preferable to apply the excitation as close as possible to the surfaces whose flutter characteristics are under

particular investigation, as it is not always possible to obtain adequate forced amplitudes of the surfaces under observation, by excitation at a remote point in the structure. This will mean that in a general flutter investigation it may be necessary to provide separate excitation equipment for the wings and tail end of the aircraft. For example, if inertial exciters were being used, it might be necessary to install an exciter outboard in each wing with the ability to operate in and out of phase and, in addition, independent vertical and lateral excitation in the rear fuselage. The detail positions of the exciters would be dictated by local space and strength consideration, always bearing in mind that the exciters must be placed as far as possible away from nodal lines for the modes of vibration of interest in the flutter problem.

Other areas which might need some attention in the test plan formulation are pilot-static calibrations, use of a back-up pilot in the safety/photo chase role, and so forth. The test plan must be thorough and explicit with regard to all responsibilities and functions. Yet it must be realistic enough that no one has any problems sticking to the rules.

During the early 50's at Wright-Patterson AFB flutter tests were conducted on the P-80 to obtain data on the effects of tip tank fuel c.g. travel. Lead weights were used to control the variables. The wing modes were excited by elevator raps for the symmetrical case and aileron raps for the anti-symmetrical case.

The test program was planned to cover a predetermined speed range for each flight. At each data point the pilot would excite the wings and take oscillograph records. After each flight the data would be analyzed and the speed range established for the next sortie.

After two uneventful flights the pilot felt that too much time was being wasted in flying and collecting the data so he decided to take the initiative to speed up the program. A few more airspeed increments were flown that the test card had called for and a wing bending-torsion flutter condition developed. Fortunately, he was able to jettison the tip tanks before a catastrophic failure occurred. However, the wings were so badly ripped that they could not be repaired. Analysis of the subcritical response on the oscillograph showed that there was sufficient flutter onset warning even

though the pilot could feel no change in the aircraft prior to the flutter occurrence. The moral is - develop a sound test plan and stick to it.

12.5.16 Flight Test Execution

There are also do's and don'ts in the flying and test plan execution.

- (1) Precision flying is a must - do not exceed the maximum intended aerodynamic pressure. Practice build-up runs should be flown so that the procedures become rote and the pilot knows exactly how the critical speeds will be approached.
- (2) There must be a minimum crew. For multi-place aircraft each crewmember must be thoroughly familiar with the egress procedures following an emergency. In past cases of flutter testing of cargo type aircraft where the risks were high, knotted ropes were secured along the floor in converging lines toward the exits. If the aircraft became uncontrollable in flight the crewmembers would be able to pull themselves toward the exits for bailout.
- (3) The pilot must be completely familiar with the recovery techniques if a flutter condition were to be encountered. There would be an immediate need to reduce the q and the pilot must fully understand the effects on the airplane of throttle chops, immediate g loadings, use of S/B, stores release, and so forth. In other words, what is the exact response for the pilot if a flutter condition were encountered.
- (4) An investigation should start at the higher altitudes, working first toward the Mach limits. In subsequent flights, the lower altitude, high q limits could be approached.
- (5) If at any time the damping becomes less than predicted, or if they reach minimum planned for levels, recover the aircraft and regroup.
- (6) The weather on test day should be near perfect. Turbulence (unless used as the excitation source) might prematurely excite the critical condition. Obstructions to vision such as cloud layers or heavy haze are not desirable during high speed dives. Strong wind shears can lead to dangerous dive attitude changes.
- (7) A decision must be made on whether to test over land or over water. There is usually less turbulence and more altitude for dive recoveries over the latter. The disadvantages are distance to the recovery base and the difficulty of wreckage retrieval should an accident occur.
- (8) Real time TM with computer hook up is highly recommended. This set-up would allow the engineers to monitor energy distribution of the excited modes and determine the adequacy of excitation at a subcritical speed. Also, the damping trends will be better defined so that engineering decisions based simply on successive oscillograph traces can be avoided.

- (9) The aircrew should monitor the data analysis to ensure that they clearly understand how the tests are proceeding. Their inputs relative to mission progression and foreseeable problems are often times invaluable. Many of the "rules" just presented are common sense in nature.

Nevertheless, they are emphasized simply because of the many occasions in previous flight tests where catastrophes happen simply because of a failure in understanding or of communication by the aircrew. Back in 1941, flutter tests were being conducted on the twin engined AT-8. Ground vibration tests in conjunction with a wing analysis predicted a bending-torsion flutter at 217K. During the preliminary flight tests, however, no large wing oscillations were encountered even at speeds up to 221 K (only small persistent oscillations were recorded).

Consequently, a 3/8 in-lb rotational unbalance shaker was placed at the 42% semi-span on the left wing rear spar. The procedure for the pilot and flutter engineer crew was to climb to 15 thousand feet, start a gentle powered dive and tune the shaker to resonance at each incremental speed build-up. Approaching 200 K, the wing oscillations became so large that the pilot became somewhat concerned. However, since he felt that the engineer in back was watching the same oscillations without getting excited the situation was under control. It turned out that the flutter engineer was on his knees controlling the knobs on the excitation and recording equipment and was not in fact observing the large oscillations.

This example illustrates the importance of each person involved knowing what his and everyone else's responsibility is in a hazardous test program. Another misconception was noted then and at other times prior and subsequent: If the flutter engineer is aboard things must be okay.

A successful test program requires that the crew thoroughly understand the problem, the aircraft capabilities and characteristics, the whys and wherefores in the data accumulation and analyses, and the individual responsibilities in the flight test execution. Like in all group efforts (and so well exemplified in the game of football), a sound game plan, followed by total concentration in individual execution is a must. Happy landing.

12.5.17 Brief Example

We will very briefly discuss the Northrop T-38 as an example of how flutter characteristics of a prototype aircraft are determined through design, analysis, tunnel and ground vibration tests. The emphasis is not on detail but on overall approach. Some of the measures taken to identify and eliminate possible problem areas will be discussed.

Non-steady aerodynamic theories are usually conservative in that the calculated speeds at which instability will occur are usually lower than actual. Because of this, and due to the limitations of beam theory analyses the basic flutter inputs into the T-38 design philosophy were to be derived from wind tunnel model tests. Analytic calculations were made mainly to define speed increments resulting from structural changes and variations in the surface boundary conditions.

Ground vibrations tests on the airplane were run primarily to verify the calculated modes and to illuminate deficiencies in the structural boundaries and the safety margins on the final wing design. Flutter flight test confirmed the safety margins on the production aircraft.

The vibration and flutter analyses of each of the T-38 aerodynamic surfaces were based on the following assumptions: (1) Spanwise distributions of bending and torsional stiffness were represented along a straight swept elastic axis; (2) Surface mass distributions were represented by inertially equivalent strips perpendicular to the elastic axis as shown in Figure 12.93; (3) Oscillating surface aerodynamic forces were approximated by two-dimensional aerodynamic forces calculated for streamwise strips as shown in Figure 12.94, and (4) A flutter mode was represented by a superposition of a finite number of natural vibration modes.

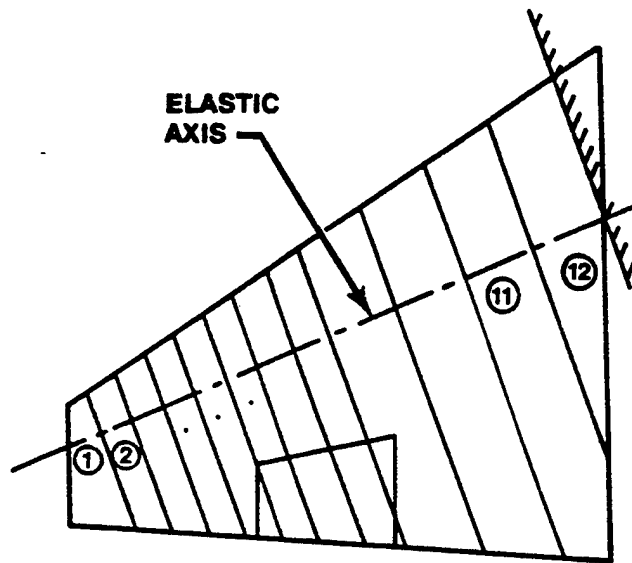


FIGURE 12.93. STRUCTURAL MODEL OF T-38 WING

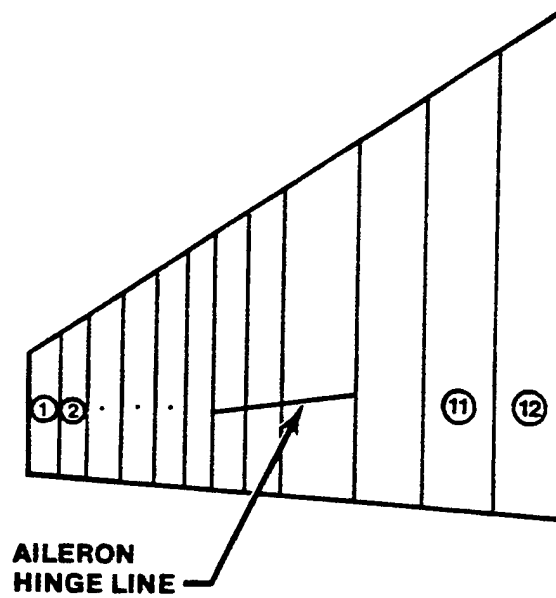


FIGURE 12.94. AERODYNAMIC MODEL OF T-38 WING

The first two assumptions lead to a static beam problem with inertia loadings induced by the mass section oscillations. The strip theory aerodynamic terms used in the flutter analysis were initially based on the incompressible flow oscillating wing section theory of Theodorsen. In follow-up analyses the lift curve slopes were adjusted from the infinite AR 2π value to wind tunnel derived ones.

The three low speed tunnel models used the spanwise mass distribution shown in Figure 12.93. The high speed models simulated the actual aircraft structure with scaled down skins and spars. All models were vibrated prior to the tunnel tests to verify the dynamic simulation.

The general results of the wing tests are as follows. Flutter boundary determination was difficult because of the high stability of the wing. No flutter occurred during the transonic tests at Cornell where 115% limit velocities were achieved at Mach between 0.78 and 0.94. A mild flutter may have occurred with the addition of aft ballast at $M = 0.86$. Based on an analytical extrapolation comparing the bare wing with the ballasted one a safety margin of 32% was predicted.

Tunnel tests at AEDC revealed a possible low damping region at $M = 0.85$ and $q = 2340$ ($V_e = 850$ K). The wing was lost at $q = 3480$. Even a conservative estimate yielded a safety margin of 38%.

The high speed wing tests at Cornell covered a range of aileron rotation to second wing bending (ω_β/ω_2) from 0.92 to 1.48. No aileron flutter or buzz instability was observed. Very briefly, the overall conclusions of the T-38 flutter characteristics were as follows:

Wing and Aileron - no special problems were found in this area.

Vertical Fin and Rudder - except for the destabilizing effect of a three pound extended fuel vent, the vertical fin did not present any major stability problems.

Horizontal Stabilizer - this was initially the most critical of the T-38 aerodynamic surfaces. Flutter problem areas were associated with actuator stiffness, torque tube bending stiffness, freeplay in the actuator system, and the possibility of fuselage vertical bending/horizontal stabilizer bending flutter. The presence of freeplay in the actuator system resulted in a significant decrease in model flutter speeds. As a result, rigging procedures were adopted to eliminate freeplay on the airplane.

The level of pitch stiffness on the stabilizer was found to be deficient during the ground vibration tests. Increases in horn size and hydraulic cylinder stiffness were required to alleviate the coupled stabilizer pitch - torsion problem. In fact, one of the more significant recommendations made in the report was that more rigid controls were required in the future on the specific problem of actuator stiffness and freeplay.

It is appropriate at this time to present a quote from the "DISCUSSION AND CONCLUSIONS" section of the report.

"Identification and elimination of the T-38 flutter problem areas has required a coordinated effort in the fields of theoretical analysis, ground vibration testing, and wind tunnel flutter model testing. No one of these investigations would have been completely effective without the additional information received from the other studies. The final confirmation of aircraft flutter freedom has come from the best possible source - flight flutter tests of the production aircraft."

BIBLIOGRAPHY

- 12.1. Cataldo, C.E. "Overview of Composites for Space Shuttle Structures," George C. Marshall Space Flight Center, Alabama.
- 12.2. Rosen, B. W. "Structural Composites - Design and Analysis," Materials Sciences Corporation, Blue Bell, PA (Drexel University Seminar).
- 12.3. Lovelace, A.M. and Tsai, S.W. "Composites Enter the Mainstream of Aerospace Vehicle Design," Astronautics and Aeronautics, pp. 56-61, July 1970.
- 12.4. Tsai, S.W. "Mechanics of Composite Materials, Part I, Introduction," AFML-TR-66-149, June 1966.
- 12.5. McQuillen, E.J. and Shih, H.L. "Graphite-Epoxy Wing for BWM-34E Supersonic Aerial Target," Journal of Aircraft, Vol. 8, No. 6, pp 480-486, June 1971.
- 12.6. Chow, P.C., Carleone, J. and Hsu, C.M. "Effective Elastic Constants of Layered Media," Report No. 71-18, Mechanics and Structures Advanced Study Group, Drexel University, Philadelphia, PA., October 1971.
- 12.7. Materials (A Scientific American Book), W.H. Freeman and Co., San Francisco, 1967.
- 12.8. Nicholls, R. "Composite Construction Materials Handbook," Prentice-Hall, Inc., Englewood Cliffs, NJ., 1976.
- 12.9. Broutman, L.J. and Krock, R.H. "Modern Composite Materials," Addison-Wesley Publishing Co., Menlo Park, CA., 1967.
- 12.10. BISPLINGHOFF, R.L., ASHLEY, H., and HALFMAN, R.L. Aeroelasticity, Adison-Wesley Publishing Co., Inc., MA, 1955.
- 12.11. ABRAMSON, H.N. The Dynamics of Airplanes, The Ronald Press Co., New York, 1958.
- 12.12. GARRICK, I.E. Editor, Aerodynamic Flutter, AIAA Selected Reprint Series, March, 1969.
- 12.13. LONG, J.A., Jr., and BERRY, R.L. X-24-B Ground Vibration Test (Strake/Aileron/Fin/Rudder), AFFTC FTC-TR-73-23, June, 1973.
- 12.14. LONG, J.A., Jr. Flutter Test Techniques as Demonstrated in the NASA F-8 Supercritical Wing Program, Flight Test Technology Branch Office Memo, Air Force Flight Test Center, January, 1973.

- 12.15 SCHWARTZ, S., and ROONEY, T.R. T-38 Flutter Characteristics Summary, NAI-58-11, Northrop Corp., Hawthorne, CA, June, 1960.
- 12.16 McCRACKEN, D.W. Flutter Boundary Testing, from the Pilots Handbook for Critical and Exploratory Flight Testing, SETP, CA. 1972.
- 12.17 TOLVE, L.A. History of Flight Flutter Testing, Lockheed Aircraft Corp., Marietta, GA.
- 12.18 MILITARY SPECIFICATION, MIL-A-008870A (USAF), Airplane Strength and Rigidity, Flutter, Divergence, and Other Aeroelastic Instabilities, 31 Mar 1971.
- 12.19 KARAMCHETI, K. Principles of Ideal-Fluid Aerodynamics, John Wiley and Sons, Inc., New York, 1966.
- 12.20 THOMSON, W.T. Vibration Theory and Applications, Prentice-Hall, Inc., New Jersey, 1965.
- 12.21 KORDES, E.E. Chairman, NASA Symposium on Flutter Testing Techniques, NASA SP-415, October 9-10, 1975.
- 12.22 THEODORSON, T. General Theory of Aerodynamic Instability and the Mechanism of Flutter, NACA Report No. 496, 1935.